

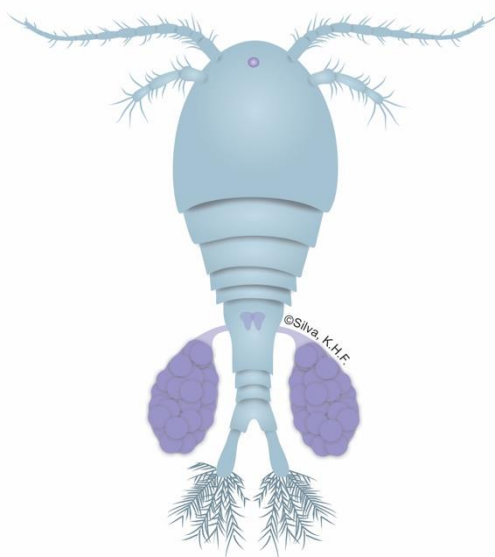


UNIVERSIDADE FEDERAL DE PERNAMBUCO
CENTRO DE TECNOLOGIA E GEOCIÊNCIAS
DEPARTAMENTO DE OCEANOGRÁFIA
PROGRAMA DE PÓS-GRADUAÇÃO EM OCEANOGRÁFIA



KAIO HENRIQUE FARIAS DA SILVA

**COMPLEXIDADE DE ÁREAS MARINHAS PROTEGIDAS: FATORES QUE GOVERNAM
A ASSEMBLEIA DE COPÉPODES MESOZOOPLANCTÔNICOS
(APÓS DERRAMAMENTO DE PETRÓLEO)**



Recife

2022

KAIO HENRIQUE FARIAS DA SILVA

**COMPLEXIDADE DE ÁREAS MARINHAS PROTEGIDAS: FATORES QUE GOVERNAM
A ASSEMBLEIA DE COPÉPODES MESOZOOPLANCTÔNICOS
(APÓS DERRAMAMENTO DE PETRÓLEO)**

Dissertação apresentada ao Programa de Pós-Graduação em Oceanografia da Universidade Federal de Pernambuco, como requisito parcial para obtenção do título de Mestre em Oceanografia.

Área de concentração: Oceanografia Biológica

Orientadora: Prof.^a Dr.^a Sigrid Neumann Leitão

Coorientadora: Dr.^a Renata Polyana de Santana Campelo

Recife
2022

Catalogação na fonte
Bibliotecário Gabriel Luz CRB-4 / 2222

S586c Silva, Kaio Henrique Farias da.

Complexidade de áreas marinhas protegidas: fatores que governam a assembleia de copépodes mesozooplâncticos (após derramamento de petróleo) / Kaio Henrique Farias da Silva. 2022.

103 f: figs., tabs., sigls.

Orientadora: Profa. Dra. Sigrid Neumann Leitão.

Coorientadora: Profa. Dra. Renata Polyana de Santana Campelo.

Dissertação (Mestrado) – Universidade Federal de Pernambuco. CTG.

Programa de Pós-graduação em Oceanografia, Recife, 2022.

Inclui referências.

1. Oceanografia. 2. Copepoda. 3. Ecossistemas costeiros. 4. Estuário tropical. 5. Biomassa. 6. Produção de copepoda. I. Leitão, Sigrid Neumann (Orientadora). II. Campelo, Renata Polyana de Santana (Coorientadora). III. Título.

UFPE

551.46 CDD (22. ed.)

BCTG / 2022 - 338

KAIO HENRIQUE FARIAS DA SILVA

**COMPLEXIDADE DE ÁREAS MARINHAS PROTEGIDAS: FATORES QUE GOVERNAM
A ASSEMBLEIA DE COPÉPODES MESOZOOPLANCTÔNICOS
(APÓS DERRAMAMENTO DE PETRÓLEO)**

Dissertação apresentada ao Programa de Pós-Graduação em Oceanografia da Universidade Federal de Pernambuco, como requisito parcial para obtenção do título de Mestre em Oceanografia.

Área de concentração: Oceanografia Biológica

Aprovada em 31 de agosto de 2022

BANCA EXAMINADORA

Prof.^a Dr.^a Sigrid Neumann Leitão (Orientadora) - Presidente
(Universidade Federal de Pernambuco – UFPE)

Prof.^a Dr.^a Xiomara Franchesca García Díaz - Titular Externo
(Universidade Federal Rural da Amazônia – UFRA)

Prof. Dr. Mauro de Melo Júnior – Titular Externo
(Universidade Federal Rural de Pernambuco - UFRPE)

Prof. Dr. Pedro Augusto Mendes de Castro Melo – Suplente Interno
(Universidade Federal de Pernambuco – UFPE)

Prof.^a Dr.^a Tâmara de Almeida e Silva – Suplente Externo
(Universidade do Estado da Bahia – UNEB)

Dedico esse trabalho aos meus amados pais (Janete Maria e Valdir Barbosa), por todo carinho e dedicação na minha criação.

AGRADECIMENTOS

Como é de concordância de todos, sozinho podemos chegar longe, mas em equipe o infinito é o limite. Felizmente nunca estive sozinho nessa caminhada!

A Profa. Dr. a. Sigrid Neumann Leitão pela orientação, ensinamentos, incentivo, oportunidades, sugestões e por ter contribuído efetivamente para minha formação pessoal e acadêmica. Obrigado por tudo e por todo suporte durante a pandemia. A senhora é luz.

A Dr.^a Renata Polyana de Santana Campelo pela coorientação, ensinamentos, contribuído efetivamente na minha jornada científica e especialmente por ter ajudado mesmo estando em um momento tão único da vida, a chegada de Maria Júlia. Você foi peça fundamental para esse trabalho acontecer, obrigado por toda dedicação, carinho e amizade.

A FACEPE por ter concedido o incentivo financeiro para a realização desse projeto.

Aos projetos PELD-TAMS e FACEPE_Agua por toda estrutura fornecida para a realização das coletas, juntamente com toda equipe de Tamandaré (CEPENE e barqueiros).

Aos laboratórios de fitoplâncton (LabFito) e ao de compostos organismos (OrganoMar) da UFPE por cederem parte dos resultados.

A todos os professores do PPGO que fizeram parte da minha formação.

Aos coordenadores do PPGO Prof. Dr. Pedro Augusto M. C. Melo e Prof. Dr. Roberto Lima Barcellos, ao secretário Nerlucyton Gomes e outros que me ajudaram todo esse período.

Aos amigos do Laboratório de Zooplâncton (Claudeilton Santana, Gabriel Farias, Gabriela Figueiredo, Ralf Cordeiro, Mikaelle Helena, Richard Wonder, Simone Jorge, Ítala Gabriela, Cynthia Lima, Simone Lira, Morgana Loyola e Nathalia Lins) por todos os conhecimentos/experiências compartilhados e pelo revezamento nas coletas em plena pandemia. Vocês são a melhor equipe/família científica que eu poderia ter em um momento tão delicado que enfrentamos.

Ao Vinícius Padilha, pelo auxílio na tradução dos capítulos e também por sempre estar presente me apoiando e ouvindo. Obrigado por ter tornado o final desse mestrado mais leve.

Aos meus amigos que a vida me deu na graduação e mestrado por sempre estarem presente quando precisei. Vocês são demais!

Ao meu irmão Klebson Farias por todo companheirismo.

Aos meus pais, Valdir Barbosa e Janete Maria, que tanto se esforçaram para me educar e ensinar os valores que hoje carrego e por ter me apoiado desde sempre. Amo vocês!

RESUMO

A presente dissertação é composta por dois capítulos em forma de manuscritos, ambos com o objetivo de avaliar a assembleia de copépodes mesozooplanctônica em duas áreas de proteção ambiental: Tamandaré (capítulo 1) e Rio Formoso (capítulo 2). As duas áreas foram impactadas pelo derramamento de petróleo que ocorreu em 2019. O capítulo 1 visou investigar a heterogeneidade espacial e temporal da assembleia de copépodes sobre um conjunto de fatores abióticos. A assembleia foi avaliada no período seco (2020) em três estações fixas em Tamandaré. Os copépodes foram analisados por classe de tamanho e os mais abundantes foram utilizados para as taxas de biomassa e produção. 38 táxons foram identificados, destes 10 foram considerados dominantes e representaram 87% de toda abundância relativa na área. Destaque para abundância, biomassa e produção das espécies *Dioithona oculata*, *Oithona nana*, *Acartia lilljeborgii* e *Parvocalanus quasimodo*. Foi registrada a ocorrência de enxame de *D. oculata* nos dois primeiros meses. Os resultados do estudo apontaram para uma heterogeneidade espaço/temporal baseada na abundância, biomassa e produção dos copépodes. O capítulo 2 objetivou investigar a variabilidade espaço-temporal da abundância, biomassa e produção da assembleia de copépodes em uma área estuarina. A assembleia foi avaliada no período seco (2020) em três estações fixas no Rio Formoso. 34 táxons foram identificados, destes 9 foram considerados dominantes e representaram 90% de toda a abundância relativa na área. As espécies *Paracalanus crassirostris*, *Acartia lilljeborgii*, *Dioithona oculata* e *Euterpina acutifrons* foram as que mais contribuíram em abundância e manutenção da biomassa e produção da cadeia alimentar local. A estação localizada na desembocadura do rio Ariquindá (um dos rios que compõem o complexo estuarino do Rio Formoso) atuou como vetor de incremento de nutriente e produtividade, o qual foi expresso em altas taxas de produtividade primária e secundária. A espécie *P. crassirostris* foi a mais favorecida pela influência dos rios adjacentes e a mesma foi considerada espécie-chave para a manutenção dos recursos pesqueiros na região.

Palavras-chave: copepoda; ecossistemas costeiros; estuário tropical; biomassa; produção de copepoda

ABSTRACT

This dissertation is composed of two chapters in manuscript form, both aiming to assess the mesozooplankton copepod assemblage in two environmental protection areas: Tamandaré (chapter 1) and Rio Formoso (chapter 2). Both areas were impacted by the oil spill that occurred in 2019. Chapter 1 aimed to investigate the spatial and temporal heterogeneity of the copepod assembly over a set of abiotic factors. The assembly was assessed during the dry period (2020) at three fixed stations in Tamandaré. Copepods were analyzed by size class and the most abundant were used for biomass and production rates. 38 taxa were identified, of these 10 were considered dominant and represented 87% of all relative abundance in the area. Highlights for abundance, biomass and production were the species *Dioithona oculata*, *Oithona nana*, *Acartia lilljeborgii* and *Parvocalanus quasimodo*. Swarming of *D. oculata* was recorded in the first two months. The results of the study pointed to a spatial/temporal heterogeneity based on the abundance, biomass and production of copepods. Chapter 2 aimed to investigate the spatio-temporal variability of abundance, biomass and production of the copepod assembly in an estuarine area. The assembly was assessed during the dry period (2020) at three fixed stations in Rio Formoso. 34 taxa were identified, of these 9 were considered dominant and represented 90% of all relative abundance in the area. The species *Paracalanus crassirostris*, *Acartia lilljeborgii*, *Dioithona oculata* and *Euterpina acutifrons* contributed the most in abundance and maintenance of biomass and production of the local food chain. The station located at the mouth of the Ariquindá river (one of the rivers that make up the estuarine complex of Rio Formoso) acted as a vector of nutrient and productivity increment, which was expressed in high rates of primary and secondary productivity. The species *P. crassirostris* was the most favored by the influence of the adjacent rivers and it was considered a key species for the maintenance of fish resources in the region.

Keywords: copepoda; coastal ecosystems; tropical estuary; biomass; copepoda production

LISTA DE FIGURAS

Figura 1	Infográfico demonstrando a interação biológica: Comportamento do petróleo na coluna d'água e a interação com os organismos zooplânctônicos.....	20
Figura 2	Interação do Zooplâncton com o petróleo: Fotografias de análises de amostras realizadas com um microscópio para categorizar visualmente o impacto do óleo no plâncton: (A e B) gotículas de óleo intercaladas entre o zooplâncton; (c) organismo planctônico oleado (Zoea) com manchas de óleo no aparelho oral.....	21
Figura 3	Localização das estações de amostragem na costa sul de Pernambuco. Círculos pretos correspondem aos pontos de amostragem: Tamandaré = TM1 – Pluma; TM2 – Baía; TM3 – Recife e RF1, RF2 e RF3 representando os pontos de amostragem no estuário do Rio Formoso.....	26

COPEPODA ASSEMBLAGE STRUCTURE IN A MARINE PROTECTED REEF AREA INFLUENCED BY ESTUARINE PLUME

Figure 1	Sampling stations along the coast of Pernambuco, Brazil. Three sampling stations in the municipality of Tamandaré (estuarine plume, bay, and reef).....	34
Figure 2	Distribution of abiotic data in Tamandaré: (A) Temporal variation of mean values of environmental variables; (B) Results of principal component analysis (PCA) of environmental variables (Temp = temperature, pH, DO = dissolved oxygen, Sal = salinity and Chl-a = Chlorophyll-a) in green; Stations: Estuarine Plume - green triangle, Bay - pink circle and Reef - blue square.....	38
Figure 3	Temporal variation of total relative abundance (%) of the Copepoda assemblage in Tamandaré, Brazil.....	39
Figure 4	Composition of the Copepoda assembly by size class: (A) Venn diagram based on the number of species among size fractions; (B) Relative abundance (%) of Copepoda assemblage by size fraction in Tamandaré, Brazil.....	42
Figure 5	Box-Plot (median and quartiles) representing the Log(X+1) of abundance, biomass and production of the Copepoda assembly by: Abundance: (A) Temporal, (B) Spatial: Estuarine Plume, Bay and Reef and (C) Size fraction: 200/500 µm, 500/1000 µm and >1000 µm. Biomass: (C) Temporal, (E) Spatial	45

and (F) Size fraction. Production: (G) Temporal, (F) Spatial and (I) Size classes. Samples collected with 200 μm mesh in 2020 in Tamandaré, Brazil....	
Figure 6 Biomass variation (mg C m^{-3}) and production ($\text{mg C m}^{-3} \text{ d}^{-1}$) of Copepoda species by: Temporal (A - E), spatial (B - F) and size class (C - G) in Tamandaré, northeast Brazil.....	46
Figure 7 Average values of the Shannon diversity index (H') in Tamandaré: (A) Temporal variation; (B) Spatial variation; (C) Variation by size class.....	47
Figure 8 Multidimensional scaling plot (MDS) for Copepod assembly in response to size fraction by: (A) abundance, (B) biomass and (C) production. 200/500 μm (yellow triangle), 500/1000 μm (blue circle) and >1000 μm (pink square).....	48
Figure 9 Principal component analysis (PCA): (A) Environmental variables vectors (Temp = temperature, pH, DO = dissolved oxygen, Sal = salinity and Chl-a = chlorophyll-a) in green vectors and dominant species in black vectors; (B) Environmental variables vectors + PAH (Polycyclic Aromatic Hydrocarbons available in seawater) green vectors, February and November sampling months (black circles) and dominant species in black vectors.	50

THE STRUCTURE OF THE COPEPOD ASSEMBLAGE IN TERMS OF ABUNDANCE, BIOMASS AND PRODUCTIVITY IN A TROPICAL ESTUARINE COMPLEX

Figure 1 Sampling stations along the coast of Pernambuco, Brazil. Three sampling stations in the Rio Formoso estuarine complex (RF1, RF2 and RF3).....	61
Figure 2 Distribution of abiotic data in Rio Formoso: (A) Temporal variation of mean values of environmental variables; (B) Results of principal component analysis (PCA) of environmental variables (Temp = temperature, pH, DO = dissolved oxygen, Sal = salinity and Chl-a = Chlorophyll-a) in green; Stations: RF1 - green triangle, RF2 - pink circle and RF3 - blue square.	65
Figure 3 Temporal variation of the total relative abundance (%) of the Copepoda assemblage in Rio Formoso, Brazil.....	66
Figure 4 Composition by size class: (A) Venn diagram based on the number of species among size fractions; (B) Relative abundance (%) of Copepoda assemblage by size fraction in Rio Formoso, Brazil.....	68

Figure 5	Box-Plot (median and quartiles) representing the Log(X+1) of abundance, biomass and production of the Copepoda assemblage by: Abundance: (A) Temporal, (B) Spatial: RF1, RF2 e RF3 and (C) Size fraction 200/500µm, 500/1000µm and >1000µm. Biomass: (C) Temporal, (E) Spatial and (F) Size fraction. Production: (G) Temporal, (F) Spatial and (I) Size classes. Samples collected using the 200µm mesh in 2020 in Rio Formoso, Brazil.....	71
Figure 6	Biomass (mg C m^{-3}) and production ($\text{mg C m}^{-3} \text{ d}^{-1}$) of Copepoda by time series species (A - E), season (B - F) and size class (C - G) in Rio Formoso, northeast of Brazil.....	72
Figure 7	Average values of the Shannon diversity index (H') in Rio Formoso: (A) Annual variability of diversity; (B) Variety in terms of spatial diversity; (C) Variety in terms of the size fractions of the diversity.	73
Figure 8	Multidimensional Scaling (MDS) for the copepod assemblage in response to the Size Fraction factor in (A) abundance, (B) biomass and (C) production: 200/500µm (yellow triangle), 500/1000µm (blue circle) and >1000µm (pink square).....	74
Figure 9	Principal component analysis (PCA) results of environmental variable vectors (Temp = temperature, pH, DO = dissolved oxygen, Sal = salinity and Chl-a = chlorophyll-a / green vectors) and black vectors dominant species.....	75

LISTA DE TABELAS

Tabela 1	a) Regressões de comprimento e peso aplicadas para estimar a biomassa dos copépodes mais abundantes. Dados de comprimento inseridos em μm ; b) Equação de regressão para estimar a taxa de crescimento instantâneo aplicada a Copepoda.....	28
----------	--	----

COPEPODA ASSEMBLAGE STRUCTURE IN A MARINE PROTECTED REEF AREA INFLUENCED BY ESTUARINE PLUME

Table 1	a) Length-weight regressions applied to estimate the biomass of the most abundant copepods. Length data entered in μm ; b) Regression equation for estimating instantaneous growth rate applied to Copepoda.....	36
Table 2	Table 2. Relative abundance (%) and abundance (mean \pm standard deviation) of taxa recorded in the mesozooplankton copepod assemblage in the estuarine plume, bay and reef (Tamandaré, Brazil) in the dry season of 2020.....	40
Table 3	Biomass (total and mean \pm SD, mg C m^{-3}) and Production (total and mean SD, $\text{mg C m}^{-3} \text{ d}^{-1}$) of the most abundant taxonomic groups of the Copepoda from Tamandaré, Brazil.....	43
Table 4	PERMANOVA analysis for the most abundant taxa (>2%) based on the abundance, biomass and production of the copepod assemblage structure in relation to the factors Size class and Spatial. P(perm) = P-value permutational e P(MC) = P-value Monte Carlo.....	48

THE STRUCTURE OF THE COPEPOD ASSEMBLAGE IN TERMS OF ABUNDANCE, BIOMASS AND PRODUCTIVITY IN A TROPICAL ESTUARINE COMPLEX

Table 1	a) Length-weight regressions applied to calculate the biomass of the most abundant copepods. Length data entered in μm ; b) Regression equation to estimate the instantaneous growth rate applied to Copepoda.....	63
Table 2	Relative abundance (RA%) and detail abundance (mean \pm standard deviation) recorded in the assemblage of mesozooplanktonic copepods at stations RF1,.....	66

RF2 and RF3 in the Rio Formoso estuary (northeastern Brazil) in the dry season of 2020.....	
Table 3 Biomass (total and mean \pm SD, mg C m $^{-3}$) and Production (total and mean SD, mg C m $^{-3}$ d $^{-1}$) of the most abundant taxonomic groups from the Copepoda assemblage captured from Rio Formoso, Brazil.	70
Table 4 PERMANOVA analysis for the most abundant taxa (>2%) based on the abundance, biomass and production of the copepod assemblage structure in relation to the factors Size class and Spatial.....	74

LISTA DE SIGLAS

ANOVA	<i>Analysis of variance</i> (Análise de variância)
C	Unidade de Carbono
d ⁻¹	Produção por dia
DO	<i>Dissolved oxygen</i> (Oxigênio dissolvido)
EPA	<i>Environmental protection área</i> (Área de proteção ambiental)
ind ⁻³	Indivíduo por metros cúbicos
ITOPF	<i>International Tanker Owners Pollution Federation Limited</i>
m ⁻³	Metros cúbicos
MDS	<i>Multidimensional scaling</i> (Escalonamento multidimensional)
mg	Miligrama
PAH	<i>Polycyclic Aromatic Hydrocarbon</i> (<i>Hidrocarbonetos Policíclicos Aromáticos</i>)
PCA	Principal Component Analysis (Análise de componentes principais)
PERMANOVA	<i>Permutational multivariate analysis of variance</i> (Análise de variância permutacional)
RA%	<i>Relative abundance</i> (Abundância relativa)
SD	Standard deviation (Desvio padrão)
SIMPER	<i>Similarity percentages Analysis</i> (Análise de Porcentagem de Similaridade)

SUMÁRIO

1	INTRODUÇÃO.....	18
1.1	DERRAMAMENTO DE PETRÓLEO.....	18
1.2	INTERAÇÃO DO ÓLEO COM O ZOOPLÂNCTON.....	19
1.3	COMUNIDADE DO MESOZOOPLÂNCTON.....	22
2	OBJETIVO.....	24
2.1	OBJETIVO GERAL.....	24
2.2	OBJETIVOS ESPECÍFICOS	24
3	METODOLOGIA.....	25
3.1	ÁREA DE ESTUDO.....	26
3.2	ESTRATÉGIA AMOSTRAL.....	26
3.3	PROCESSAMENTO DO ZOOPLÂNCTON.....	27
3.4	ANÁLISE DOS DADOS.....	27
3.4.1	Abundância e diversidade.....	27
3.4.2	Biomassa e Produtividade.....	28
3.4.3	Analises estatísticas.....	29
4	ESTRUTURA DA DISSERTAÇÃO	30
5	RESULTADOS.....	31
5.1	ARTIGO 1 – COPEPODA ASSEMBLAGE STRUCTURE IN A MARINE PROTECTED REEF AREA INFLUENCED BY ESTUARINE PLUME.....	31
5.1.1	Introduction.....	32
5.1.2	Materials and Methods.....	33
5.1.2.1	Study area.....	33
5.1.2.2	Sampling of environmental variables and plankton.....	34
5.1.2.3	Mesozooplankton analysis.....	35
5.1.2.4	Statistical analyses.....	36
5.1.3	Results.....	37
5.1.3.1	Environmental variables and phytoplanktonic biomass (chlorophyll-a).....	37
5.1.3.2	Composition and abundance of the copepod assemblage.....	38
5.1.3.3	Composition of the copepod assemblage by size class.....	41
5.1.3.4	Biomass and secondary production.....	42
5.1.3.5	Diversity.....	46

5.1.3.6	Structure of the copepod assemblage.....	47
5.1.4	Discussion.....	50
5.1.4.1	Environmental variable and phytoplanktonic biomass (chlorophyll-a)	50
5.1.4.2	Composition and abundance of the copepod	51
5.1.4.3	Copepod assemblage structure and ecological indices.....	53
5.1.4.4	Biomass and secondary productivity.....	54
5.1.4.5	Selectivity by size class.....	55
5.1.5	Conclusions.....	56
5.1.6	Acknowledgments.....	57
5.2	ARTIGO 2 – THE STRUCTURE OF THE COPEPOD ASSEMBLAGE IN TERMS OF ABUNDANCE, BIOMASS AND PRODUCTIVITY IN A TROPICAL ESTUARINE COMPLEX.....	58
5.2.1	Introduction.....	59
5.2.2	Materials and Methods.....	60
5.2.2.1	Study area.....	60
5.2.2.2	Sampling of environmental variables and plankton.....	61
5.2.2.3	Mesozooplankton analysis.....	62
5.2.2.4	Statistical analyses.....	63
5.2.3	Results.....	64
5.2.3.1	Environmental variables and phytoplanktonic biomass (chlorophyll-a).....	64
5.2.3.2	Composition and abundance of the copepod assemblage.....	65
5.2.3.3	Composition of the copepod assemblage by size class.....	67
5.2.3.4	Biomass and secondary production.....	69
5.2.3.5	Diversity.....	73
5.2.3.6	Structure of the copepod assemblage.....	73
5.2.4	Discussion.....	76
5.2.4.1	Environmental variables and phytoplanktonic biomass (chlorophyll-a).....	76
5.2.4.2	Composition and abundance of the copepod assemblage.....	77
5.2.4.3	Biomass and secondary productivity.....	79
5.2.5	Conclusions.....	80
5.2.6	Acknowledgments.....	81
7	CONSIDERAÇÕES FINAIS.....	82
	REFERÊNCIAS.....	84

1 INTRODUÇÃO

1.1 DERRAMAMENTO DE PETRÓLEO

As Áreas Marinhais Protegidas (AMPs) foram criadas com a proposta de proteger as espécies de impactos locais como sobrepesca e poluição (BATES *et al.*, 2019; WILSON *et al.*, 2020). Com o crescimento econômico e populacional, a humanidade se tornou a principal força motora para a mudança dos ecossistemas e isso acabou fortalecendo a importância das áreas protegidas (HUGHES *et al.*, 2018). Apesar de serem refúgio para a vida marinha, as AMPs estão sendo ameaçadas constantemente pelas ações antrópicas. Seja por ameaças globais como mudanças climáticas, ou mudanças locais como a poluição marinha (HUGHES *et al.*, 2018; WILLIAMS *et al.*, 2019).

Recentemente, o Brasil foi alvo de um evento de derramamento de petróleo, o qual foi considerado o maior desastre ambiental litorâneo já documentado na costa tropical do Oceano Atlântico (CAMPELO, *et al.*, 2021; LOURENÇO *et al.*, 2020; SILVA, L. S. C. D. *et al.*, 2020; SOARES *et al.*, 2020). O vazamento foi incialmente registrado entre o fim de agosto e início de setembro de 2019 , com as ultimas manchas sendo reportadas em julho de 2020 no estado da Bahia (ESCOBAR, 2019; SILVA, L. S. C. D. *et al.*, 2020; SOARES *et al.*, 2020). Ao longo desse período, mais de 5000 toneladas de resíduo do óleo foram coletadas ao longo da costa brasileira, principalmente nos estados de Alagoas e Pernambuco (BRUM *et al.*, 2020). Um total de 11 estados brasileiros foram afetados, caracterizando esse desastre ambiental como o maior já registrado na história do Brasil (IBAMA, 2020; LOURENÇO *et al.*, 2020; SOARES *et al.*, 2020).

A extensão do acidente foi de aproximadamente 3000 km ao longo da costa brasileira (ESCOBAR, 2019) e, segundo o Ibama (2020), afetou mais de 55 AMPs, sendo duas delas as maiores do Atlântico Sul: Área de Proteção Ambiental (APA) Costa dos Corais e Parque Nacional Marinho de Abrolhos, sendo a APA Costa dos Corais a maior unidade de conservação federal em extensão ($>3.000\text{km}$) no território Brasileiro. Sabendo da importância dessas regiões e ecossistemas associados, o monitoramento em escala de curto, médio e longo prazo se faz importante, uma vez que o efeito do petróleo pode afetar a estrutura/funcionamento da cadeia trófica (GARCIA; LA ROVERE, 2011; RAMSEUR, 2010; ZIOLLI, 2002).

Assim que se popularizaram as notícias da chegada das manchas de óleo bruto, a população civil se mobilizou em ações de limpeza. Muitos sem conhecimento dos malefícios causados pelo petróleo e gás tóxico, que esse poluente libera no ar, se expuseram sem apoio de equipamentos de proteção individual e máscara de gás (Figura 1) (ARAÚJO *et al.*, 2020), porém, sem essa ajuda

prestada pelos voluntários, o impacto causado nas praias pelo óleo teria tomado proporções ainda maiores, já que a ação governamental foi lenta (SOARES *et al.*, 2020).

As consequências causadas por tal catástrofe acometida no Brasil ainda são incertas, pois logo após o desastre do óleo, a população global enfrentou uma pandemia causada pelo vírus SARS-CoV-2 (Coronavírus - COVID-19) (primeiro caso confirmado no Brasil em fevereiro de 2020) (CIOTTI *et al.*, 2020). A necessidade de adotar medidas preventivas obrigatórias como o *lockdown* pelo governo estadual (pois cada estado brasileiro tomou decisões diferentes) para desacelerar a propagação do Coronavírus (SILVA, L. *et al.*, 2020), impactou diretamente os trabalhos de pesquisas que estavam em andamento sobre o óleo. Todavia, mesmo com todas as dificuldades (praias fechadas e risco de contaminação), alguns estudos imediatos/emergenciais foram realizados.

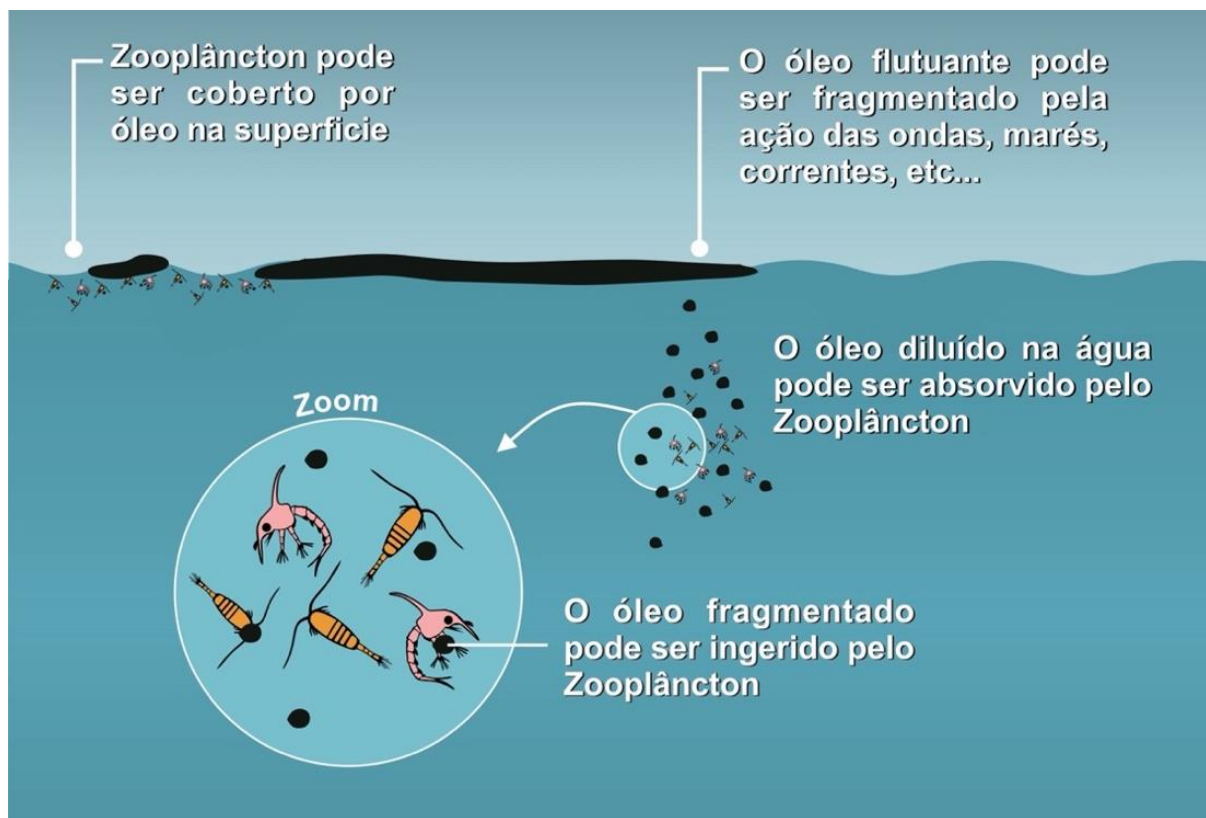
Os resultados das pesquisas emergenciais sobre o impacto do derramamento de óleo sobre a comunidade biológica costeira revelaram um impacto agudo em equinodermos (CERQUEIRA, 2021), poliquetas (por exemplo, *Branchiosyllis*), esponjas (CRAVEIRO *et al.*, 2021; LIRA *et al.*, 2021) e interação entre os organismos zooplânctônicos e o óleo (CAMPELO, R. P. D. S. *et al.*, 2021; SOARES *et al.*, 2020). Resultados de ensaios de laboratório demonstram que o carbono do petróleo bruto é incorporado à biomassa celular do endossimbionte *Symbiodinium glynnii* com uma alteração concomitante do valor isotópico $\delta^{13}\text{C}$ e impactos negativos na fisiologia e na taxa de crescimento (MÜLLER *et al.*, 2021).

1.2 INTERAÇÃO DO ÓLEO COM O ZOOPLÂNCTON

Quando ocorrem derramamentos de petróleo, além do próprio óleo bruto (parte visível), há os impactos de compostos relacionados ao mesmo, que são capazes de atingir uma extensão maior, incluindo áreas não alcançadas pelas manchas de óleo (ABESSA *et al.*, 2018; DASGUPTA *et al.*, 2018). Por ter densidade menor que a água do mar, ele geralmente se move pela superfície (BEYER *et al.*, 2016). No entanto, ao estar disponível no ambiente, o óleo sofre processos físico-químicos (evaporação, dissolução, oxidação, sedimentação e biodegradação) que podem modificar a sua composição e toxicidade (DEL VIGNE; SWEENEY, 1988). Esses processos quebram as manchas de óleo em fragmentos menores (1–100 μm de diâmetro), semelhante ao processo que ocorre com o microplástico, afetando ainda mais organismos (ALMEDA *et al.*, 2014) (Figura 1). Outro aspecto importante é o tempo de exposição dos organismos ao contaminante e a condição do mesmo durante o contato (intemperizado, emulsificado, fragmentação, etc). As duas formas principais em que o petróleo provoca impactos nos organismos aquáticos são o efeito físico consequente do recobrimento

e o efeito químico, agregado à toxicidade dos compostos presentes (SZEWCZYK *et al.*, 2006).

Figura 1 – Infográfico demonstrando a interação biológica: Comportamento do petróleo na coluna d’água e a interação com os organismos zooplânctônicos.

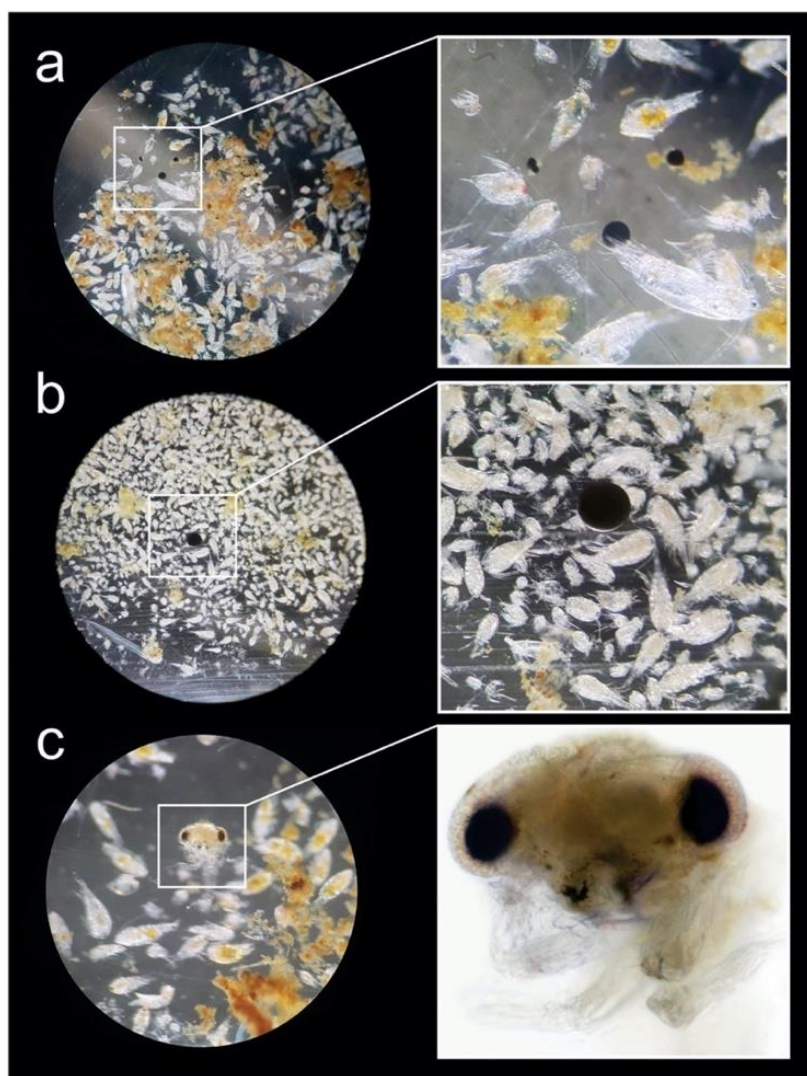


Fonte: O autor, 2022.

As manchas maiores podem afetar organismos maiores como aves, peixes, tartarugas e macroalgas, levando muitas vezes a mortalidade, mas também podem afetar microrganismos que estão na base da cadeia alimentar (LOURENÇO *et al.*, 2020; SOARES *et al.*, 2020). O poluente em questão age como barreira física impedindo a penetração da luz solar na coluna d’água, limitando a taxa fotossintética, e também pode agir como fator desencadeador para o aumento das florações e modificações no crescimento algal (HÄDER; GAO, 2015; HUANG *et al.*, 2011). Após a fragmentação das manchas, o óleo acaba se dispersando para mais lugares e ficando disponível para organismos menores. Os fragmentos acabam ficando dentro do espectro de tamanho alimentar de vários grupos do zooplâncton, facilitando a interação entre os organismos (ALMEDA *et al.*, 2013; CAMPELO, *et al.*, 2021) (Figura 2). Essa interação no ambiente foi recentemente demonstrada, como resultado de análises das amostras de zooplâncton coletadas pós-derramamento de petróleo na costa

pernambucana (CAMPELO, *et al.*, 2021). Neste estudo, foram registradas evidências de ingestão de gotículas de óleo por grupos do zooplâncton como Copepoda e Zoea (larva de Decapoda) (Figura 2).

Figura 2 – Interação do Zooplâncton com o petróleo: Fotografias de análises de amostras realizadas com um microscópio para categorizar visualmente o impacto do óleo no plâncton: (a e b) gotículas de óleo intercaladas entre o zooplâncton; (c) organismo planctônico oleado (Zoea) com manchas de óleo no aparelho oral.



Fonte: Campelo, *et al.* (2021) / © Claudeilton Santana.

O zooplâncton é formado por protozoários e pequenos metazoários (BOLTOVSKOY, 1981). Esses organismos desempenham um importante papel no controle da produção do fitoplâncton (consequentemente na transferência de energia para os níveis tróficos superiores), ciclismo biogeoquímico e recrutamento de peixes (BRANDINI *et al.*, 1997). No entanto, apesar de sua importância em ambientes marinhos, nosso conhecimento sobre as interações entre zooplâncton e desastres ambientais de origem antropogênicas é bastante limitado (ALMEDA *et al.*, 2013).

Sabe-se que a mistura de hidrocarbonetos (HAP) é altamente tóxica para os consumidores primários e podem biomagnificar e serem transferidos ao longo da cadeia trófica (BERROJALBIZ *et al.*, 2009). Como revisado por Almeda *et al.* (2013), sobre interação do zooplâncton com poluentes, existem três principais tipos de interações: A primeira, os poluentes podem exercer efeitos diretos com o zooplâncton, incluindo efeitos subletais (mal desenvolvimento, mutações) e letais (mortalidade) (WALSH, 1978); A segunda interação está na capacidade do zooplâncton influenciar nas características físico-químicas dos poluentes na coluna d'água, a partir da absorção, transformação e eliminação (MUSCHENHEIM; LEE, 2002; WALSH, 1978); E, por último, o zooplâncton pode desempenhar um papel importante na bioampliação de contaminantes químicos xenobióticos nas teias tróficas, por meio da biomagnificação (GRAY, 2002; WALSH, 1978).

1.3 COMUNIDADE DO MESOZOOPLÂNCTON

Os organismos zooplanctônicos podem ser classificados de acordo com suas dimensões corporais, em microzooplâncton (20–200µm) (ex.: foraminíferos), **mesozooplâncton** (200µm–2mm) (ex.: cladóceros, copépodes), macrozooplâncton (2–20mm) (ex.: pterópodes, copépodes, quetognatos) e megazooplâncton (20–200 mm) (ex.: taliáceos, cífozoários) (OMORI; IKEDA, 1992; SIEBURTH *et al.*, 1976). Além disso podem ser agrupados em dois grupos distintos, em relação à duração a vida planctônica: Holoplâncton e Meroplâncton. Os organismos holoplanctônicos que passam todo o seu ciclo de vida como componentes do plâncton e os meroplanctônicos os que dependem desse ambiente apenas em uma parte de seu ciclo de vida, geralmente na fase larval (OMORI; IKEDA, 1992).

Os representantes mais numerosos do holoplâncton marinho e estuarino são os copépodes. Dominantes em biomassa e abundância (chegam a alcançar aproximadamente 60–80% da produção total do zooplâncton), além disso, são o grupo mais diversificado dentre os crustáceos (HUYS, 1991; KIØRBOE, 1997). Essa representatividade pode ser observada em todos os ambientes aquáticos com destaque aos costeiros (DIAS, 1999; DIAS; BONECKER, 2009; FIDELIS, 2014; FIGUEIRÊDO, 2014; MAGALHÃES, 2014; MELO-JUNIOR *et al.*, 2016). Segundo Kiørboe (2010), esse sucesso se deve por conta a sua plasticidade na forma de se alimentar, reproduzir e estratégias de sobrevivência na coluna d'água.

Por estarem dispersos na coluna d'água, as condições bióticas e abióticas do meio influenciam diretamente essa comunidade. Essa variabilidade do meio pode afetar o crescimento do zooplâncton acarretando alterações significativas na estrutura trófica desses organismos em todos os níveis intra/interespecíficos (ANACLETO; GOMES, 2006; GORSKY *et al.*, 2010). Devido ao caráter

resiliente, sensível e dinâmico (curto ciclos de vida) os copépodes são considerados excelentes bioindicadores das variações ecossistêmicas (NEUMANN-LEITÃO, 2010). Estas variações tem efeito direto em importantes descritores da assembleia de copépodes tais como: abundância, biomassa e produtividade (GROSS; GROSS, 1996; NEUMANN-LEITÃO *et al.*, 1998). Os resultados podem representar um alerta a respeito da saúde dos ambientes investigados.

O estudo da biomassa e produção secundária em ambientes aquáticos permitem conhecer o fluxo de energia e matéria na teia alimentar planctônica, bem como o estado fisiológico e nutricional dos organismos (KIMMERER, 1987; OMORI; IKEDA, 1992; PAGANO; LUCIEN SAINT-JEAN, 1989). Segundo Downing (1984) e Day *et al.* (2012), diversos fatores podem influenciar a produção secundária de um determinado local, entre eles: as atributos da população (biomassa, duração do ciclo de vida, número de gerações/ano, idade, tamanho dos organismos, diversidade e estado trófico), os fatores ambientais (temperatura, salinidade, oxigênio dissolvido, pH e clorofila-a), predação e competição inter/intraespecíficas. Além disso, o estudo desses caracteres também permitem avaliar a resposta do zooplâncton à exposição de poluição xenobiótica (DOWNING, 1984).

Neste contexto, tendo em vista a magnitude do impacto causado na costa tropical brasileira pelo derramamento de petróleo, o desenvolvimento de pesquisas sobre a resposta da comunidade do zooplâncton ao impacto são de extrema importância. O presente estudo tem como objetivo investigar a heterogeneidade espacial da estrutura da assembleia de copépodes planctônicos em habitats costeiros (Tamandaré e Rio Formoso) após o derramamento do petróleo. Desafios particulares incluíram o fato de que não haverem amostragem durante o impacto do derramamento do óleo (setembro~dezembro de 2019) e nem coleta recorrente dos valores de HPA na água (devido ao *lockdown*), além disso, existem poucos dados de linha de base da comunidade do zooplâncton para a área estudada. Desta forma, a estrutura da assembleia de copépodes teve que ser avaliada dentro do contexto de grande complexidade espacial do ecossistema costeiro.

2 OBJETIVO

2.2 OBJETIVO GERAL

Investigar a heterogeneidade espaço-temporal da estrutura da assembleia de copépodes mesozooplâncticos em duas áreas de proteção ambiental após derramamento de petróleo.

2.2 OBJETIVOS ESPECÍFICOS

- a) Caracterizar a estrutura da assembleia de copépodes (ao menor nível taxonômico) de dois ambientes costeiros (Tamandaré e Rio Formoso) em diferentes escalas (espacial, temporal e classes de tamanho);
- b) Verificar as associações existentes entre as espécies de copépodes e quais os fatores abióticos (salinidade, temperatura, pH e oxigênio dissolvido) que influenciam na estruturação/distribuição da assembleia;
- c) Estimar a biomassa e produtividade dos copépodes pelágicos dominantes dos dois ecossistemas costeiros e verificar as espécies que mais contribuem na introdução de carbono.

3 METODOLOGIA

3.1 ÁREA DE ESTUDO

O presente estudo foi realizado no âmbito dos projetos de pesquisa: PELD-TAMS (Programa Ecológico de Longa duração – Tamandaré Sustentável) e FACEPE_Agua (Monitoramento de petróleo na água e seu impacto na base da teia alimentar na costa de Pernambuco: Implicações ecológicas em dois locais de amostragem Tamandaré e Rio Formoso, Pernambuco, Brasil).

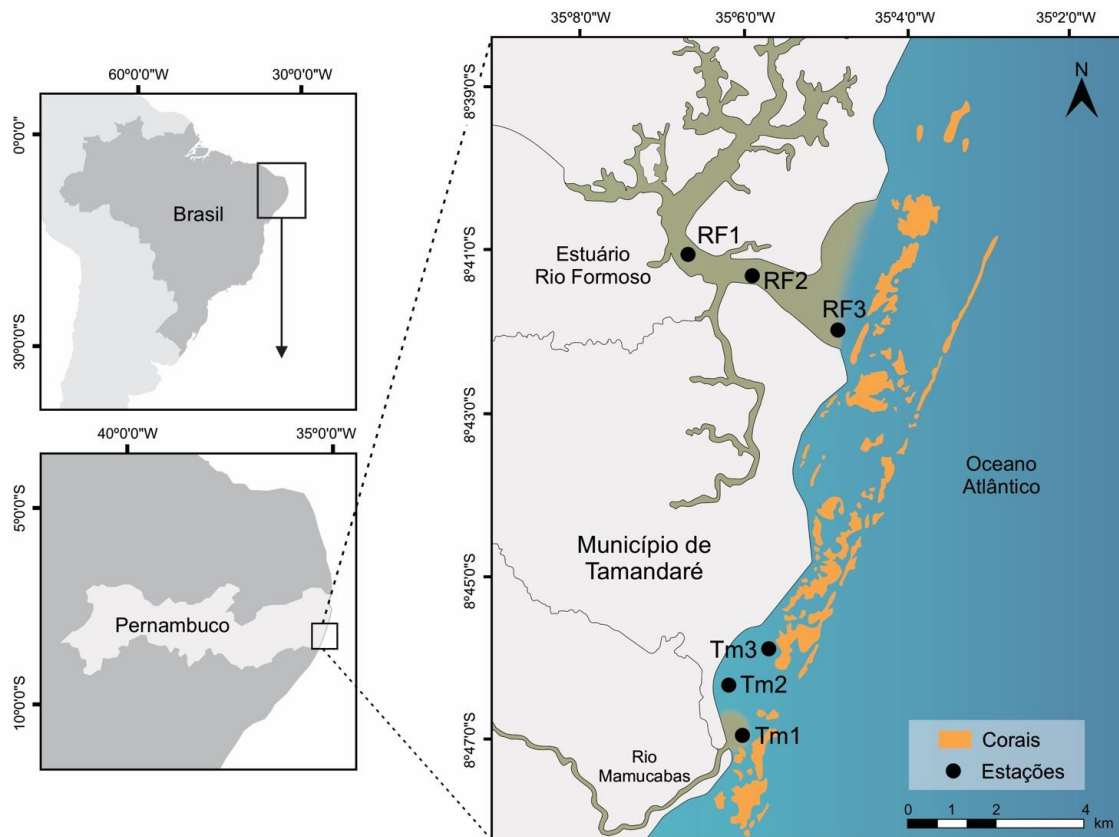
A primeira área está localizada no município de Tamandaré (litoral Sul do estado de Pernambuco), a cerca de 110km da cidade do Recife. Possui aproximadamente 9km de costa dividida em três áreas: Praia dos Carneiros, Praia dos Campas e a Baía de Tamandaré (MAIDA & FERREIRA, 1995; CAMARGO *et al.*, 2007) (Figura 3). A Baía de Tamandaré está localizada entre a Latitude 08°44' a 08°47'30"S e Longitude 35°05' a 35°07'W, e recebe a influência estuarina de três rios: rios Ilhetas, Mamucabas e Una. A baía trata-se de uma enseada aberta, que possui uma extensão de cerca 4 km² em forma semicircular voltada para o leste (profundidade média 7 ~ 10 metros) (Figura 1) (MOURA, 1991; MOURA & PASSAVANTE, 1993). A baía destacasse por possuir um complexo recifal que separa o mar-aberto da linha da costa, constituindo um “quebra-mar” natural (REBOUÇAS, 1966). Este complexo recifal faz parte da maior Unidade de conservação Marítima em extensão no Brasil, a Área de Proteção Ambiental (APA) Costa dos Corais (FERREIRA *et al.*, 2001).

A segunda área encontra-se ao lado de Tamandaré (cerca de 4 km ao Norte), o município de Rio Formoso. Este município está inserido em duas APAs: a APA de Guadalupe e a APA Costa dos Corais (BOTELHO *et al.*, 2000; FERREIRA; MAIDA, 2006; HONORATO DA SILVA *et al.*, 2009) (Figura 3). Hidrograficamente este município está inserido nas bacias de cinco rios: rios a noroeste - Formoso, dos Passos, Lemenho e Porto das Pedras, e ao sul - rio Ariquindá. Neste complexo, destaca-se o estuário do Rio Formoso que apresenta uma área aproximada de 2.724 hectares e está situado entre as coordenadas geográficas 8°39' - 8°42'S e 35°10' - 35°05'W (Figura 1) (FIDEM, 1987). A área estuarina é do tipo planície costeira, de morfologia sinuosa e influenciada por pequenas descargas continentais é margeado em toda sua extensão por mangues, recebe efluentes domésticos, resíduos provenientes da agroindústria açucareira e atividade de carcinicultura (HONORATO DA SILVA *et al.*, 2004, 2009).

As regiões apresentam um clima do tipo litorâneo, tipicamente quente e úmido do tipo AS', segundo o sistema de classificação de Köppen, caracterizado por um período seco e um período de chuva (ALVARES *et al.*, 2013). Conta um uma variação média de temperatura de 25° - 30° C, e é

fortemente influenciada pela ação moderada dos ventos alísios, que sopram de sudeste a nordeste (MOURA, 1991; MOURA & PASSAVANTE, 1995). A pluviosidade anual na faixa costeira de Pernambuco oscila entre 1.850 e 2.364 mm e conta com um período de seco estende-se de setembro a março e chuvoso de abril a agosto (ANDRADE, 1971; NIMER, 1979; LIMA, 2001).

Figura 3 – Localização das estações de amostragem na costa sul de Pernambuco. Círculos pretos correspondem aos pontos de amostragem: Tamandaré = TM1 – Pluma; TM2 – Baía; TM3 – Recife e RF1, RF2 e RF3 representando os pontos de amostragem no estuário do Rio Formoso.



Fonte: O autor, 2022.

3.2 ESTRATÉGIA AMOSTRAL

As amostragens foram realizadas na região Nordeste do Brasil e abrange a camada subsuperficial da coluna d'água da baía de Tamandaré (Pluma estuarina – Tm1 [originária do rio Mamucabas e Ilhetas] Baía – Tm2 e Recife – Tm3) e do estuário do Rio Formoso (RF1, RF2 e RF3 [pontos definidos acompanhando registros de petróleo pós-derramamento]) (Figura 3).

As amostragens em Tamandaré e Rio Formoso foram realizadas no ano de 2020, ambas no período seco, maré vazante, diurnas e pontos únicos (fixos). Tamandaré contou com 6 meses de amostragem

(Fevereiro, Março, Setembro, Outubro, Novembro e Dezembro), totalizando 18 unidades amostrais. O estuário do Rio Formoso contou com 4 meses de amostragem (Fevereiro, Março, Setembro e Outubro), totalizando 12 unidades amostrais.

Amostras de água foram coletadas para o teor de clorofila-a (UNESCO, 1966). Os parâmetros ambientais (temperatura da superfície do mar, pH, salinidade e oxigênio dissolvido) foram medidos à superfície usando um sensor multiparâmetro pré-calibrado de qualidade da água (HORIBA - U50). Os dados pluviométricos foram obtidos do Instituto Nacional de Meteorologia.

Arrastos subsuperficiais diurnos com rede de plâncton de malha de 200 µm (com diâmetro de boca de 30 cm) foram realizados para a coleta do mesozooplâncton. Os arrastos foram efetuados com uma velocidade 1,5 a 2,5 nós por 3 minutos. Um fluxômetro foi acoplado na boca da rede para estimar o volume de água filtrada através da rede. As amostras de zooplâncton foram preservadas imediatamente em uma solução de formaldeído a 4% e tamponadas com bórax (0,5 g*L⁻¹) (NEWELL; NEWELL, 1963).

3.3 PROCESSAMENTO DO ZOOPLÂNCTON

As amostras foram fracionadas em três classes de tamanho utilizando um conjunto de peneiras com tamanhos de malha de 1000, 500 e 200 µm (HEAD *et al.*, 1999). Posteriormente, as diferentes classes de tamanho (200/500µm, 500/1000µm, e >1000µm) foram fracionadas utilizando um equipamento de classificação tipo MOTODA para uma análise mínima de 300 copépodes (OMORI; IKEDA, 1984). As amostras foram analisadas em uma câmara de contagem Bogorov sob um estereomicroscópio. Para identificação taxonômica, foram consultadas bibliografias especializadas: Bjornberg (1981) e Boltovskoy *et al.* (2002). Após a identificação, os copépodes foram medidos usando um software Zen.

3.4 ANÁLISE DOS DADOS

3.4.1 Abundância e diversidade

A abundância (ind m⁻³) e a abundância relativa de copépodes (%) foram calculadas para descrever a estrutura da comunidade (espécies de copépodes com abundância relativa $\geq 2\%$ foram consideradas dominantes e utilizadas para as análises multivariadas). O índice de diversidade Shannon (H') foi aplicado para estimar a diversidade do conjunto (SHANNON, 1948), onde os valores

encontrados indicam: alta diversidade se $H' > 3,0$ bits ind^{-1} , média diversidade se $2,0 < H' \leq 3,0$ bits ind^{-1} , baixa diversidade se $1,0 < H' \leq 2,0$ bits ind^{-1} , e muito baixa diversidade se $H' < 1,0$ bits ind^{-1} .

3.4.2 Biomassa e Produtividade

Para estimar a biomassa, um total de 30 indivíduos das espécies mais abundantes (abundância relativa >2%) foram medidos considerando apenas o comprimento do prossoma. Biomassa (B, mg C m^{-3}) de um determinado táxon com base em sua abundância (A, $ind\ m^{-3}$) e peso de carbono individual (CW, mg C): $B = A * CW$. O CW foi definido usando regressões de comprimento e peso disponíveis na literatura (Tabela 1a). O cálculo da Produção ($mg\ C\ m^{-3}\ dia^{-1}$) foi baseado em sua biomassa e taxas de crescimento específicas: $P_i = C_i * B_i$. Onde (P_i) a produção do grupo i, (C_i) taxa de crescimento da biomassa do grupo i e (B_i) do grupo i. A taxa de crescimento (C) foi baseada no modelo global de Hirst *et al.* (2003) (Adultos e jovens foram considerados juntos / Tabela 1b).

Tabela 1 – a) Regressões de comprimento e peso aplicadas para estimar a biomassa dos copépodes mais abundantes. Dados de comprimento inseridos em μm ; b) Equação de regressão para estimar a taxa de crescimento instantâneo aplicada a Copepoda.

a) Equações de regressão para o comprimento-peso

Taxa	Equações	Referencias
<i>Acartia lilljeborgii</i>	$CW = 6.177 \times 10^{-9} \times L^{3.029}$	Ara (2001)
Oithonidae	$\ln CW = 1.10 \ln PL - 7.07$	Chisholm e Roff (1990)
Paracalanidae	$\ln CW = 2.78 \ln PL - 16.52$	Webber e Roff (1995)
<i>Labidocera</i> spp.	$CW = 1.666 \times 10^{-8} \times TL^{2.837}$	Ara (2001)
Harpacticoida	$\log CW (\mu g) = -8.51 + 3.26 \times \log TL$	Hirota (1986)
Náuplio (Copepoda)	$\ln AFDW = 2.48 \ln TL - 15.7$	Båmstedt <i>et al.</i> (1986)

b) Equação de regressão para a taxa de crescimento

Taxa	Equações	Reference
Copepoda	$\log_{10} C = 0.0186 \times T - 0.288 \times \log_{10}(CW) + 0.417 \times \log_{10}(Cl) - 1.209$	Hirst e Bunker (2003)

CW, Peso de Carbono; PL, Comprimento do Prossoma; TL, Comprimento Total; C, Carbono; Cl, Clorofila-a; T, Temperatura

Fonte: O auto, 2022.

3.4.3 Analises estatísticas

As informações relacionadas às variáveis dependentes: abundância (ind m⁻³), biomassa (mg C m⁻³) e produção (mg C m⁻³ d⁻¹) de copépodes planctônicos, foram testadas estatisticamente a partir de rotinas desenvolvidas em software matemático. A análise de variância (ANOVA) foi utilizada para analisar os efeitos de primeira ordem (não-interação) de múltiplas variáveis independentes: espacial (pluma estuarina versus baía versus recife), temporal (meses versus meses) e classe de tamanho (200/500µm versus 500/1000µm versus >1000µm). A heterogeneidade das variações foi investigada com o teste de Levene e a normalidade dos dados foi investigada pelo teste de Kolmogorov-Smirnov. Quando necessário, os dados foram transformados em Log(X+1). Uma vez verificado o significado ($P < 0,05$), foi aplicado o teste Tukey-HSD (post-hoc).

A estrutura da assembleia de copépodes foi investigada usando análises multivariadas. A análise permutacional de variância (PERMANOVA) foi aplicada para testar a hipótese de que a estrutura da assembleia de copépodes varia em resposta aos fatores espaciais e de classe de tamanho testados (o fator temporal foi deixado de fora das análises multivariadas devido ao desequilíbrio e porque todas as amostras eram de um único período). No caso de diferenças significativas, foi realizado um teste emparelhado entre diferentes níveis de fator(s) significativo(s). Para identificar padrões de similaridade entre as amostras e, portanto, possíveis mudanças na distribuição dos copépodes, foi usado o escalonamento multidimensional (MDS) para representá-los graficamente.

Tanto o PERMANOVA quanto o MDS foram baseados em uma matriz de similaridade Bray-Curtis construída a partir do Log(X+1) da abundância de espécies transformadas com relativa abundância $\geq 2\%$. A análise da porcentagem de similaridade (SIMPER) foi realizada para identificar taxas/espécies representativas e suas contribuições para a dissemelhança. A análise de componentes principais (PCA) também foi calculada usando os dados e parâmetros ambientais padronizados e espécies de Copepoda para avaliar as associações entre eles.

4 ESTRUTURA DA DISSERTAÇÃO

Esta dissertação está formatada como manuscrito para publicação na revista *Estuarine, Coastal and Shelf Science* e apresenta a distribuição da assembleia de copépodes em dois ambientes costeiros tropicais na costa Brasileira.

As análises foram conduzidas a partir da abundância total, abundância relativa, biomassa e produtividade dos copépodes e análises multivariadas em uma série de dados (espacial, entre meses do período seco e classes de tamanho). A dissertação está estruturada em dois artigos produzidos:

- O Artigo 1 é focado na assembleia de copépodes na costa de Tamandaré (Pernambuco, Brasil) em três ambientes (pluma estuarina, baía e recife), tem como título: *Copepoda assemblage structure in a marine protected reef area influenced by estuarine plume*;
- O Artigo 2 é focado na assembleia de copépodes no complexo estuarino do Rio Formoso (Pernambuco, Brasil) com a proposta de ser o primeiro a investigar a biomassa e produção dos copépodes no local, tem como título: *The structure of the copepod assemblage in terms of abundance, biomass and productivity in a tropical estuarine complex*.

5 RESULTADOS

5.1 ARTIGO 1 – COPEPODA ASSEMBLAGE STRUCTURE IN A TROPICAL MARINE PROTECTED REEF AREA INFLUENCED BY ESTUARINE PLUME

Kaio H. F. da Silva^a; Renata P. de S. Campelo^a & Sigrid Neumann-Leitão^a

^aDept. of Oceanography, Federal University of Pernambuco,
Av. Arquitetura s/n, Recife, Pernambuco, 50740-550, Brazil

Abstract

The research was carried out in one of the largest Environmental Protection Areas called Costa dos Corais, located in northeastern Brazil. The area is composed of a complex extensive reef zone influenced by an estuarine plume. In 2019 an oil spill occurred on the Brazilian coast affecting this area. To understand the extent of the impact of the oil on mesozooplanktonic copepods it was carried out an investigation about the spatial and temporal heterogeneity of the copepod assemblage on a set of abiotic factors. Samples were obtained in Tamandaré (Pernambuco, Brazil) and comprised three sites (estuarine plume, bay and reef zone). Horizontal subsurface hauls were performed during the ebb tide in six months of the dry period (February, March, September, October, November and December/2020) with a plankton net 200 µm mesh size. In addition, size class methodology was used to analyze the samples, after which the biomass and productivity (model of Hirst and Bunker, 2003) of the most abundant species were estimated. A total of 38 taxonomic groups were identified, of these 10 were dominant and accounted to 87% of all relative abundance in the area. We highlight the contributions in abundance, biomass and production for the species: *Dioithona oculata*, *Oithona nana*, *Acartia lilljeborgii* and *Paracalanus quasimodo*. The results of the study point to a space-time heterogeneity based on the abundance, biomass and production of copepods, where although statistical differences have not been verified, we suggest that these parameters fluctuate locally by the influence of the estuarine plume, contributing nutrients and increasing productivity and by patterns related to predator-prey relationships, especially in the reef area. It is noteworthy that the region presents a period referring to the months of October, November and December considered of high productivity in the region, being recorded the highest numerical values of abundance, biomass and production of copepods in this period.

Keywords: copepods; biomass; production of copepoda; coastal ecosystems

5.1.1 Introduction

Estuaries and reefs are among the richest coastal habitats in natural resources and have a relevant ecological role, because they are favorable environments for the life cycle of several species, serving as nurseries, and migration pathways, especially during the breeding season (CHUWEN *et al.*, 2009; FERREIRA *et al.*, 2001; GREGO *et al.*, 2009). These habitats are classified in the highest levels of sensitivity, with protection priorities. Due to this importance, the area where the research was carried out is part of an Environmental Protection Area (EPA), called Costa dos Corais (Tamandaré, Pernambuco - Brazil). Being one of the largest (3000 km) and most important EPAs in Brazilian territory (FERREIRA *et al.*, 2001). In addition, the studied environment was affected by the oil spill that hit the Brazilian coastal zone in late 2019, bringing hazards to the affected coastal habitats and associated organisms (CAMPELO *et al.*, 2021).

In these important habitats, zooplankton play a vital role in the structuring and functioning of the pelagic community. It controls phytoplankton production, provides a food source for higher trophic levels, and it is an important link between the food web and the microbial loop (CALBET; LANDRY, 2004; SHERR; SHERR, 2002). Besides, zooplankton are important in biomonitoring programs, because of the short life cycle, responding quickly to natural and/or anthropogenic environmental variations (GROSS; GROSS, 1996; NEUMANN-LEITÃO *et al.*, 1998).

Since they are dispersed in the water column, the environmental conditions directly influence this community. The temporal and spatial variations of the zooplankton community are subject to several factors, such as the physical and chemical variations of the water column and the continental runoff that, consequently, affects the food resources of this group (AGUILAR, 2013). Changes in these factors can directly affect the abundance and productivity of local species (BEGON; TOWNSEND, 2020). Therefore, investigating this combination of factors helps to understand how organisms respond to changes in the environment.

Among the mesozooplankton organisms ($\geq 200 \mu\text{m}$), copepods (Crustacea) account for more than 70% of the relative abundance and are the main secondary producers in these environments (CHISHOLM; ROFF, 1990; KIORBOE; SABATINI, 1995). Due to this dominance and resilience, copepods can be used as an ecosystem bioindicator reflecting in species abundance, composition and diversity (GROSS; GROSS, 1996; NEUMANN-LEITÃO *et al.*, 1998). These organisms are typically sampled with a plankton net 200 μm mesh size, however, even though it aims to collect organisms $\geq 200 \mu\text{m}$, the plankton net is capable of collecting other size spectra such as the range between 450~1000 μm (HOPCROFF *et al.*, 2001), causing an overestimation of the larger species

(SKJOLDAL *et al.*, 2013). In the study area, researches have been conducted to better understand the distribution of abundance, biomass and productivity of copepods (BRITO-LOLAIA *et al.*, 2020; FARÍAS, 2019; FIDELIS, 2014; FIGUEIRÊDO, 2014), however none of these took into consideration the analysis of size classes and all were done at a single point (reef area).

The sampling program for the present study was conducted after the oil spill reached Tamandaré. In this context, it was considered the magnitude of the impact caused by the oil spill and the importance of the associated ecosystems and biological communities. The main objective of the present study was to investigate the spatial and temporal heterogeneity of the assembly structure of mesozooplankton copepods in coastal habitats.

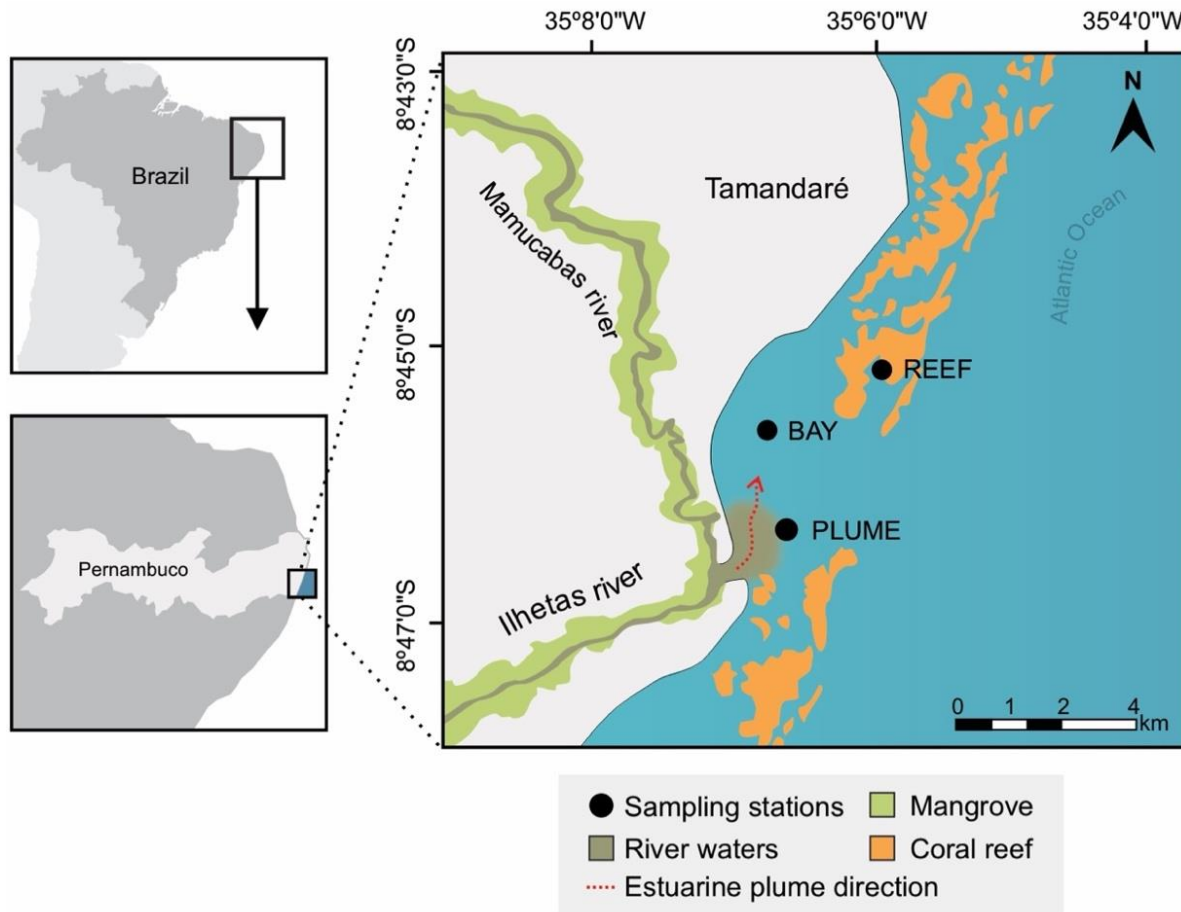
5.1.2 Materials and Methods

5.1.2.1 Study area

The municipality of Tamandaré (southern coast of the state of Pernambuco, Brazil) is located about 110 km from the city of Recife. It has approximately 9 km of coastline that is divided into three areas: Carneiros beach, Campas beach and the Bay of Tamandaré (MAIDA; FERREIRA, 1995). Tamandaré Bay ($08^{\circ}44'$ and $08^{\circ}47'30"S$; $35^{\circ}05'$ and $35^{\circ}07'W$) receives the estuarine influence of three rivers: Ilhetas, Mamucabas and Una. The bay is an open cove, which has an extension of about 4 km^2 in a semicircular shape facing east (average depth 7~10m) (Figure 1) (MOURA, 1991; MOURA; PASSAVANTE, 1993). In the bay a reefline complex divides the open sea from the coastline, constituting a natural "breakwater" (REBOUÇAS, 1966). This reef complex is part of the largest marine conservation unit in Brazil, *Costa dos Corais* Environmental Protection Area (EPA) (FERREIRA *et al.*, 2001).

The region has a coastal climate, warm and humid of type AS', according to the Köppen classification system, characterized by a dry season (September to March) and a rainy season (April to August) (ALVARES *et al.*, 2013). The annual rainfall in the coastal of Pernambuco oscillates between 1.850 and 2.364mm. It presents an average temperature variation of 25°-30°C, and is strongly influenced by the moderate action of the trade winds, which blow from southeast to northeast (MOURA; PASSAVANTE, 1995).

Figure 1 – Sampling stations along the coast of Pernambuco, Brazil. Three sampling stations in the municipality of Tamandaré (estuarine plume, bay, and reef).



Source: The author, 2022.

5.1.2.2 Sampling of environmental variables and plankton

The sampling was carried out in the subsurface layer of the Tamandaré Bay water column (stations: estuarine plume, bay and reef) (Figure 1). A total of 18 samples were collected during daytime ebb tides in February, March, September, October, November, and December 2020. Water samples were collected for chlorophyll-a content. In the laboratory, spectrophotometric analysis was performed for chlorophyll-a estimation according (UNESCO, 1966). The environmental parameters (sea surface temperature - °C, pH, salinity and dissolved oxygen) were measured at surface using a pre-calibrated multiparameter water quality sensor (HORIBA - U50). The rainfall data were obtained from the National Institute of Meteorology data.

Subsurface hauls with a plankton net 200 µm mesh size (mouth diameter 30cm) were performed to collect mesozooplankton (UNESCO, 1968). The hauls were carried out at a speed of 1.5

to 2.5 knots for 3 minutes. A flowmeter was attached to the mouth of the net to estimate the volume of water filtered. Zooplankton samples were preserved immediately in a 4% formaldehyde solution buffered with borax 0.5 g*L⁻¹) (GIFFORD; CARON, 2000; NEWELL; NEWELL, 1963). Polycyclic Aromatic Hydrocarbon (PAH) concentrations for February and November were obtained from water samples, the mean values were provided by OrganoMAR (partner laboratory for chemical analysis).

5.1.2.3 Mesozooplankton analysis

The samples were fractionated into three size classes using a set of sieves with mesh sizes of 1000, 500 and 200 µm (HEAD et al., 1999). Afterwards, the different size classes (200/500µm, 500/1000µm, and >1000µm) were fractionated using a MOTODA type grading equipment for a minimum analysis of 300 copepods (OMORI; IKEDA, 1984). The samples were analyzed in a Bogorov counting chamber under a stereomicroscope. For taxonomic identification, specialized bibliographies were consulted: Bjornberg (1981) and Boltovskoy et al. (2002). Following identification, the copepods were measured using Zen software.

The abundance (ind m⁻³) and relative abundance of copepods (%) were calculated to describe the community structure (copepod species with relative abundance ≥ 2% were considered dominant and used for the multivariate analyses). The Shannon diversity index (H') was applied to estimate the diversity of the assembly (SHANNON, 1948), where the values found indicate: high diversity if H' > 3.0 bits ind⁻¹, medium diversity if 2.0 < H' ≤ 3.0 bits ind⁻¹, low diversity if 1.0 < H' ≤ 2.0 bits ind⁻¹, and very low diversity if H' < 1.0 bits ind⁻¹.

To estimate biomass, a total of 30 individuals of the most abundant taxa were measured considering only the length of the prosoma. Biomass (B, mg C m⁻³) of a given taxon based on its abundance (A, ind m⁻³) and individual carbon weight (CW, mg C): B = A * CW. CW was defined using length-weight regressions available in the literature (Table 1a). The calculation of Production (mg C m⁻³ day⁻¹) was based on its biomass and specific growth rates: Pi = Ci * Bi. Where (Pi) the production of group i, (Ci) growth rate of group i and (Bi) biomass of group i. The growth rate (C) was based on the global model of Hirst et al. (2003) (Adults and juveniles were considered together / Table 1b).

Table 1 – a) Length-weight regressions applied to estimate the biomass of the most abundant copepods. Length data entered in μm ; b) Regression equation for estimating instantaneous growth rate applied to Copepoda.

a) Regression equations for length-weight		
Taxa	Equation	References
<i>Acartia lilljeborgii</i>	$\text{CW} = 6.177 \times 10^{-9} \times L^{3.029}$	Ara (2001)
Oithonidae	$\ln \text{CW} = 1.10 \ln \text{PL} - 7.07$	Chisholm e Roff (1990)
Paracalanidae	$\ln \text{CW} = 2.78 \ln \text{PL} - 16.52$	Webber e Roff (1995)
<i>Labidocera</i> spp.	$\text{CW} = 1.666 \times 10^{-8} \times TL^{2.837}$	Ara (2001)
Harpacticoida	$\log \text{CW} (\mu\text{g}) = -8.51 + 3.26 \times \log \text{TL}$	Hirota (1986)
Nauplii (Copepod)	$\ln \text{AFDW} = 2.48 \ln \text{TL} - 15.7$	Båmstedt <i>et al.</i> (1986)

b) Regression equations for growth rate		
Taxa	Equation	Reference
Copepoda	$\log_{10} \text{C} = 0.0186 \times T - 0.288 \times \log_{10}(\text{CW}) + 0.417 \times \log_{10}(\text{Cl}) - 1.209$	Hirst e Bunker (2003)

CW, Carbon weight; PL, Prossome length; TL, Total length; C, Carbon; Cl, Chlorophyll-a; T, Temperature

Source: The author, 2022.

5.1.2.4 Statistical analyses

The information related to the dependent variables: abundance (ind m^{-3}), biomass (mg C m^{-3}) and production ($\text{mg C m}^{-3} \text{ d}^{-1}$) of planktonic copepods, were statistically tested from routines developed in mathematical software. Analysis of variance (ANOVA) was used to analyze the first-order (non-interacting) effects of multiple independent variables: spatial (estuarine Plume vs. bay vs. reef), Temporal (months vs. months) and size class (200/500 μm vs. 500/1000 μm vs. >1000 μm). Heterogeneity of variances was investigated with Levene's test and normality of the data was investigated by Kolmogorov-Smirnov test. When necessary, the data were $\text{Log}(X+1)$ transformed. Once significance was verified ($P < 0.05$), the Tukey-HSD (post-hoc) test was applied.

The structure of the copepod assemblage was investigated using multivariate analyses. Permutational analysis of variance (PERMANOVA) was applied to test the hypothesis that copepod assemblage structure varies in response to the spatial and size class factors tested (the temporal factor was left out of the multivariate analyses due to unbalance and because all samples were from a single period). In the case of significant differences, a paired test was performed between different levels of significant factor(s). To identify patterns of similarity between the samples and therefore possible changes in copepod distribution, multidimensional scaling (MDS) was used to represent them graphically.

Both PERMANOVA and MDS were based on a Bray-Curtis similarity matrix constructed from the Log(X+1) of the abundance of transformed species with relative abundance $\geq 2\%$. Percentage of Similarity (SIMPER) analysis was performed to identify representative taxa/species and their contributions to dissimilarity. Principal component analysis (PCA) was also calculated using the data and standardized environmental parameters and Copepoda species to assess the associations between them.

5.1.3 Results

5.1.3.1 Environmental variables and phytoplanktonic biomass (chlorophyll-a)

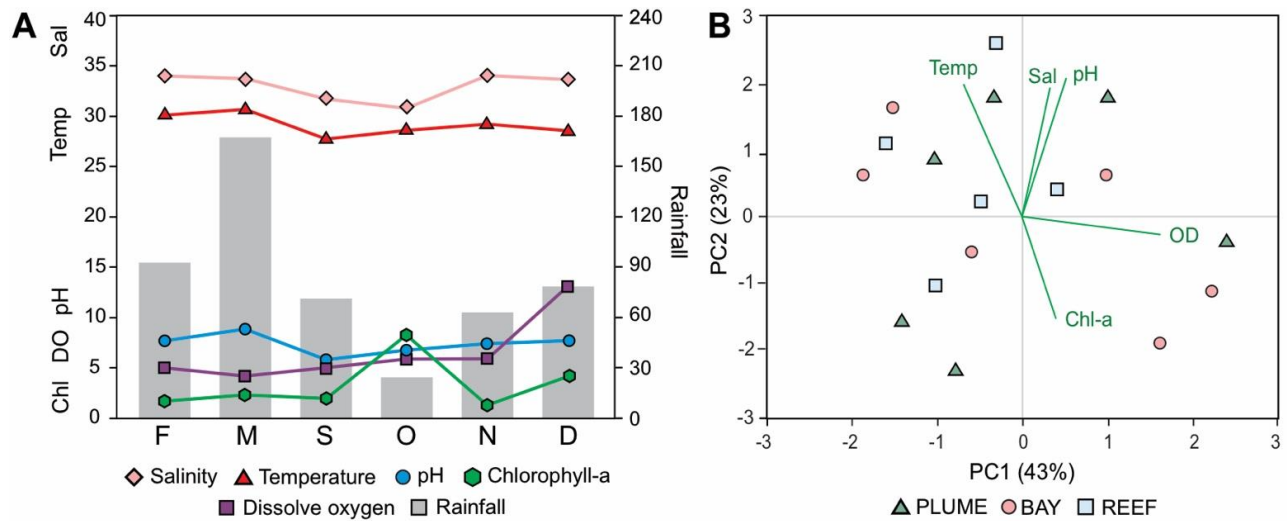
The temporal and spatial effect was not identified on the abiotic variables investigated. The rainfall values obtained from the National Institute of Meteorology data can be observed in Figure 2a, where March recorded the highest cumulative value (171mm). The sea surface temperature ranged from 31.27°C (March - plume) to 27.3°C (December - bay) (Figure 2a). Between stations, the mean values recorded were $29.4 \pm 1.4^\circ\text{C}$, $29.2 \pm 1.2^\circ\text{C}$ and $29.5 \pm 1.0^\circ\text{C}$, in the estuarine plume, bay and reef, respectively.

Salinity ranged from 33.0 (March - plume) to 35.1 (November - bay) (Figure 2a). A salinity gradient towards the Reef was recorded, however, statistical differences were not significant. The estuarine plume recorded a mean salinity equivalent to 31.7 ± 2.9 , the bay 34.1 ± 1.1 and the reef 34.3 ± 0.4 . The pH ranged from 5.7 (September - plume) to 8.8 (March - bay) (Figure 2a). The estuarine plume recorded an average pH of 7.3 ± 1.3 , bay 7.7 ± 0.5 and the reef 7.5 ± 1.3 . Dissolved oxygen values ranged from 3.1mg L^{-1} (October - reef) to 19.0 mg L^{-1} (December - plume) (Figure 2a). Mean DO range from: $6.2 \pm 3.5\text{mg L}^{-1}$, $7.6 \pm 5.7\text{mgL}^{-1}$ and $6.2 \pm 2.2\text{ mg L}^{-1}$, in the estuarine plume, bay and reef, respectively.

Chlorophyll-a concentration showed values ranging from 0.15 mg m^{-3} at the reef station to 16.96 mg m^{-3} at the estuarine plume station, both in October 2020. ANOVA main effects analysis identified spatial differences for phytoplankton biomass ($p = 0.04$), where the Estuarine plume area showed a mean phytoplankton biomass of $6.6 \pm 5.9\text{ mg m}^{-3}$, significantly higher (Tukey HSD, $p = 0.04$) than the reef station $0.6 \pm 0.4\text{ mg m}^{-3}$. The mean recorded for the bay was $2.7 \pm 1.0\text{ mg m}^{-3}$. Temporally, statistical differences were not identified, but the mean phytoplankton biomasses were $1.9 \pm 1.2\text{ mg m}^{-3}$; $1.9 \pm 1.2\text{ mg m}^{-3}$; $2.1 \pm 1.7\text{ mg m}^{-3}$; $7.0 \pm 8.8\text{ mg m}^{-3}$; $1.5 \pm 0.4\text{ mg m}^{-3}$ and 4.4 ± 5.2

mg m^{-3} were recorded in February, March, September, October, November and December, respectively.

Figure 2 – Distribution of abiotic data in Tamandaré: (A) Temporal variation of mean values of environmental variables; (B) Results of principal component analysis (PCA) of environmental variables (Temp = temperature, pH, DO = dissolved oxygen, Sal = salinity and Chl-a = Chlorophyll-a) in green; Stations: Estuarine Plume - green triangle, Bay - pink circle and Reef - blue square.



Source: The author, 2022.

Principal component analysis applied to the environmental variable data explained 66% of the data variation in the first two axes (Figure 2b). Axis 1 accounted for 43%, while Axis 2 explained 23% of the data variation. There was no clustering among stations and months, however, it was observed that temperature, salinity and pH explained the distribution of data in most samples.

5.1.3.2 Composition and abundance of the copepod assemblage

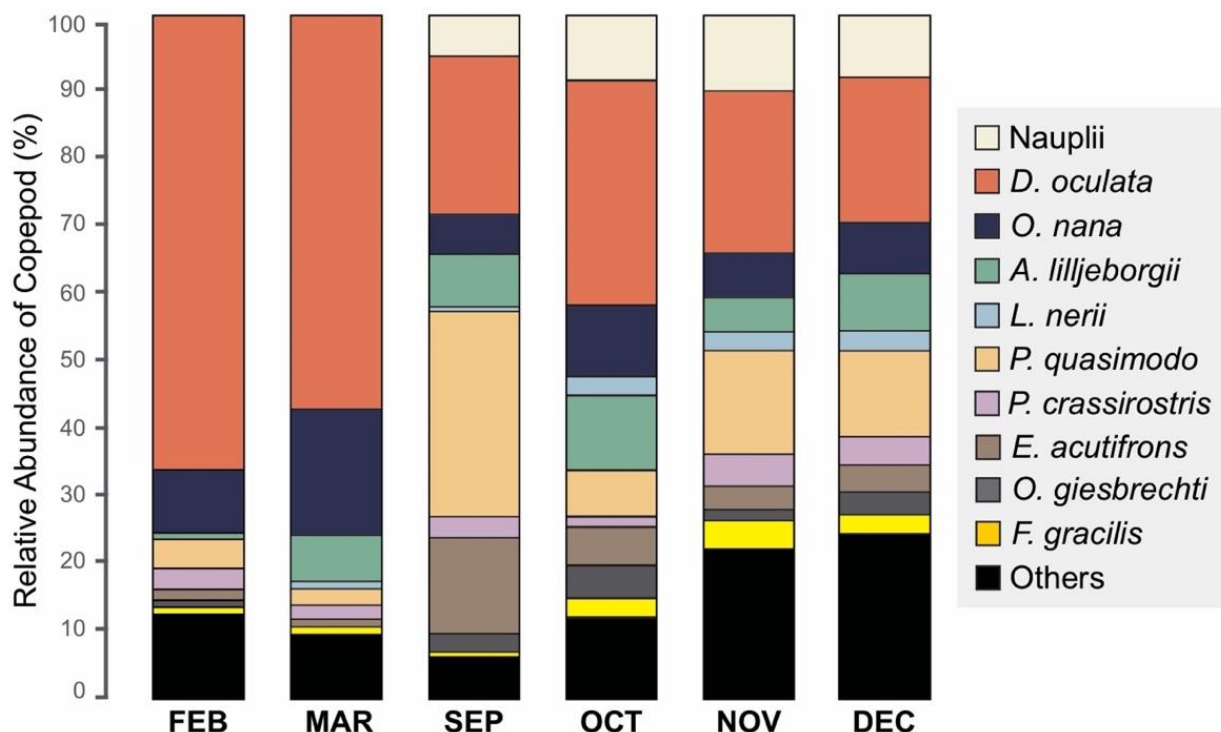
A total of 38 taxonomic groups contributed to the total abundance in the studied area with the orders Calanoida (24), Polyarthra (1), Cyclopoida (9) and Harpacticoida (4) (Table 2). Among the 38 taxa identified, 10 were considered dominant and these represented 87% of the overall relative abundance (Figure 3).

In Figure 3 it is possible to observe the temporal variation of these taxa, where *D. oculata* dominated in the first two months of the study, equivalent to 67.1% and 58.4% of all relative abundance in February and March, respectively. The important contribution of *P. quasiomodo* also stands out, where in September it reached 30.4% and in the other months it was below this value, but

values above other species (5.0% February, 2.8% March, 7.3% October, 16.5% November and 14.3% December). The species *A. lilljeborgii* did not reach such high values when compared to *D. oculata* and *P. quasimodo*, but recorded equivalent values (7.1% March, 8.3% September, 12.1% October, 6.7% November, and 9.9% December), with the exception of February, which had a low relative abundance (0.3%).

The values of copepod mean abundances among the study months were: 92.7 ± 386.7 ind m^{-3} February, 86.2 ± 326.6 ind m^{-3} March, 38.4 ± 96.1 ind m^{-3} September, 49.2 ± 112.5 ind m^{-3} October, 82.6 ± 158.5 ind m^{-3} November and 209.1 ± 360.1 ind m^{-3} December, besides that, no significant differences among abundances were identified. Despite not registering statistical differences, it was possible to observe an increase in abundance in the last two months of the year (Figure 5a). The mean abundance values among stations were: 207.8 ± 531.1 ind m^{-3} , 203.8 ± 415.9 ind m^{-3} and 146.7 ± 425.5 ind m^{-3} respectively recorded in estuarine plume, bay and reef, however, no significant differences were identified either (Figure 5b).

Figure 3 – Temporal variation of total relative abundance (%) of the Copepoda assemblage in Tamandaré, Brazil.



Source: The author, 2022.

Table 2 – Relative abundance (%) and abundance (mean \pm standard deviation) of taxa recorded in the mesozooplankton copepod assemblage in the estuarine plume, bay and reef (Tamandaré, Brazil) in the dry season of 2020.

Taxa	RA% Genera	Estuarine plume		Bay		Reef	
		RA%	ind m ⁻³	RA%	ind m ⁻³	RA%	ind m ⁻³
Copepoda nauplii	6.3	7.1	140.1 \pm 200.5	5.3	101.8 \pm 95.2	6.4	90.1 \pm 45.5
<i>Acartia lilljeborgii</i>	7.6	6.8	33.4 \pm 72.5	8.0	38.6 \pm 102.6	8.2	26.8 \pm 49.5
<i>Undinula vulgaris</i>	1.0	>0.1	0.4 \pm 0.3	2.3	16.0 \pm 34.6	0.5	6.0 \pm 6.3
<i>Calocalanus pavo</i>	0.5	0.4	6.0 \pm 12.0	1.0	40.1 \pm 38.4		
<i>Dioithona oculata</i>	36.3	39.9	525.1 \pm 515.0	26.4	341.0 \pm 241.6	44.9	416.9 \pm 330.0
<i>Oithona nana</i>	9.8	8.2	130.0 \pm 96.6	7.4	95.109.1	15.3	142.2 \pm 128.6
<i>Oithona similis</i>	>0.1	>0.1	0.8 \pm 1.7				
<i>Oithona oswaldoocruzi</i>	0.3	0.4	8.9 \pm 9.3	0.2	8.1 \pm 2.1	0.1	2.1 \pm 0.3
<i>Oithona simplex</i>	>0.1	>0.1	0.5 \pm 1.0	>0.1	0.2 \pm 0.4	0.1	0.5 \pm 1.1
<i>Temora stylifera</i>	0.9	1.8	23.9 \pm 34.6	0.4	14.7 \pm 16.6	0.4	8.4 \pm 5.2
<i>Paracalanus quasimodo</i>	11.8	10.6	140.1 \pm 138.0	19.0	245.1 \pm 289.2	3.6	33.5 \pm 14.0
<i>Clausocalanus furcatus</i>	0.1	0.1	2.3 \pm 5.0				
<i>Euterpinina acutifrons</i>	4.0	5.4	38.7 \pm 67.2	4.5	70.0 \pm 47.1	1.5	10.2 \pm 12.2
<i>Farranula gracilis</i>	2.0	2.0	12.9 \pm 20.9	2.1	14.5 \pm 26.5	1.9	11.6 \pm 8.9
<i>Onychocorycaeus giesbrechti</i>	2.2	1.1	8.9 \pm 18.9	3.9	37.5 \pm 76.9	1.5	11.8 \pm 12.9
<i>Corycaeus speciosus</i>	0.1	>0.1	0.2 \pm 0.2	0.2	2.3 \pm 3.7	>0.1	0.3 \pm 0.8
<i>Corycaeus amazonicus</i>	0.2	0.5	6.2 \pm 7.5				
<i>Centropages velificatus</i>	0.4	0.6	4.7 \pm 7.1	0.2	2.6 \pm 3.3	0.2	1.6 \pm 2.1
<i>Paracalanus crassirostris</i>	3.0	1.7	27.3 \pm 42.0	5.0	96.8 \pm 104.8	2.1	23.1 \pm 14.4
<i>Pontella</i> spp.	0.1	>0.1	0.1 \pm 0.1	0.2	5.3 \pm 3.9	>0.1	0.8 \pm 1.0
<i>Labidocera fluviatilis</i>	0.2	0.3	2.8 \pm 2.2	0.1	1.0 \pm 0.9	0.1	2.2 \pm 1.2
<i>Labidocera nerii</i>	2.1	2.7	35.3 \pm 64.1	1.0	6.8.1	2.7	21.8 \pm 23.1
<i>Lucicutia flavigaster</i>	0.1	0.2	5.2 \pm 7.4	0.1	5.1 \pm 6.3		
<i>Calanopia americana</i>	0.3	0.1	3.1 \pm 3.9	0.2	1.8 \pm 5.5	0.8	6.1 \pm 17.9
<i>Pseudodiaptomus</i> spp.	0.2	0.0	0.1 \pm 0.2	0.6	16.4 \pm 27.4	0.1	1.0 \pm 1.2
<i>Paracalanidae</i>	>0.1					0.2	2.1 \pm 5.1
<i>Longipedia coronata</i>	>0.1					>0.1	0.1 \pm 0.1

Continuation of Table 2...

<i>Pseudodiaptomus acutus</i>	>0.1	0.2	2.6 ± 2.6	0.1	1.6 ± 3.6	0.1	0.2 ± 0.6
<i>Clytemnestra rostrata</i>	0.2	0.1	1.4 ± 2.5	0.0	0.9 ± 0.8	0.5	5.7 ± 7.2
<i>Miracia efferata</i>	1.2	2.1	28.1 ± 60.4	0.6	7.15.3	0.6	8.5 ± 15.7
<i>Macrosetella gracilis</i>	0.1	0.1	1.4 ± 2.7	0.0	0.6 ± 0.0		
Copepodites:							
Calanidae	0.9	1.4	37.1 ± 62.1	0.3	12.3 ± 3.3	1.1	20.9 ± 18.2
<i>Temora</i>	0.1	0.2	4.7 ± 9.4				
<i>Centropages</i>	>0.1	0.1	1.4 ± 2.0	0.0	0.4 ± 0.9	0.1	0.1 ± 0.1
Paracalanus	>0.1			0.1	1.6 ± 3.5	0.1	0.5 ± 1.1
<i>Acartia</i>	3.4	1.2	18.6 ± 25.7	5.8	90.5 ± 128.5	3.3	26.4 ± 30.9
<i>Labidocera</i>	2.8	0.7	10.4 ± 8.0	4.3	110.6 ± 94.6	3.7	41.5 ± 35.9

Source: The author, 2022.

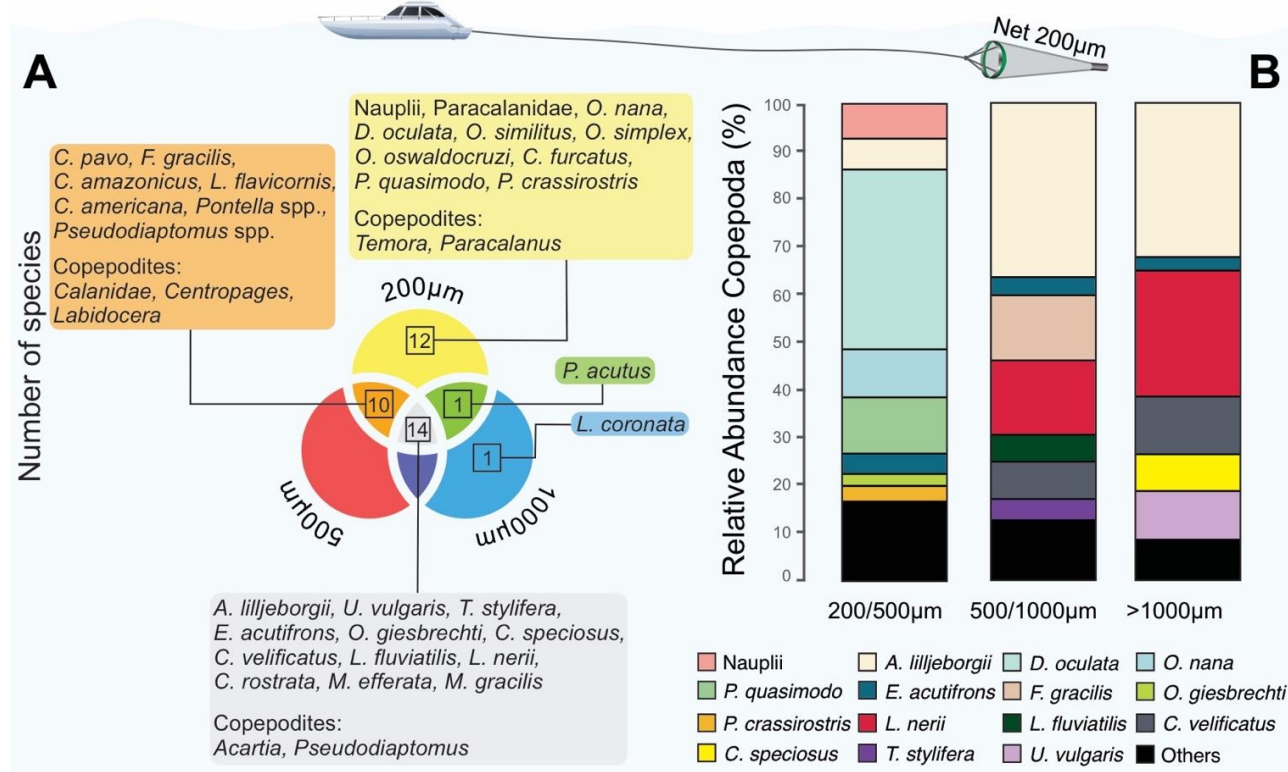
5.1.3.3 Composition of the copepod assemblage by size class

The Vann diagram showed that the number of copepod species (14) was highest at the intercession between the three size classes, occurring in all three spectra (Figure 4a). Twelve species (all small-sized, including juvenile stages) were retained in the smallest size class (200 µm) (Figure 4a). Ten species remained in the 200~500 µm intercession, these were medium-sized species and juvenile stages of large species (Figure 4a). One species was in the 200-1000 µm intercession (Figure 4a). Only one species occurred exclusively in the largest size class (1000 µm) (Figure 4a).

A total of eight, seven and six taxa were considered dominant in the 200-500µm, 500-1000µm and > 1000µm fractions, representing 81.8%, 86.1% and 89.8% of the total abundance of the copepod assemblage, respectively (Figure 4b). We emphasized the important contribution of the small-sized species (<1.5mm) *D. oculata* in the 200-500µm fraction (37%) and the medium-sized species *A. lilljeborgii* for the 500-1000µm (36.5%) and >1000µm (32%) fractions.

Statistically significant differences were identified (Kruskall-Wallis, $p = 0.0000$), where the 200/500 µm size class showed significantly higher mean copepod abundance (524.1 ± 1312.7 ind m^{-3}) ($p = 0.0001$) than that recorded in the 500/1000µm (9.1 ± 28.9 ind m^{-3}) ($p = 0.0001$) and >1000µm (0.9 ± 2.6 ind m^{-3}) ($p = 0.0001$) classes (Figure 5c).

Figure 4 – Composition of the Copepoda assembly by size class: (A) Venn diagram based on the number of species among size fractions; (B) Relative abundance (%) of Copepoda assemblage by size fraction in Tamandaré, Brazil.



Source: The author, 2022.

5.1.3.4 Biomass and secondary production

The total biomass (most abundant species) recorded in the area was 8.3 mg C m^{-3} , ranging from 0.6 mg C m^{-3} (September and October, reef respectively) to 3.2 mg C m^{-3} (December - plume). As with abundance, an increase in total copepod biomass was observed in the last three months (0.6 mg C m^{-3} October, 1.1 mg C m^{-3} November and 3.2 mg C m^{-3} December). Among the stations, the estuarine plume (3.1 mg C m^{-3}) and the bay (3.4 mg C m^{-3}) showed the highest values of total biomass and the reef (1.8 mg C m^{-3}) the lowest.

No statistics differences were identified between study months (Figure 5d), however, the mean copepod biomass recorded for February was equivalent to $0.13 \pm 0.27 \text{ mg C m}^{-3}$; March $0.13 \pm 0.18 \text{ mg C m}^{-2}$; September and October $0.06 \pm 0.08 \text{ mg C m}^{-3}$; November $0.11 \pm 0.08 \text{ mg C m}^{-3}$ and December $0.32 \pm 0.26 \text{ mg C m}^{-3}$. Among the sampling stations, the average biomass was $0.31 \pm 0.30 \text{ mg C m}^{-2}$ in the estuarine plume, $0.33 \pm 0.30 \text{ mg C m}^{-3}$ in the bay, and $0.17 \pm 0.20 \text{ mg C m}^{-3}$ in the reef, besides that, no statistical differences were recorded (Figure 5e).

Among size classes, the mean biomass was $0.77 \pm 0.71 \text{ mg C m}^{-3}$ 200/500 μm , $0.04 \pm 0.09 \text{ mg C m}^{-3}$ 500/1000 μm and $0.01 \pm 0.03 \text{ mg C m}^{-3}$ $>1000\mu\text{m}$. The effect of size was recorded on copepod biomass (Kruskal-Wallis, $p = 0.000$), where values recorded for the 200/500 μm class were significantly higher than that recorded for the 500/1000 μm and $>1000\mu\text{m}$ classes (Multiple comparisons a posteriori test: 200/500 μm vs. 500/1000 μm , $p = 0.0004$; 200/500 μm vs. $>1000\mu\text{m}$, $p = 0.0000$) (Figure 5f).

The species that had the highest contribution in total biomass/overall mean of the assembly were: *D. oculata*, *P. quasimodo*, *A. lilljeborgii*, *E. acutifrons* and *P. crassirostris* (Table 3). Among the months, in terms of total biomass, we can observe that *D. oculata*, *P. quasimodo* and *A. lilljeborgii* were the species that had the highest contributions of total biomass of the assembly (Figure 6a). *D. oculata* reached the highest values in February, March, and December. *A. lilljeborgii* in March and December. *P. quasimodo* in November and had a significant increase in December (Figure 6a).

Spatially, in terms of total biomass, in the estuarine plume we highlighted the species *D. oculata*, *P. quasimodo*, *A. lilljeborgii* and *E. acutifrons*. For the bay station we highlighted the species *P. quasimodo* and *D. oculata* and in the reef only the species *D. oculata* (Figure 6b). Among the size classes, all species had their highest values in the 200/500 μm size class, where the species *D. oculata* and *P. quasimodo* were the species that most contributed in this size class. In the 500/1000 μm size class, *A. lilljeborgii* and *L. nerii* most contributed, and these same species contributed the $>1000\mu\text{m}$ size class (Figure 6c).

Table 3 – Biomass (total and mean \pm SD, mg C m^{-3}) and Production (total and mean SD, $\text{mg C m}^{-3} \text{ d}^{-1}$) of the most abundant taxonomic groups of the Copepoda from Tamandaré, Brazil.

Taxa	Biomass		Production	
	Total	Mean \pm SD	Total	Mean \pm SD
Copepoda nauplii	0.17	0.01 ± 0.02	-	-
<i>Dioithona oculata</i>	2.35	0.13 ± 0.12	5.94	0.99 ± 0.82
<i>Oithona nana</i>	0.58	0.03 ± 0.03	1.47	0.24 ± 0.18
<i>Acartia lilljeborgii</i>	1.05	0.04 ± 0.03	2.52	0.42 ± 0.40
<i>Labidocera nerii</i>	0.25	0.01 ± 0.01	0.61	0.10 ± 0.11
<i>Paracalanus quasimodo</i>	1.73	0.09 ± 0.16	4.17	0.70 ± 0.83
<i>Parvocalanus crassirostris</i>	0.55	0.03 ± 0.05	1.32	0.22 ± 0.22
<i>Euterpina acutifrons</i>	0.82	0.03 ± 0.05	1.92	0.32 ± 0.30
<i>Onychocorycaeus giesbrechti</i>	0.42	0.02 ± 0.04	0.98	0.16 ± 0.16
<i>Farranula gracilis</i>	0.32	0.01 ± 0.01	0.78	0.13 ± 0.11

The total production (most abundant species) recorded in the area was $20.2 \text{ mg C m}^{-3} \text{ d}^{-1}$ and ranged from $1.3 \text{ mg C m}^{-3} \text{ d}^{-1}$ (September - reef) to $7.9 \text{ mg C m}^{-3} \text{ d}^{-1}$ (December - plume). The first two months of the study showed similar production: $3.3 \text{ mg C m}^{-3} \text{ d}^{-1}$ February and $3.5 \text{ mg C m}^{-3} \text{ d}^{-1}$ March. Like the total biomass of copepods, an increasing production was observed in the last three months ($1.4 \text{ mg C m}^{-3} \text{ d}^{-1}$ October, $2.6 \text{ mg C m}^{-3} \text{ d}^{-1}$ November and $7.9 \text{ mg C m}^{-3} \text{ d}^{-1}$ December). Among the stations, an estuarine plume ($7.9 \text{ mg C m}^{-3} \text{ d}^{-1}$) and the bay ($8.3 \text{ mg C m}^{-3} \text{ d}^{-1}$) showed the high values and the reef ($3.9 \text{ mg C m}^{-3} \text{ d}^{-1}$) a low value.

Temporal effect was not recorded on the average copepod production in the study region (Figure 5g), however, the average production recorded in February was $0.33 \pm 0.67 \text{ mg C m}^{-3} \text{ d}^{-1}$; March $0.35 \pm 0.50 \text{ mg C m}^{-3} \text{ d}^{-1}$; September $0.13 \pm 0.17 \text{ mg C m}^{-3} \text{ d}^{-1}$; October $0.14 \pm 0.09 \text{ mg C m}^{-3} \text{ d}^{-1}$; November $0.25 \pm 0.19 \text{ mg C m}^{-3} \text{ d}^{-1}$ and December $0.80 \pm 0.64 \text{ m}^{-3} \text{ d}^{-1}$. Spatial effect was also not observed on the mean copepod production, but values of $0.79 \pm 0.79 \text{ mg C m}^{-3} \text{ d}^{-1}$; $0.83 \pm 0.73 \text{ mg C m}^{-3} \text{ d}^{-1}$ and $0.39 \pm 0.47 \text{ mg C m}^{-3} \text{ d}^{-1}$ were respectively recorded in the estuarine plume, bay and reef (Figure 5h).

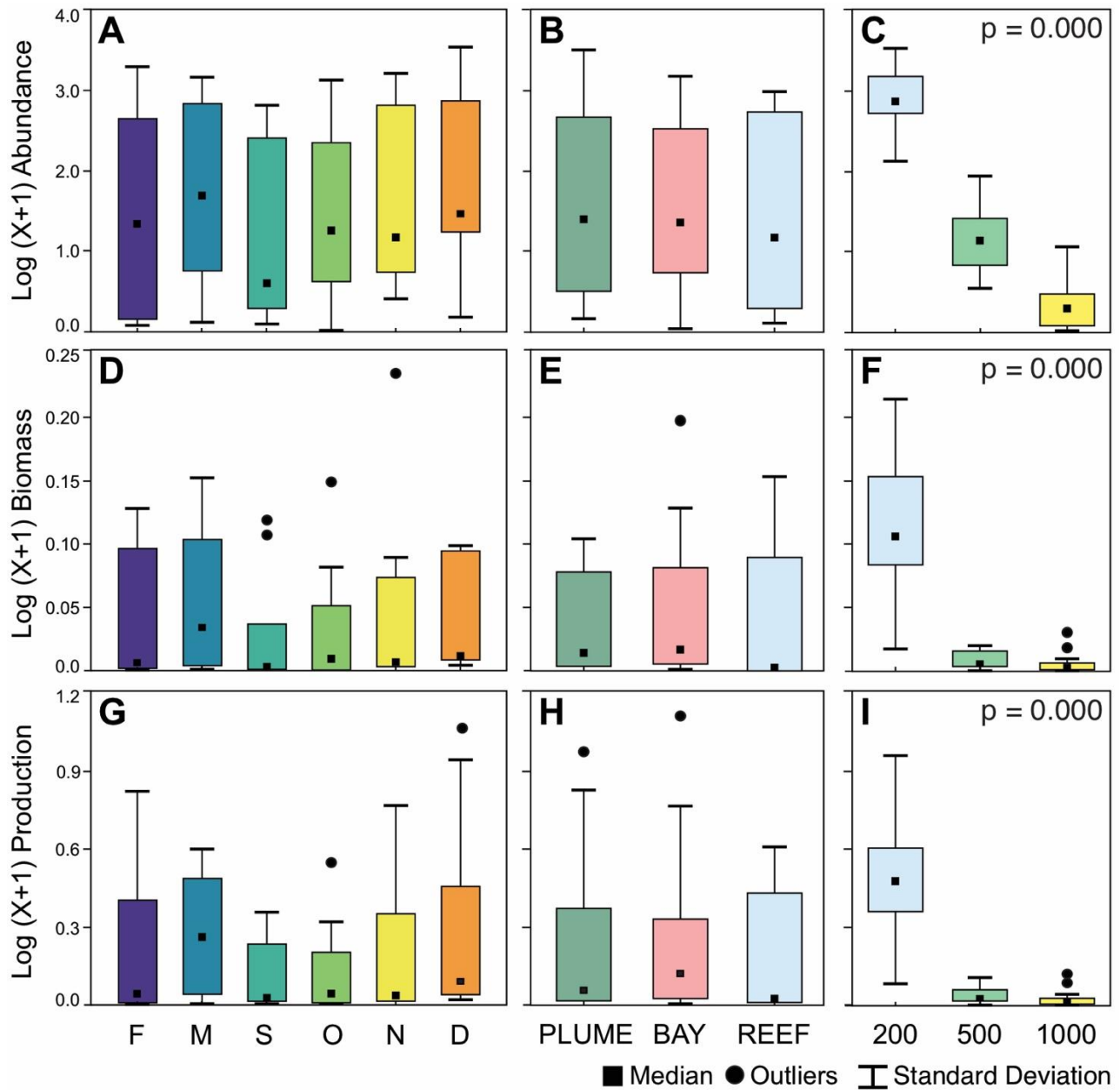
Among the size classes, the average production was $1.89 \pm 1.79 \text{ mg C m}^{-3} \text{ d}^{-1}$ $200/500 \mu\text{m}$, $0.10 \pm 0.22 \text{ mg C m}^{-3} \text{ d}^{-1}$ $500/1000 \mu\text{m}$ and $0.02 \pm 0.04 \text{ mg C m}^{-3} \text{ d}^{-1}$ $>1000 \mu\text{m}$. Size classes statistical differences was recorded on copepod production (Kruskal-Wallis, $p = 0.000$), where values recorded for the $200/500 \mu\text{m}$ class were higher than those recorded for the $500/1000 \mu\text{m}$ and $>1000 \mu\text{m}$ classes (Multiple comparisons a posteriori test: $200/500\mu\text{m}$ vs. $500/1000 \mu\text{m}$, $p = 0.0004$; $200/500 \mu\text{m}$ vs. $>1000 \mu\text{m}$, $p = 0.000$) (Figure 5i).

The species with the highest contribution to total production/overall average were: *D. oculata*, *P. quasimodo* and *A. lilljeborgii* (Table 3). Among the months, in terms of total production, *D. oculata* was most productive in February, March and December. *P. quasimodo* reached the highest values in November and December. *A. lilljeborgii* in March and December (Figure 6e).

Among the stations, in terms of total production, in the estuarine plume we highlighted the species *D. oculata*, *P. quasimodo*, *A. lilljeborgii* and *E. acutifrons*. For the bay station we highlighted the species *P. quasimodo* and *D. oculata* and for the reef station the species that most contributed was *D. oculata* (Figure 6f).

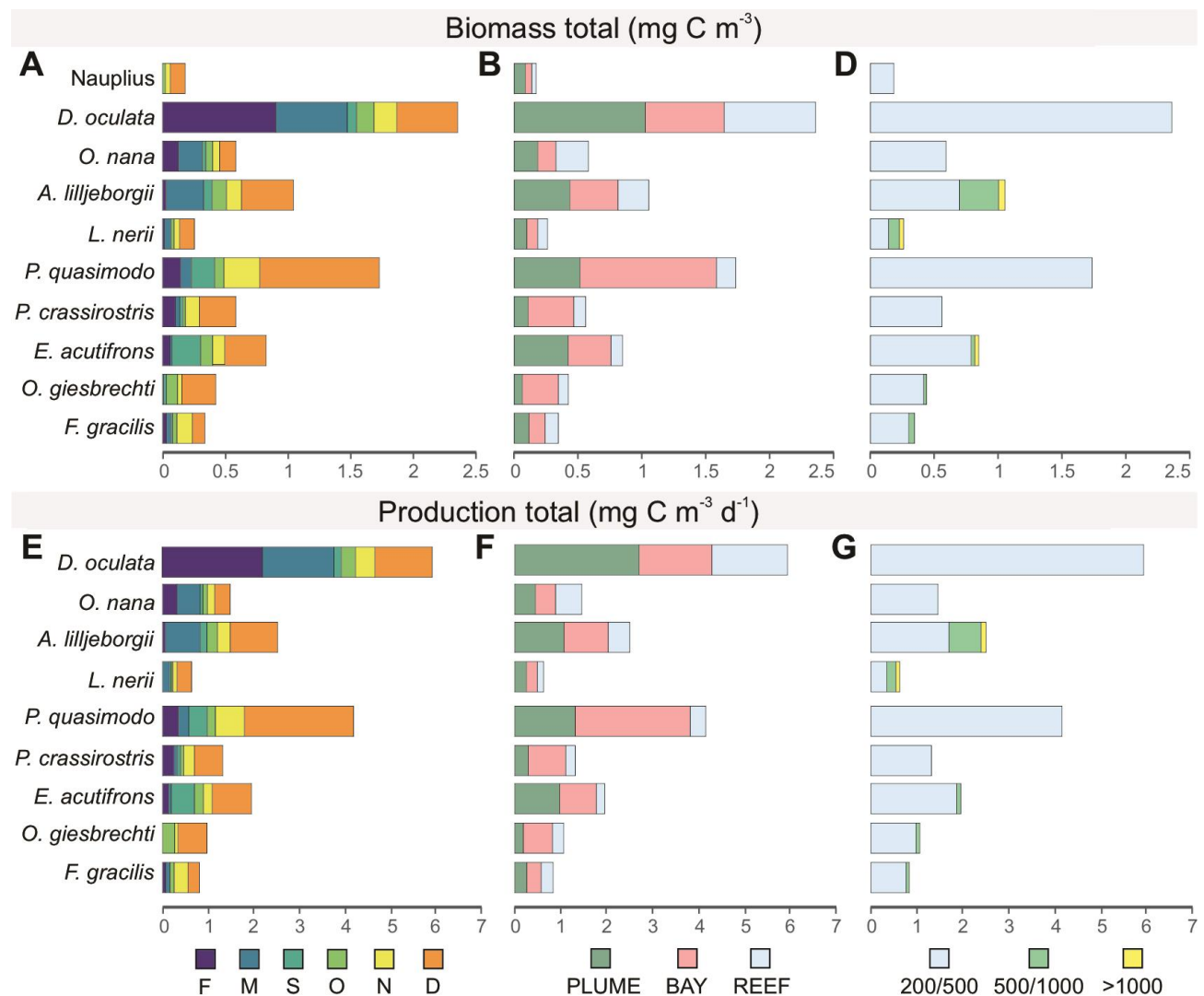
Between size classes, in terms of total production per specific contribution, as well as abundance and biomass, most species had their highest values in the $200/500 \mu\text{m}$ size class (Most contributed: *D. oculata*, *P. quasimodo* and *A. lilljeborgii*). In the $500/1000 \mu\text{m}$ class the medium/large size species *A. lilljeborgii* and *L. nerii* were most productive, and these same species contributed in the $>1000 \mu\text{m}$ class (Figure 6g).

Figure 5 – Box-Plot (median and quartiles) representing the Log(X+1) of abundance, biomass and production of the Copepoda assembly by: **Abundance:** (A) Temporal, (B) Spatial: Estuarine Plume, Bay and Reef and (C) Size fraction: 200/500 μm , 500/1000 μm and >1000 μm . **Biomass:** (D) Temporal, (E) Spatial and (F) Size fraction. **Production:** (G) Temporal, (H) Spatial and (I) Size classes. Samples collected with 200 μm mesh in 2020 in Tamandaré, Brazil.



Source: The author, 2022.

Figure 6 – Biomass variation (mg C m^{-3}) and production ($\text{mg C m}^{-3} \text{ d}^{-1}$) of Copepoda species by: Temporal (A - E), spatial (B - F) and size class (C - G) in Tamandaré, northeast Brazil.

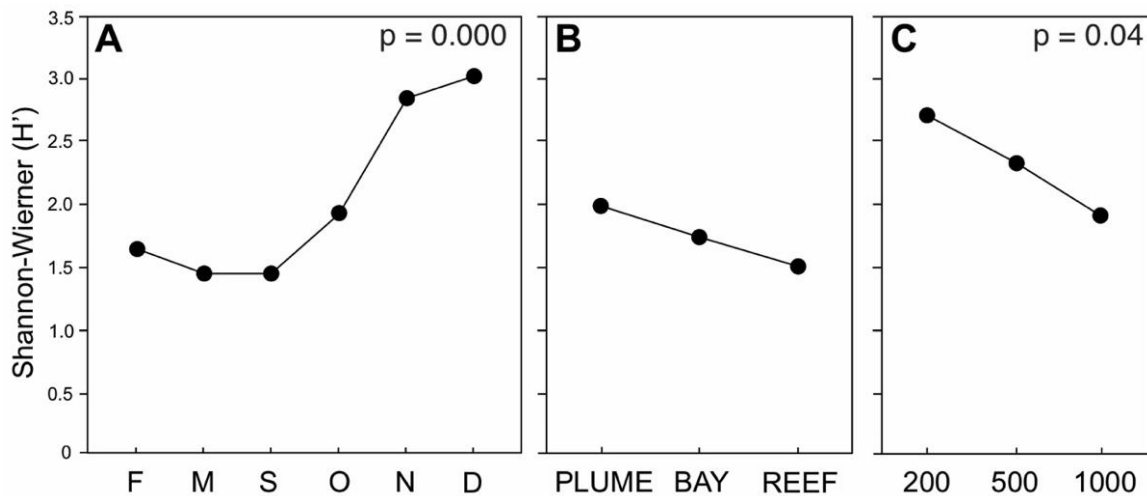


Source: The author, 2022.

5.1.3.4 Diversity

The mean values of the Shannon-Wiener species diversity index (H') observed in the coastal region of Tamandaré on the tested factors (spatial, temporal and size class), indicate low taxonomic diversity in the first three months (1.6 ± 0.6 bits ind^{-1} February, 1.3 ± 0.5 bits ind^{-1} March and 1.3 ± 0.9 bits ind^{-1} September) of study and high in the other three subsequent months (1.9 ± 1.1 bits ind^{-1} October, 2.6 ± 0.4 bits ind^{-1} November and 3.1 ± 0.4 bits ind^{-1} December). The temporal factor showed a statistically significant difference (ANOVA, $p = 0.0001$), where diversity recorded in December and November were higher than those in the other months (Tukey HSD, $p = 0.0006$) (Figure 7a).

Figure 7 – Average values of the Shannon diversity index (H') in Tamandaré: (A) Temporal variation; (B) Spatial variation; (C) Variation by size class.



Source: The author, 2022.

In spatial terms it was possible to observe a numerical gradient between the means of the analyzed stations: Estuarine plume (2.5 ± 0.9 bits ind^{-1}) → Bay (2.0 ± 0.9 bits ind^{-1}) → Reef (1.6 ± 0.8 bits ind^{-1}), but no significant differences were recorded (Figure 7b). Numerically the estuarine plume showed the highest mean diversity scores. Regarding size classes, all classes had the following mean diversity values: 200/500μm 2.3 ± 0.6 bits ind^{-1} , 500/1000μm 2.1 ± 1.7 bits ind^{-1} and >1000μm 1.6 ± 0.7 bits ind^{-1} (Figure 7c) and significant differences were identified (ANOVA, $p = 0.04$). Where the mean diversity value observed in the >1000 μm size class was lower than that recorded for the 200/500 μm class (Tukey HSD, $p = 0.03$).

5.1.3.6 Structure of the copepod assemblage

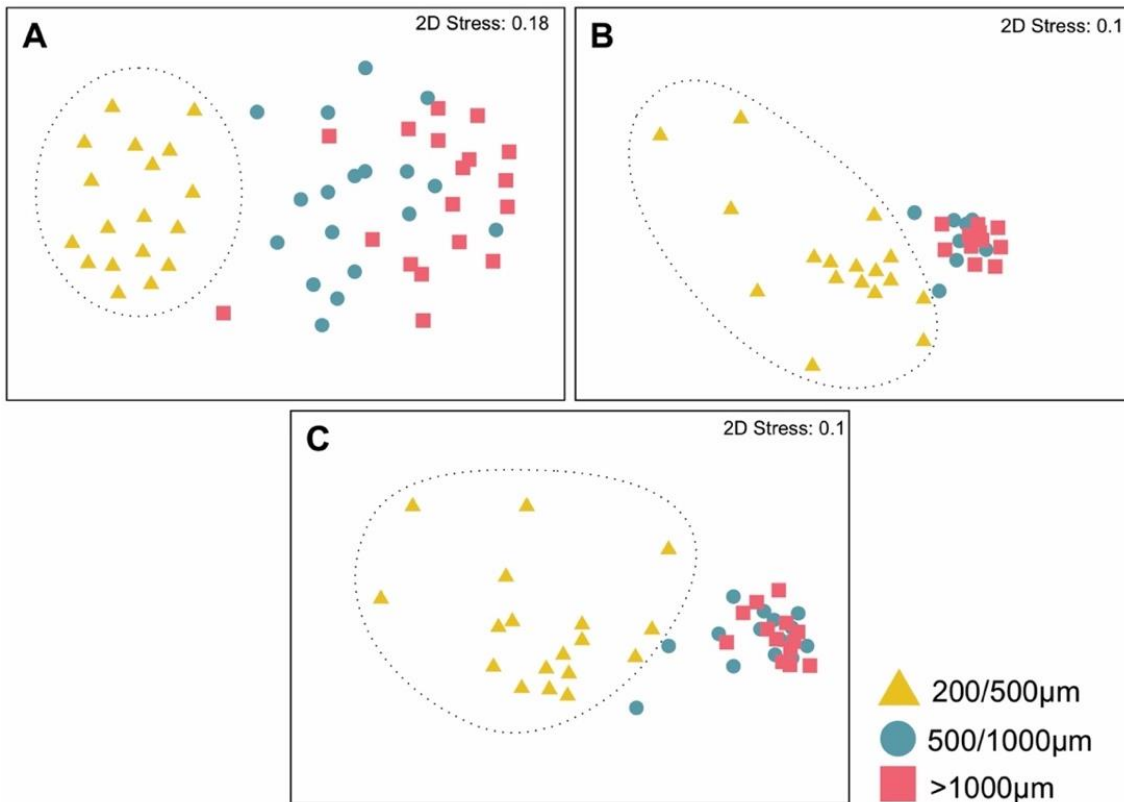
PERMANOVA was applied on abundance, biomass and production over spatial and size class factors. The analysis identified differences in community structure (abundance, biomass and production) only in relation to size class ($P(\text{perm}) = 0.001 / P(\text{MC}) = 0.001$), reinforcing the results of the descriptive statistics (Table 4). Paired tests for the size class factor (abundance, biomass, and production) showed that the three classes (200/500 μm vs. 500/1000 μm vs. >1000 μm) differed significantly from each other in the taxonomic composition of the copepod assembly. The MDS graphically represents the differences recorded by PERMANOVA in copepod assembly structure in response to the size class factor (abundance, biomass and production) (Figure 8).

Table 4 – PERMANOVA analysis for the most abundant taxa (>2%) based on the abundance, biomass and production of the copepod assemblage structure in relation to the factors Size class and Spatial. P(perm) = P-value permutational e P(MC) = P-value Monte Carlo.

PERMANOVA	df	MS	Pseudo-F	P (perm)	P(MC)
Abundance					
Size Class	2	140.35	52.909	0.001	0.001
Spatial	2	11363	0.6535	0.59	0.828
Size class x Spatial	4	214.77	0.8052	0.56	0.454
Biomass					
Size Class	2	903.06	33.684	0.001	0.001
Spatial	2	16.402	0.61181	0.581	0.549
Size class x Spatial	4	9.811	0.36595	0.863	0.848
Production					
Size Class	2	140.27	1.0716	0.001	0.001
Spatial	2	211.43	1.6152	0.288	0.278
Size class x Spatial	4	196.32	1.4998	0.26	0.285

Source: The author, 2022.

Figure 8 – Multidimensional scaling plot (MDS) for Copepod assembly in response to size fraction by: (A) abundance, (B) biomass and (C) production. 200/500 µm (yellow triangle), 500/1000 µm (blue circle) and >1000 µm (pink square).



Source: The author, 2022.

The MDS formed two distinct groups. The first corresponds to the size class 200/500 µm and the second a merged group of the classes 500/1000 µm and >1000 µm (Figure 8 a, b and c).

In abundance, SIMPER shows a 97.1% dissimilarity between the 200/500 µm vs. 500/1000µm size classes, where the taxa *D. oculata* (44.2%), *P. quasimodo* (13.9%), *O. nana* (11.8%) and Copepoda nauplii (7.5%) contribute 77.5% of this dissimilarity. Between the 200/500 µm vs. >1000 µm classes there was 99.7% dissimilarity and the same taxa above mentioned (*D. oculata* 44.9%, *P. quasimodo* 13.84%, *O. nana* 11.8% and Copepoda nauplii 7.5%) contributed 71.9%. Between the 500/1000 µm vs. >1000 µm fractions there was 87.6% dissimilarity and the species *F. gracilis* (36.7%) and *A. lilljeborgii* (34.3%) contributed with 71.0%.

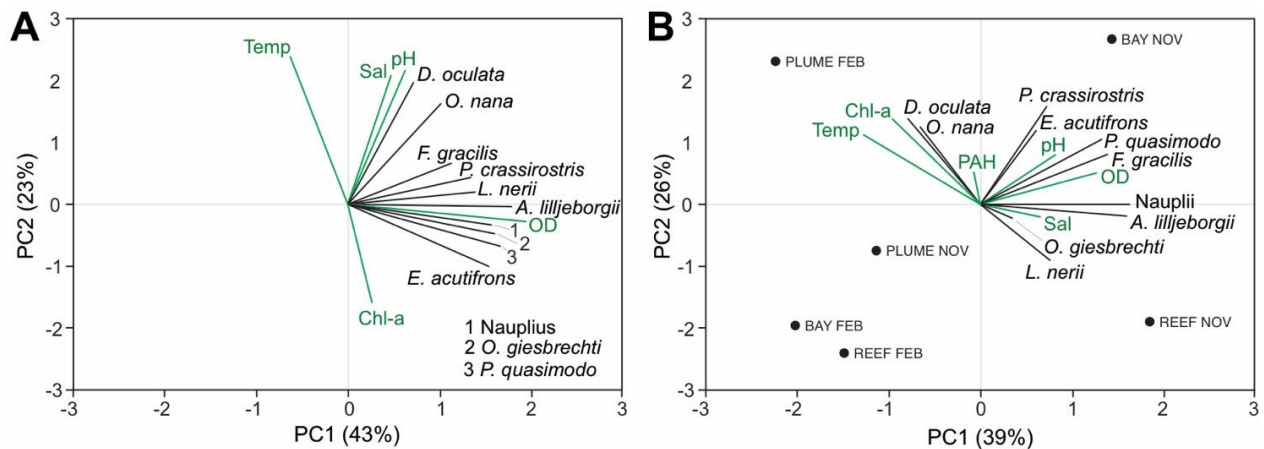
SIMPER, for biomass, shows 93.1% dissimilarity between the 200/500 µm vs. 500/1000 µm size classes, where the species *D. oculata* (32.7%), *P. quasimodo* (18.3%), *E. acutifrons* (11.0%) and *A. lilljeborgii* (9.3%) contribute 71.2% of this dissimilarity. Between classes 200/500 µm vs. >1000 µm there was 97.3% dissimilarity, where species *D. oculata* (33.0%), *P. quasimodo* (18.5%), *E. acutifrons* (11.3%) and *O. nana* (8.9%) contributed with 72%. For production SIMPER showed a 92.3% dissimilarity between the 200/500 µm vs. 500/1000 µm size classes where the species *D. oculata* (28.5%), *P. quasimodo* (23.7%), *A. lilljeborgii* (12.4%) and *O. nana* (8.9%) contributed 73.5%. Between the 200/500 µm vs. >1000 µm classes there was 96.0% dissimilarity as *D. oculata* (29.0%), *P. quasimodo* (24.2%), *A. lilljeborgii* (10.6%) and *O. nana* (9.1%) contributed with 72.9%.

Principal component analysis (PCA) explained 66% of the data variation (Figure 9a); axis1 explained 43% (PC1) and axis2 explained 23% (PC2). Salinity and pH were the main factors responsible for the distribution of *D. oculata*, *O. nana*, *P. crassirostris* and *F. gracilis*. Dissolved oxygen and chlorophyll-a were the factors that best explained the distribution of *E. acutifrons*, *P. quasimodo*, Copepoda nauplii, *A. lilljeborgii*, while temperature showed a negative relationship with these species.

A PCA was also performed on the months of February and November (the only months with PAH records in the water for the work). The PCA explained 65% of the distribution of the assembly in these two months (Figure 9b), where the first axis explained 39% (PC1) and the second explained 26% (PC2). From the analysis of the graph, it is possible to observe a positive relationship in relation to the distribution of *D. oculata* and *O. nana* on the environmental factor's chlorophyll-a, temperature and PAH, but observing the proximity and size of the vectors in relation to the species, chlorophyll-a and temperature explained better the distribution of these two species in February for the plume, month that *D. oculata* dominated in the samples. It is also possible to observe that the distribution of the others species are related to the other environmental factors, being dissolved oxygen and pH the

factors that best explain the distribution of *P. crassirostris*, *E. acutifrons*, *P. quasimodo* and *F. gracilis*, and salinity and the Copepoda species *A. lilljeborgii*, *L. nerii* and nauplii in November.

Figure 9 – Principal component analysis (PCA): (A) Environmental variables vectors (Temp = temperature, pH, DO = dissolved oxygen, Sal = salinity and Chl-a = chlorophyll-a) in green vectors and dominant species in black vectors; (B) Environmental variables vectors + PAH (Polycyclic Aromatic Hydrocarbons available in seawater) green vectors, February and November sampling months (black circles) and dominant species in black vectors.



Source: The author, 2022.

5.1.4 Discussion

The spatial and temporal variation of attributes related to abundance, biomass and production of the copepod assemblage of a complex reef system influenced by an estuarine plume was investigated in the present study. Although the spatial effect was not verified on the above descriptors, the integrated evaluation of our results suggests and reinforces that the estuarine plume is a site of intense biological activity, consequently of high productivity reflecting in the high numerical values verified for the investigated planktonic organisms.

5.1.4.1 Environmental variable and phytoplanktonic biomass (chlorophyll-a)

In coastal environments factors such as temperature, salinity, pH, and dissolved oxygen are determinants for the distribution and life cycle success of most aquatic organisms (JACOBS; GRANT, 1978; ODUM; BARRETT, 1971; ZARAUZ *et al.*, 2008). The continental shelf of Pernambuco is characterized by higher temperatures and higher salinity especially in the dry season (COSTA *et al.*,

1985). Among the environmental factors analyzed in this study, temperature, salinity, pH, and DO were the main responsible for the distribution found in most of the samples, as evidenced in the principal component analysis.

The variations in sea surface temperature, salinity, pH and DO were within the historical range expected for the dry season and also by the influence of the plume of the Ilhetas and Mamucabas rivers. The results corroborate other studies that have been done in the region for the dry season (NASCIMENTO-VIEIRA *et al.*, 2010; SILVA *et al.*, 2009; SILVA *et al.*, 2019). Temperature and salinity are important hydrological impact factors, which directly interfere with the distribution of planktonic organisms, especially species sensitive to changes in the water column (CAVALCANTI *et al.*, 2008; GRAHAME, 1976; MISHRA; PANIGRAHY, 1999; NASCIMENTO-VIEIRA *et al.*, 2010; NEUMANN-LEITÃO *et al.*, 2009; PATIL *et al.*, 2002).

The estuarine plume registered higher values of phytoplankton biomass compared to the bay and the reef, being classified as mesotrophic (PASSAVANTE, 2003). These biomass values for the estuarine plume were already expected, since estuarine waters are richer in nutrients compared to adjacent coastal waters. This region of the mouths of Ilhetas and Mamucabas rivers, which form the studied estuarine plume, is already known for its high phytoplankton activity in the dry period (LOSADA *et al.*, 2003). On the other hand, the low phytoplankton biomass value verified in Tamandaré Bay was already evidenced in other studies in the area (MOURA; PASSAVANTE, 1993; 1995) and showed that, even though the estuarine plume waters spread nutrients throughout the region, consequently raising the phytoplankton biomass, it can be quickly consumed by the zooplankton grazing pressure, so that the region can be characterized as an oligotrophic environment, with a tendency to mesotrophic in some months of the year, depending on the amplitude of the estuarine plume. Regarding the phytoplankton biomass chlorophyll-a contents found in the reefs, were similar to values recorded in other coral reef areas around the world (BRODIE *et al.*, 2007; DUYL *et al.*, 2002; TADA *et al.*, 2003) characterizing it as an oligotrophic environment (PASSAVANTE, 2003).

5.1.4.2 Composition and abundance of the copepod

The results presented here indicate that the taxonomic groups that were identified are similar to those verified by previous studies conducted in the Tamandaré region, as well as the dominant species in the region: *Dioithona oculata*, *Paracalanus quasimodo* e *Acartia lilljeborgii* (BRITO-LOLAIA *et al.*, 2020; FARIAS, 2019; FIDELIS, 2014; FIGUEIRÊDO, 2014). However, the total

number of taxa identified in this study was higher than those verified by other authors and may be related to the sampling strategy, tidal timing, and type of net used.

The Copepoda assemblage was influenced by three complex systems (estuary, oceanic waters and reef environment), characterized by the presence of freshwater, estuarine, coastal and oceanic species. Nevertheless, it is notable the dominance in the region of species classified as neritic/estuarine (*D. oculata* and *P. quasimodo*) and estuarine (*A. lilljeborgii*, *O. nana* and *P. crassirostris*) (BJORNBERG, 1981; BOLTOVSKOY *et al.*, 2002; LOPES *et al.*, 1998). It is known that the coastal zone is highly influenced by the continent, being inhabited by species well adapted to large variations in temperature, salinity, freshwater and runoff (BRADFORD-GRIEVE *et al.*, 1999). Brito-Lolaia *et al.* (2020) could observe this fluctuation as to the origin when studying the Tamandaré reef community, especially the copepod assemblage, demonstrating the strong influence of the estuarine plume on the reefs and the adaptive plasticity of the species to environmental variations.

Regarding the most abundant species, *Acartia lilljeborgii* was among those that contributed the most to the composition of the assembly. This species is commonly dominant in tropical and subtropical coastal/estuarine environments, due to its high tolerance to salinity and temperature variation (BJÖRNBERG, 1972; LIRA, 1996; TEIXEIRA *et al.*, 1965; TUNDISI; TUNDISI, 1968). Because they are considered medium to large species, usually copepods of the genus *Acartia* dominate the biomass in most bays, lagoons and estuaries (AZEITERIO *et al.*, 2005; LEANDRO *et al.*, 2007). Despite being among the most relevant, presented higher contribution, and (as classically reported), and this may be related to: 1 - Efficiency of the net in collecting organisms of larger size spectrum (see session 4.4), because when we compared our results using 300 µm nets, *A. lilljeborgii* is the species that contributes most in abundance and biomass (SILVA *et al.*, 2004); 2 - vertical migration behavior to escape predators (FORWARD, 1988; ROBERTIS, 2002).

P. quasimodo and *P. crassirostris* occurrence outranked in the area and both are very tolerant to salinity and temperature variation, common to estuarine regions with strong marine influence (ESKINAZI-SANT'ANNA; TUNDIST, 1996; LOPES, 1994; MATSUMURA-TUNDISI, 1972). They are herbivorous species that feed on particle selection and picoplankton and nanoplankton (BJORNBERG, 1981; CALBET *et al.*, 2000). This characteristic of food selection by size is a particularity of species that perform grazing by zooplankton (BERGGREEN *et al.*, 1988; HANSEN *et al.*, 1994; WILSON, 1973). As mentioned in section 4.1, according to Moura Passavante (1993; 1995), Tamandaré bay has a high grazing pressure on the phytoplankton carried by the estuarine plume to the bay. The success of these two species may be associated with the food abundance found there, as observed by Dias & Bonecker (2009) in the Bay of Camamu (Bahia, Brazil).

The high abundances of the species *Dioithona oculata* in the first two months of the study drew attention by the expressiveness of the values. At first it was believed that the high abundances were related to the presence of oil in the water (since the study area was affected by the spill only 2 months before) and this was shown in the principal component analysis. The correlation between environmental variables and abundance showed that chlorophyll-a and temperature were the variables that best explained the distribution of the species in February and not PAH concentrations, as initially thought. According to Knap *et al.* (1986) and Marchand (1980), PAH concentrations above 1.00g L^{-1} are typically found in marine regions affected by the introduction of petroleum hydrocarbons or derivatives. The concentration of PAH found in the February month was $0.17 \pm 0.13\text{g L}^{-1}$, well below what is found in affected coastal regions.

Since there was not enough correlation to support that the oil affected the abundance of this species, a literature survey was done on the ecology of the species. It was found that, *D. oculata* feeds on particles and is able to form aggregations of individuals (swarms) during the day and disperse in the water column at night (AMBLER *et al.*, 1991), behavior has been reported by other papers in the region (FARIAS, 2019; FIGUEIRÊDO, 2014; MELO *et al.*, 2010). This behavior can provide greater reproductive success, reduce the chance of involuntary dispersal by currents and protect from predation (BUSKEY *et al.*, 1996), and is more frequent at the reef top (MELO *et al.* (2010)).

5.1.4.3 Copepod assemblage structure and ecological indices

The diversity of the copepod assemblage varied from low (Reef) to medium/high (Estuarine plume), with the lowest values recorded in the first three months of the study. According to Neumann-Leitão (1994) lower diversities occur when a single species becomes dominant in the community, usually during its reproductive or food supply period. This may be attributed to the predominance of *D. oculata* in the first two months (February and March) and the predominance of *P. quasimodo* in the third month of the study (September).

It was possible to observe an increase in the last three months (abundance and diversity). These results corroborate the research by Nascimento-Vieira *et al.* (2010) in Tamandaré, where they suggested the existence of a favorable period for mesozooplankton from November to February (mainly in the dry season). The explanation would be the increase in temperature, decrease in continental drainage and spawning season of corals caused by environmental conditions. This pattern was also observed by Fidelis (2014) and Silva *et al.* (2019), reinforcing our results.

All investigated parameters pointed to a spatial decrease between estuarine plume, bay and reef (abundance and diversity). Studies using plankton abundance and diversity as descriptive characters, show that corals are able to remove 20 to 80% of the holoplankton due to the strong efficiency in the filtering process and food capture in the water column (GLYNN, 1973; JOHANNES; GERBER, 1974; LEFÈVRE, 1985; TRANER; GEORGE, 1972). Suggesting that the values recorded on reef tops may be underestimated due to the dynamics of reef ecosystems (FIDELIS, 2014; SOROKIN, 1990a; b).

5.1.4.4 Biomass and secondary productivity

Studying the biomass and productivity of species makes it possible to observe the feeding conditions of a species and its role in the food chain (OMORI; IKEDA, 1984). Although, the comparison between secondary production data is challenging, since there is no standardization in the methodologies for obtaining such rates. To obtain the secondary production of copepods, besides biomass values, it is necessary to determine the daily growth rates of the species. This is where the difficulty lies, due to the existence of various methodologies for obtaining this (MELO-JUNIOR et al., 2016). The most widely used are those that use body weight and temperature (HUNTLEY; LOPEZ, 1992) and the one that uses body weight, temperature and chlorophyll-a (HIRST; BUNKER, 2003). The first and older model ignores the fact that growth rates can be influenced by food rate and therefore results in comparative work tend to overestimate (BURKILL; KENDALL, 1982; KLEPPEL et al., 1996; PETERSON et al., 1991). Therefore, we used the Hirst and Bunker (2003) model because it uses a food descriptor and our comparisons were made with papers that followed the same methodology.

In Tamandaré, for the 200 µm mesh size, only two studies were conducted and both were on corals. The first by Fidelis (2014), in the dry period recorded a biomass of 1.4 mg C m^{-3} and a productivity of $0.4 \text{ mg C m}^{-3} \text{ d}^{-1}$. The second work by Farias (2019), recorded a biomass $\cong 17\%$ higher than that of Fidelis (71.4 mg C m^{-3}) and a production $\cong 250\%$ higher ($281.9 \text{ mg C m}^{-3} \text{ d}^{-1}$). Farias (2019) used the entire mesozooplankton community to estimate biomass and production, whereas Fidelis (2014) used only the dominant Copepoda species in the region. Comparing the present study with Fidelis (2014) (for having a similar methodology), we observed a slight increase in total biomass (in this study: 1.8 mg C m^{-3}) and a $\cong 97\%$ higher total secondary production (in this study: $3.9 \text{ mg C m}^{-3} \text{ d}^{-1}$). This increase in biomass and production in the samples of the present research may be linked to the fact that we recorded swarms of *D. oculata* in two consecutive months.

Regarding the estuarine plume and the bay, as the study was carried out at ebb tide, the hydrographic conditions of the two regions were equivalent to estuarine and to a system strongly influenced by estuarine waters. The values recorded for biomass ($0.31 \pm 0.30 \text{ mg C m}^{-3}$) and secondary production ($0.79 \pm 0.79 \text{ mg C m}^{-3} \text{ d}^{-1}$) in the estuarine plume were on par with values recorded in other estuaries. In the Taperaçu estuarine complex (Amazonas, Brazil) biomass ($0.29 \pm 1.0 \text{ mg C m}^{-3}$) and production ($6.9 \pm 2.4 \text{ mg C m}^{-3} \text{ d}^{-1}$) were similar to those recorded in this study, but production was higher and was linked to the greater abundance of medium to large species (MAGALHÃES *et al.*, 2011). The production recorded for Tamandaré Bay ($0.83 \pm 0.73 \text{ mg C m}^{-3} \text{ d}^{-1}$) in this study was higher than that recorded for Santos Bay (São Paulo, Brazil) (mean $0.21 \text{ mg C m}^{-3} \text{ d}^{-1}$) (PEREIRA, 2011). The difference between data from Tamandaré Bay and Santos Bay may reflect local pollution, in Santos it is reported the presence of sewage outfall and pollution from upstream rivers (BRAGA *et al.*, 2000; MIRANDA *et al.*, 1998).

D. oculata was the species that produced the most in the estuarine plume and reefs, which can be associated with the due swarms record, corroborating with Farias (2019). And for the Bay, the species *P. quasimodo* contributed the most to biomass and production. *P. quasimodo* also showed this dominance pattern in Santos Bay and would be tied to the higher salinity rates, lower temperature and low nutrient concentrations (PEREIRA, 2011). In this study these values reflect the grazing performed by this species on phytoplankton, as mentioned in section 4.1, since there are no large variations between the regions between the environmental parameters. Ara (2004) when studying the zooplankton composition in the estuarine-lagoon complex of Cananeira (São Paulo, Brazil), found that the biomass of herbivorous copepods would have been favored by input of phytoplankton biomass in the region.

5.1.4.5 Selectivity by size class

In our results, small species were dominant in all analyzed attributes (abundance, biomass and production), reinforcing the importance of small species in maintaining the trophic web in coastal environments. This pattern has been observed in work already conducted in the region with various plankton net sizes (BRITO-LOLAIA *et al.*, 2020; CAMPELO *et al.*, 2021; FARIAS, 2019; FIGUEIRÊDO, 2014) and in other studies around the globe in coastal regions (ESTRADA *et al.*, 2012; GARCIA *et al.*, 2021; MELO-JUNIOR *et al.*, 2016; NEUMANN-LEITÃO *et al.*, 1998; NEUMANN-LEITÃO; MATSUMURA-TUNDISI, 1998). It is worth mentioning the size of the net of great magnitude, the increase of most species, but also the reduction of filtration water for animals

(SKJOLDAL *et al.*, 2013). Despite the fact that the net eventually selects for size classes, the results of studies using a variety of plankton nets show that in the coastal region small species dominate regardless of the net flow (FULTON, 1984; HOPCROFF *et al.*, 2001; PAFFENHÖFER, 1983; TURNER, 1994). Reinforcing the points: 1 - The importance of using methodologies that avoid overestimation of large species in smaller nets; 2 - The efficiency that the 200 µm net has in suspension in the size range 450-1400 µm (HOPCROFF *et al.*, 2001).

5.1.5 Conclusions

- The estuarine plume strongly influences the region, allowing the entrance of estuarine species and contributing to the increase of biological productivity in this area. This point is confirmed by the high numerical values of phytoplankton biomass, biomass abundance and productivity of the copepod assembly;
- A period of high biological productivity occurring in the last months of the year (October, November and December) is reinforced in the present study, evidenced by the records of high abundances, biomass, productivity and diversity of copepods; in Tamandaré, in the last months of the dry period, there is a favorable period for general zooplankton;
- In general, the species *D. oculata*, *P. quasimodo*, *A. lilljeborgii* and *E. acutifrons* contributed the most in biomass and production in the assembly, suggesting that they are the main Copepoda species for the maintenance of the food web in Tamandaré;
- The Copepoda *Dithona oculata* is a key species in the coastal habitats of Tamandaré, and its dominance may be related to its feeding plasticity, low ingestion, mortality and metabolism rates, which makes it more stable, based on its high abundance, biomass and production rates, for all areas and months investigated;
- We encourage that new studies using the 200 µm net in the coastal zone be carried out using the size class analysis methodology, as this will avoid overestimation of medium/large species that is not efficiently collected by the net;
- Among the studies published in Tamandaré, it was possible to observe a pattern of results, considering the compartments phytoplankton, zooplankton, or assemblages of species. For this reason, we stimulate the creation of a review of the plankton studies, making a compilation and comparisons of the publications in the area.

5.1.6 Acknowledgments

This work was financed by the Fundação de Amparo à Ciência e Tecnologia de Pernambuco - FACEPE under the grant number PBPG-0069-1.08/20. And to the same organ, we would like to express our thanks for granting the scholarship to the first author. We thank the research projects PELD-TAMS and FACEPE Água for providing all the necessary structure for the collections. To the Phytoplankton Laboratory (LabFito/UFPE) for granting the data of chlorophyll-a and phytoplankton biomass. To the laboratory Organic Compounds in Coastal and Marine Ecosystems (OrganoMar/UFPE) for granting the PAH concentrations from February and November/2020 and to the Oceanography Department of the Federal University of Pernambuco, for granting the use of the Zooplankton Laboratory (LabZoo/UFPE).

5.2 ARTIGO 2 – THE STRUCTURE OF THE COPEPOD ASSEMBLAGE IN TERMS OF ABUNDANCE, BIOMASS AND PRODUCTIVITY IN A TROPICAL ESTUARINE COMPLEX

Kaio H. F. da Silva^a; Renata P. de S. Campelo^a & Sigrid Neumann-Leitão^a

^aDept. of Oceanography, Federal University of Pernambuco,
Av. Arquitetura s/n, Recife, Pernambuco, 50740-550, Brazil

Abstract

The research was carried out in the Rio Formoso Estuarine Environmental Protection Area, located in northeastern Brazil. The area has a total of 2.724 hectares, formed by the contribution of coastal rivers and near the coastline has reefs. The estuary itself is already characterized as a complex environment full of life, however, affected by anthropic actions such as continental pollution and recently hit by the oil spill (2019). Due to its great importance in maintaining local aquatic life, understanding how biological communities are distributed and cope with exogenous stressors is of paramount importance. The paper aimed to investigate the spatial-temporal variability of copepod assemblage in an estuarine area affected by the impact of the 2019 oil spill. And for the first time to study the copepod assembly in terms of biomass and productivity. Samples were obtained in Rio Formoso and comprised three fixed sampling stations along the estuary. Mesozooplankton (200 µm) was collected by horizontal hauls during the ebb tide in four months of the dry period (February, March, September and October/2020). In addition, size class methodology was used to analyze the samples, after which the biomass and productivity (model of Hirst and Bunker, 2003) of the most abundant species were estimated. A total of 34 taxonomic groups were identified, of these 9 were considered dominant and accounted to 90% of all relative abundance in the area. The species *Paracalanus crassirostris*, *Acartia lilljeborgii*, *Dioithona oculata* and *Euterpina acutifrons* stand out for their contributions in abundance, biomass and production. The station located at the mouth of the Ariquindá river acted as a vector of nutrient and productivity increment, which was expressed in high rates of primary and secondary productivity. The species *P. crassirostris* was the most favored by the influence of the adjacent rivers and was considered a key species for the maintenance of fish resources in the region.

Keywords: copepods; estuarine complex; biomass; production of copepoda

5.2.1 Introduction

Estuaries are complex environments whose dynamics are governed by large fluctuations in salinity, tide, freshwater flow, sea current, temperature, salinity, sedimentation and turbidity (TUNDISI; TUNDISI, 1968; TUNDISI, 1970). These physicochemical changes can occur in the short, medium and long term, which directly influence the resident aquatic communities (AKIN *et al.*, 2003). Besides natural forcing, estuarine ecosystems also suffer from anthropic impact caused by irregular discharge of domestic effluents, aquaculture, tourism and unregulated exploitation of natural sources (ESKINAZI-LEÇA *et al.*, 2004). Because of the complexity of the ecosystem, estuarine waters are biologically more productive if compared to the river upstream and the sea downstream. This productivity is reflected throughout the trophic chain, with emphasis on primary and secondary production (KENNISH, 1990). With this, the estuary becomes a favorable environment for feeding and reproduction of many species of invertebrates and vertebrates (TUNDISI; ESTUARINO, 1970), being considered a hotspot of marine life and a driving force in the fluctuation of biological population dynamics, especially the planktonic ones (HOFFMEYER, 2004; KENNISH, 1990).

The mesozooplankton (200 µm), plays a key role in coastal and estuarine ecosystems, because it acts as a fundamental link between phytoplankton and higher trophic levels; it controls phytoplankton populations through grazing; it acts as a link between the microbial loop and the classical trophic chain (BRANDINI, 1997). Among all the organisms that constitute the mesozooplankton, copepods stand out because they are dominant in abundance, biomass and productivity in aquatic environments (HUYSEN, 1991; KIØRBOE, 1997). Due to this success, copepods represent an important component in the diet of numerous animals, thus being considered a key group in the pelagic environment (BLAXTER *et al.*, 1998; UYE *et al.*, 2000).

Due to the large geographic extension, wide biomass range and many endemic groups that occur in the Neotropical region, conducting studies and biodiversity conservation become increasingly urgent (HUGHES *et al.*, 2013; MORRONE, 2014). The increase in environmental interference in coastal ecosystems as a result of human activities increasingly threaten biodiversity and ecosystem services provided by these environments. Therefore, understanding how these impacts affect the functioning and structuring of these areas is necessary to be able to carry out mitigation measures (AZEVEDO-SANTOS *et al.*, 2019; NEUMANN-LEITÃO, 2010). An excellent descriptor for understanding the impacts on the zooplankton community are estimates of biomass and production, as they provide essential data for understanding the ecological dynamics and the flow of energy and carbon through trophic webs (WEBBER; ROFF, 1995; WILLIAMSON; GRIBBIN, 1991). Due to the

dynamic character of zooplankton, any changes in the community have direct consequences on its abundance, directly influencing the biomass and production of the communities (MILLER, 2004).

The study was conducted in the Environmental Protection Area (EPA) called "Rio Formoso Estuarine Complex" (northeastern Brazil) and has as its main objective to contribute to the conservation, preservation, recovery and restoration of associated ecosystems (FERREIRA *et al.*, 2001; FIDEM, 1987; LIRA; FONSECA, 1980; SILVA *et al.*, 2009). However, despite being an EPA it is threatened due to anthropic actions (HONORATO DA SILVA *et al.*, 2004). In the region it has been reported the appearance of oil slicks caused by the oil spill that hit the Brazilian coast in 2019-2020 (CAMPELO *et al.*, 2021).

Due to the importance of the environment, studies on the micro/mesoplankton communities and the analysis of the contribution of organic and inorganic particles in the zooplankton community have been carried out (LIMA *et al.*, 2012; NEUMANN-LEITÃO *et al.*, 1995; SANTANA-BARRETO *et al.*, 1991; SILVA *et al.*, 2019), but none with the objective of understanding the biomass flux and production of the resident copepods.

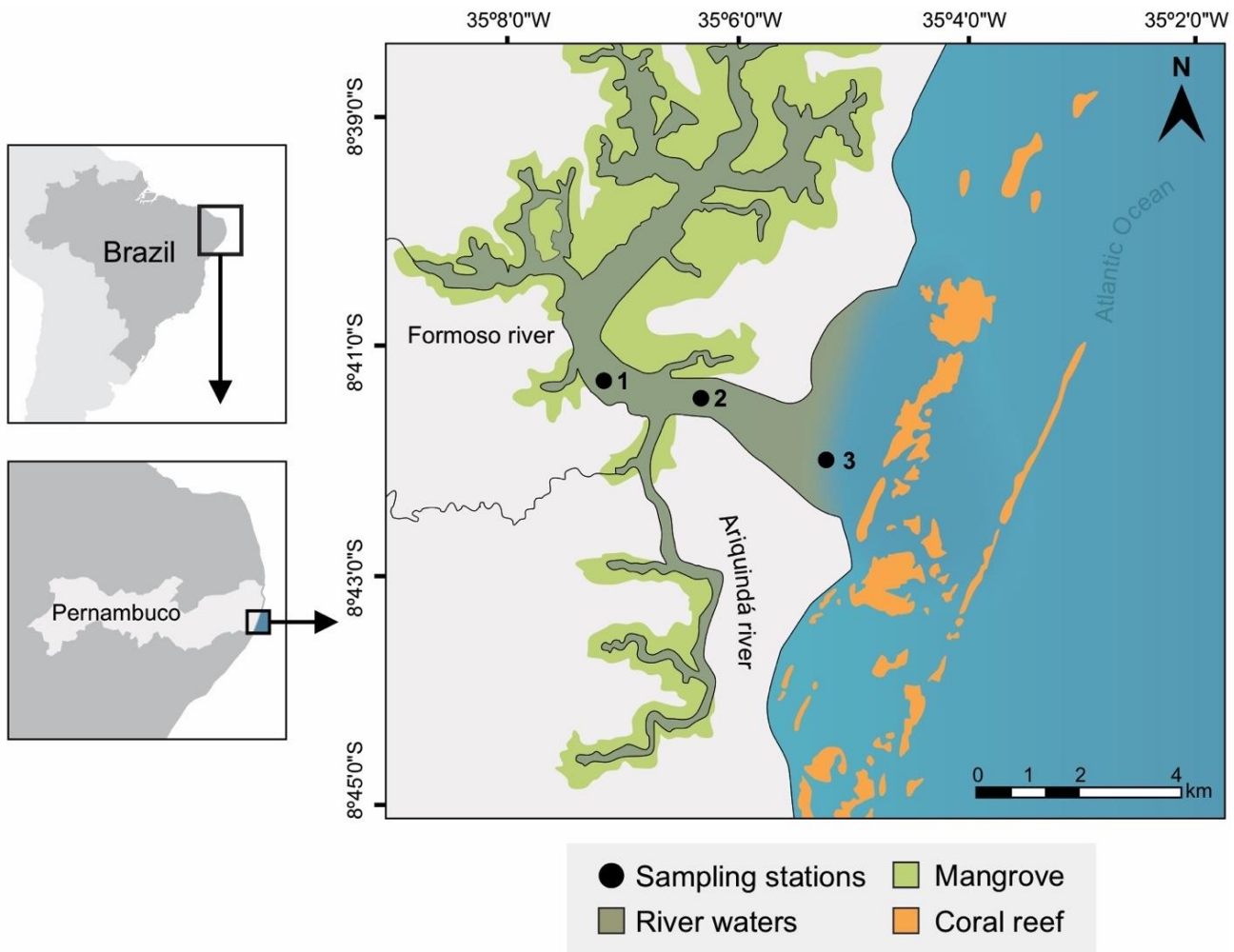
Knowing all the complexity and importance of Rio Formoso, it is of major importance to understand how the biological communities are distributed in the environment and how exogenous stressors act on the organisms. Therefore, the present study aimed to investigate the spatio-temporal variability of copepod assemblage abundance, biomass and production in a protected estuarine area.

5.2.2 Materials and Methods

5.2.2.1 Study area

The estuarine EPA of Rio Formoso, located in the municipalities of Sirinhaém and Rio Formoso, has an area of approximately 2.724 hectares and is located between the municipalities of Sirinhaém and Rio Formoso (FERREIRA *et al.*, 2001; FIDEM, 1987; LIRA; FONSECA, 1980; SILVA *et al.*, 2009) (Figure 1). The estuarine area is a type of coastal plain, with sinuous morphology and bordered along its entire length by mangroves (LIRA *et al.*, 1979). Along its length it receives domestic effluents, waste from the sugar industry and carciniculture activity (HONORATO DA SILVA *et al.*, 2004). It has a coastal climate classified, warm and humid type AS', according to the Köppen classification system, characterized by alternating dry season (September to March) and rainy season (April to August) (ALVARES *et al.*, 2013).

Figure 1 – Sampling stations along the coast of Pernambuco, Brazil. Three sampling stations in the Rio Formoso estuarine complex (RF1, RF2 and RF3).



Source: The author, 2022.

5.2.2.2 Sampling of environmental variables and plankton

The sampling was carried out in the subsurface layer of the water column of the Rio Formoso estuary (three fixed points: RF1, RF2 and RF3) (Figure 1). The sampling was carried out during the dry period, at low tide. A total of 12 samples were collected in the Formoso River estuary, which sampling occurred in the months (February, March, September and October 2020).

Diurnal hauls were carried out at a speed of 1.5 to 2.5 knots for 3 minutes with a plankton net 200 µm mesh size (with a mouth diameter of 30 cm) (UNESCO, 1968). A flowmeter was attached to the mouth of the net to estimate the volume of water filtered. Zooplankton samples were preserved

immediately in a 4% formaldehyde solution and buffered with borax (0.5 g L^{-1}) (GIFFORD; CARON, 2000; NEWELL; NEWELL, 1963).

Water samples were collected for chlorophyll-a content. In the laboratory, spectrophotometric analysis was performed for chlorophyll-a estimation according (UNESCO, 1966). The environmental parameters (surface temperature - $^{\circ}\text{C}$, pH, salinity and dissolved oxygen DO - ml l^{-1}) were measured superficially using a pre-calibrated water quality multiparameter probe (HORIBA - U50). The rainfall data were obtained from the National Institute of Meteorology data.

5.2.2.3 Mesozooplankton analysis

In order to avoid underestimating the larger individuals, the samples were fractionated into three size classes using a set of sieves with mesh sizes of 1000, 500 and 200 μm (HEAD *et al.*, 1999). Subsequently, the different size classes (200-500 μm , 500-1000 μm and $>1000\mu\text{m}$) were fractionated using a MOTODA type grading equipment for a minimum analysis of 300 copepods (OMORI; IKEDA, 1984). The samples were analyzed in a Bogorov counting chamber under a stereomicroscope. Taxonomic identifications followed the bibliographies: BJORNBERG (1981) e BOLTOVSKOY et al. (2002). The copepods were measured using the Zen software under a stereomicroscope.

The abundance (ind m^{-3}) and relative abundance of copepods (%) were calculated to describe the community structure (copepod species with relative abundance $\geq 2\%$ were considered dominant and used for the multivariate analyses). Shannon's diversity index (H') (SHANNON, 1948), was applied to estimate the diversity of the assembly, where the values found indicate: high diversity if $H' > 3.0 \text{ bits ind}^{-1}$, medium diversity if $2.0 < H' \leq 3.0 \text{ bits ind}^{-1}$, low diversity if $1.0 < H' \leq 2.0 \text{ bits ind}^{-1}$, and very low diversity if $H' < 1.0 \text{ bits ind}^{-1}$.

A total of 30 individuals of the most abundant taxa were measured to perform biomass calculations. Biomass (B , mg C m^{-3}) of a given taxon based on its abundance (A , ind.m^{-3}) and individual carbon weight (CW , mg C): $B = A * CW$. CW was defined using length-weight regressions available in the literature (Table 1a). The calculation of Production ($\text{mg C m}^{-3} \text{ day}^{-1}$) was based on its biomass and specific growth rates: $P_i = C_i * B_i$. Where (P_i) the production of group i, (C_i) growth rate of group i and (B_i) biomass of group i. The growth rate (C) was based on the model of HIRST e BUNKER (2003) (Adults and juveniles were considered together/Table 1b).

5.2.2.4 Statistical analyses

The information related to the dependent variables: abundance, biomass and production of planktonic copepods, were statistically tested from routines developed in mathematical software. Before testing the data, the Kolmogorov-Smirnov normality test and Levene's heterogeneity test were applied. When necessary, the data were Log(X+1) transformed. Analysis of variance (ANOVA) was used to analyze the first-order (non-interacting) effects of multiple independent variables: spatial (RF1 x RF2 x RF3), temporal (months x months) and size fraction (200/500 x 500/1000 x >1000 µm). Once significance was verified ($p < 0.05$), the Tukey-HSD (post-hoc) test was applied. To access the variability in copepod assembly structure among the factors (spatial and size fraction/temporal cannot be used due to unbalancing and being from a single period) a PERMANOVA was run. To graphically visualize the PERMANOVA results an MDS was used. Similarity Percentage analysis (SIMPER) was performed to identify representative taxa/species and their contributions to dissimilarity. Principal Component Analysis (PCA) was also calculated using the data and standardized environmental parameters and Copepoda species to assess the associations between them.

Table 1 – a) Length-weight regressions applied to calculate the biomass of the most abundant copepods. Length data entered in µm; b) Regression equation to estimate the instantaneous growth rate applied to Copepoda.

a) Regression equations for length-weight		
Taxa	Equation	References
<i>Acartia lilljeborgii</i>	$PS = 6,177 \times 10^{-9} \times L^{3,029}$	Ara (2001)
Oithonidae	$\ln PS = 1,10 \ln P - 7,07$	Chisholm e Roff (1990)
Paracalanidae	$\ln PS = 2,78 \ln P - 16,52$	Webber e Roff (1995)
<i>Pseudodiaptomus</i> spp.	$PS = 1,306 \times 10^{-9} P^{3,361}$	Ara (2001)
Harpacticoida	$\log PS (\mu g) = - 8.51 + 3.26 \times \log TL$	Hirota (1986)
Copepod nauplii	$\ln AFDW = 2.48 \ln TL - 15.7$	Båmstedt <i>et al.</i> (1986)

b) Regression equations for growth rate		
Taxa	Equation	Reference
Copepod	$\log_{10} C = 0.0186 \times T - 0.288 \times \log_{10}(PS) + 0.417 \times \log_{10}(Cl) - 1.209$	Hirst e Bunker (2003)

CW, Carbon weight; PL, Prossome length; TL, Total length; C, Carbon; Cl, Chlorophyll-a; T, Temperature

Source: The author, 2022.

5.2.3 Results

5.2.3.1 Environmental variables and phytoplanktonic biomass (chlorophyll-a)

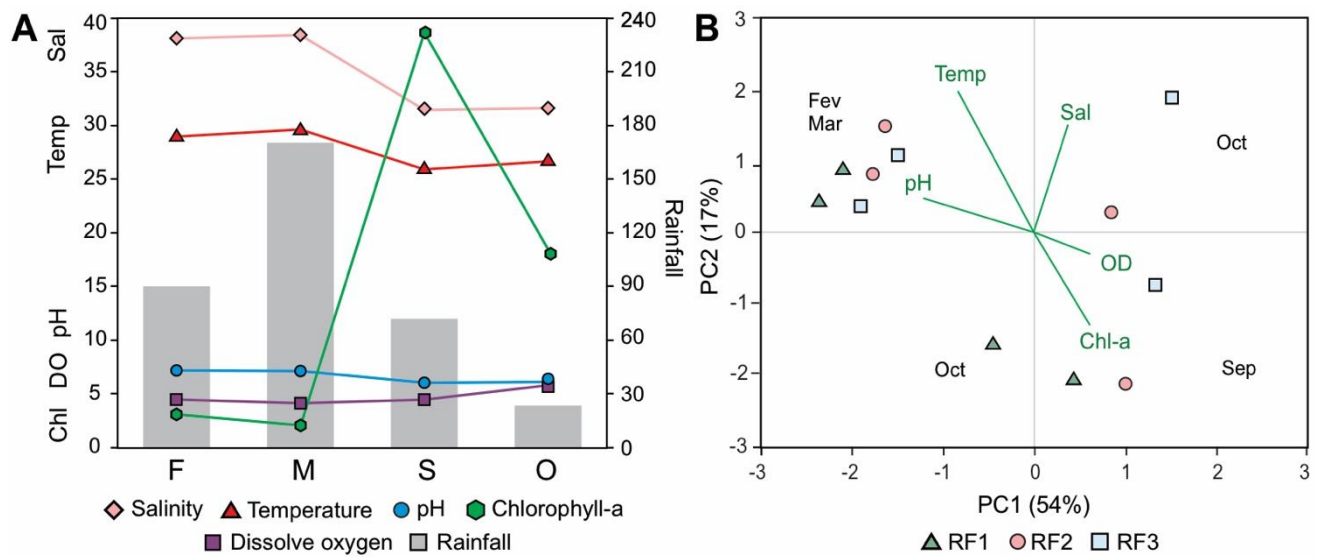
The values of rainfall were obtained from data from the National Institute of Meteorology. Considering all months of the study, there was a higher cumulative rainfall value for the month of March (157.8 mm) and a lower cumulative value for the month of October (25.4 mm) (Figure 2a). The water surface temperature in the Rio Formoso estuary varied between 30.1°C (March - RF1) and 27.1°C (September - RF3). Between stations, the mean values recorded were 29.3 ± 1.0 (RF1), 29.4 ± 1.2 (RF2) and 28.9 ± 1.3 (RF3) (Figure 2a). No statistical spatial and temporal differences were identified.

The salinity did not record differences in temporal and spatial terms, as well as pH and dissolved oxygen, however, for salinity there was a variation between the months of 33‰ (September - RF1) to 41‰ (March - RF3) (Figure 2a). Between stations the averages recorded were: $32.7 \pm 2.6\text{‰}$ (RF1), $33.1 \pm 0.6\text{‰}$ (RF2) and $34.0 \pm 1.7\text{‰}$ (RF3). The pH ranged from 6.6 (September - RF2) to 8.1 (February - RF1) (Figure 2a). Station RF1 recorded an average pH equivalent of 7.1 ± 0.8 , RF2 7.7 ± 0.9 and RF3 8.1 ± 1.2 . Dissolved oxygen (DO) ranged from 3.4 mg L^{-1} (February - RF1) to 6.6 mg L^{-1} (October - RF3) (Figure 2a). The stations recorded the following mean DO: $4.4 \pm 1.4 \text{ mg L}^{-1}$ (RF1), $5.2 \pm 0.9 \text{ mg L}^{-1}$ (RF2) and $5.5 \pm 0.5 \text{ mg L}^{-1}$ (RF3).

The chlorophyll-a concentration of phytoplankton showed values ranging from 2.35 mg m^{-3} at station RF3 in February and March 2020 to 63.90 mg m^{-3} at station RF2 in September 2020 (Figure 2a). No spatial and temporal differences were identified for phytoplankton biomass in the Rio Formoso estuary, however, numerically station RF2 showed a high mean concentration $21.8 \pm 28.2 \text{ mg m}^{-3}$ compared to station RF1 $18.6 \pm 28.6 \text{ mg m}^{-3}$ and RF3 $14.7 \pm 14.7 \text{ mg m}^{-3}$. The averages recorded in February, March, September and October 2020 were $4.10 \pm 1.85 \text{ mg m}^{-3}$; $3.78 \pm 1.98 \text{ mg m}^{-3}$; $16.93 \pm 14.57 \text{ mg m}^{-3}$ and $10.07 \pm 2.79 \text{ mg m}^{-3}$ respectively.

Principal component analysis applied to the environmental variables data explained 71% of the variation in the data on the first two axes (Figure 2b). Axis 1 accounted for 57%, while axis 2 explained 17% of the variation in the data. There was a clustering of samples from stations RF1, RF2 and RF3 from the months of February and March being correlated with the temperature and pH variables. The September samples (RF1, RF2 and RF3) focused oppositely on temperature and pH and positively on chlorophyll-a and dissolved oxygen.

Figure 2 – Distribution of abiotic data in Rio Formoso: (A) Temporal variation of mean values of environmental variables; (B) Results of principal component analysis (PCA) of environmental variables (Temp = temperature, pH, DO = dissolved oxygen, Sal = salinity and Chl-a = Chlorophyll-a) in green; Stations: RF1 - green triangle, RF2 - pink circle and RF3 - blue square.



Source: The author, 2022.

5.2.3.2 Composition and abundance of the copepod assemblage

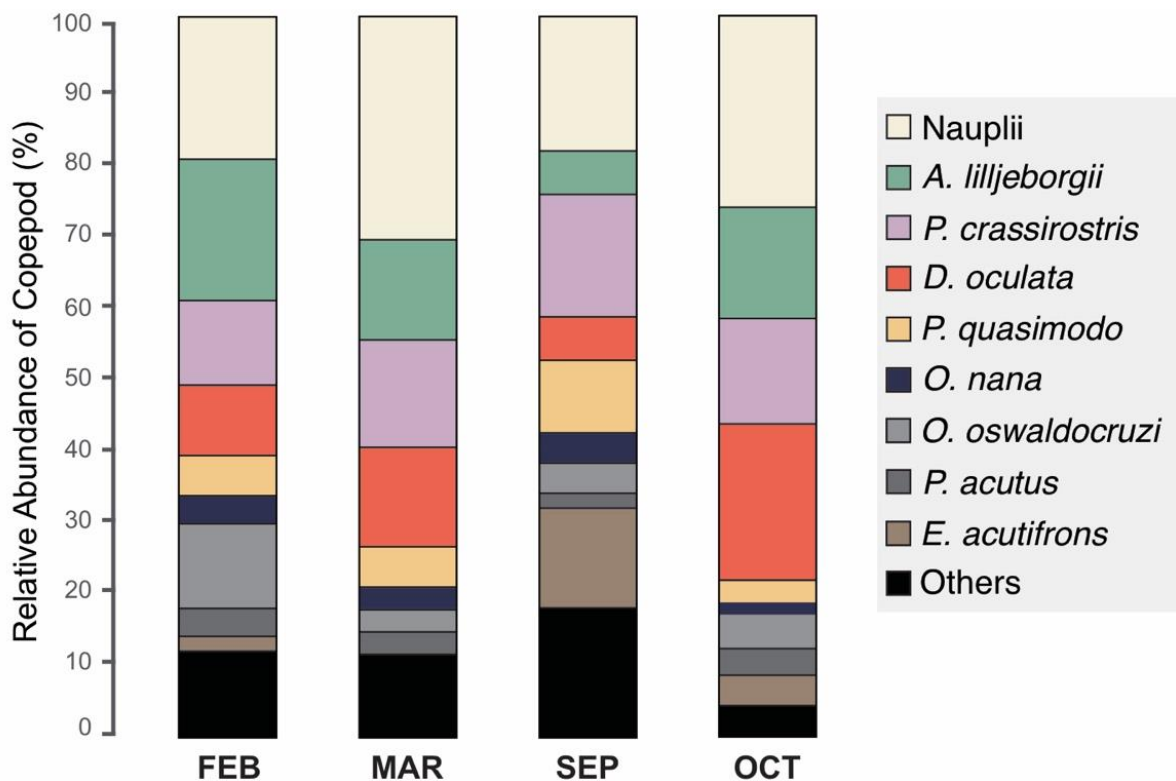
A total of 34 taxa were recorded in the Rio Formoso estuary region, with the orders Calanoida (22), Cyclopoida (9) and Harpacticoida (4) (Table 5). Among the 34 taxa identified, 9 were considered dominant and accounted for 90% of all overall relative abundance (Table 2).

In Figure 3 it is possible to observe the temporal variation of the relative abundance of these species and it is evident the high contribution of the Copepoda nauplii to the assembly, reaching 31.3% in March and 17.5% (February), 18.0% (September) and 27.0% (October). The species that were dominant during all months were: *P. crassirostris* (11.3% February, 14.6% March, 17.0% September and 14.1% October), *A. lilljeborgii* (19.9% February, 14.1% March, 6.2% September and 15.2% October) and *D. oculata* (10.1% February, 13.4 March, 5.9% September and 22.2% October) remained constant in all months (except September for *A. lilljeborgii* and *D. oculata*). In contrast, September was the month with the highest relative abundance recorded for *E. acutifrons* (1.7% February, 17.5% September, and 2.9% October) and for *P. quasimodo* (4.7% February, 5.3 March, 10.1% September, and 3.3% October).

The values of copepod mean abundances among the study months were: $67.8 \pm 79.1 \text{ ind m}^{-3}$ February, $157.2 \pm 245.3 \text{ ind m}^{-3}$ March, $276.5 \pm 403.7 \text{ ind m}^{-3}$ September and $555.8 \pm 971.3 \text{ ind m}^{-3}$

October, however, no significant differences were identified among the months (Figure 5a). The mean abundance values among stations were: $72.2 \pm 149.6 \text{ ind m}^{-3}$, $357.7 \pm 357.7 \text{ ind m}^{-3}$ and $505.7 \pm 971.3 \text{ ind m}^{-3}$ respectively recorded in RF1, RF2 and RF3, however, no significant differences were identified either (Figure 5b).

Figure 3 – Temporal variation of the total relative abundance (%) of the Copepoda assemblage in Rio Formoso, Brazil.



Source: The author, 2022.

Table 2 – Relative abundance (RA%) and detail abundance (mean \pm standard deviation) recorded in the assemblage of mesozooplanktonic copepods at stations RF1, RF2 and RF3 in the Rio Formoso estuary (northeastern Brazil) in the dry season of 2020.

Taxa	RA% General	RF1		RF2		RF3	
		RA%	ind m ⁻³	RA%	ind m ⁻³	RA%	ind m ⁻³
Copepod nauplii	24.7	35.5	192.2 ± 181.1	24.1	495.2 ± 580.9	23.5	951.1 ± 1190.6
<i>Acartia lilljeborgii</i>	12.9	8.7	20.9 ± 25.5	16.1	132.1 ± 206.5	11.8	212.2 ± 527.2
<i>Oithona</i> spp.	0.5	2.2	24.2 ± 28.0			0.5	28.2 ± 49.1
<i>Dithona oculata</i>	16.3	11.3	81.9 ± 89.2	8.8	181.1 ± 173.7	20.7	1116.8 ± 1535.5
<i>Oithona nana</i>	2.4	6.1	26.4 ± 29.6	1.7	35.2 ± 32.0	2.3	92.2 ± 105.8
<i>Oithona hebes</i>	0.6	0.3	1.4 ± 3.2	1.5	60.0 ± 54.6	0.3	20.1 ± 19.6
<i>Oithona oswaldoocruzi</i>	4.9	2.5	17.8 ± 10.9	7.8	161.4 ± 177.9	3.7	148.1 ± 138.4

Continuation of Table 2..

<i>Temora turbinata</i>	1.5	0.2	0.6 ± 1.5	0.9	17.1 ± 35.4	1.9	78.0 ± 118.8
<i>Temora stylifera</i>	0.7	0.2	1.2 ± 1.3	1.2	20.0 ± 36.8	0.5	14.1 ± 15.4
<i>Paracalanus quasimodo</i>	5.5	5.3	28.6 ± 19.9	4.4	89.5 ± 57.5	6.0	243.2 ± 272.1
<i>Euterpina acutifrons</i>	6.5	8.5	61.5 ± 81.8	9.2	377.6 ± 493.2	4.8	195.6 ± 180.5
<i>Paracalanus indicus</i>	0.3	3.6	26.0 ± 15.2	>0.0	0.1 ± 1.0		
<i>Onychorycaeus giesbrechti</i>	0.4	0.5	5.0 ± 2.7	0.1	2.0 ± 4.1	0.5	20.5 ± 37.5
<i>Corycaeus speciosus</i>	0.4	>0.0	0.1 ± 0.1	0.2	7.0 ± 10.2	0.5	44.0 ± 63.2
<i>Corycaeus amazonicus</i>	0.1	0.2	0.6 ± 1.6			0.1	4.0 ± 7.9
<i>Farranula gracilis</i>	>0.0					>0.0	2.0 ± 1.0
<i>Centropages velificatus</i>	0.3	0.1	0.2 ± 0.2	0.1	0.1 ± 0.6	0.4	16.0 ± 27.5
<i>Paracalanus crassirostris</i>	14.8	9.2	39.7 ± 59.4	16.7	274.1 ± 336.3	14.7	474.3 ± 572.8
<i>Labidocera nerii</i>	0.2	0.3	1.8 ± 1.5	0.1	3.0 ± 4.9	0.2	20.1 ± 25.9
<i>Labidocera fluviatilis</i>	0.3	0.2	2.7 ± 3.5			0.53	28.2 ± 48.0
<i>Calanopia americana</i>	>0.0					>0.0	1.0 ± 1.0
<i>Subeucalanus pileatus</i>	>0.0	0.2	1.1 ± 2.2			>0.0	0.1 ± 0.5
<i>Pseudodiaptomus</i> spp.	0.1	0.3	2.9 ± 3.0	0.2	2.0 ± 6.3		
<i>Pseudodiaptomus marshi</i>	0.1			0.2	4.0 ± 3.9		
<i>Pseudodiaptomus acutus</i>	2.4	0.1	0.2 ± 0.3	3.5	47.2 ± 29.1	2.1	49.0 ± 70.0
<i>Clytemnestra rostrata</i>	1.0	0.3	2.2 ± 2.6	0.3	11.1 ± 3.3	1.4	78.2 ± 103.4
<i>Miracia efferata</i>	>0.0	0.1	0.3 ± 0.3	>0.0	0.0 ± 0.2	>0.0	0.1 ± 0.1
<i>Lucicutia</i> spp.	0.6					0.9	51.0 ± 88.0
<i>Copilia</i> spp.	>0.0					>0.0	0.1 ± 0.1
Copepodites:							
<i>Calanidae</i>	0.2	0.7	3.6 ± 1.3	0.4	15.0 ± 19.3	>0.0	1.3 ± 1.5
<i>Pontelina</i>	0.3	0.3	1.2 ± 2.9			0.5	25.1 ± 44.6
<i>Acartia</i>	1.7	2.1	15.1 ± 14.4	2.5	75.1 ± 59.8	1.2	63.1 ± 110.1
<i>Paracalanus</i>	0.1	0.8	8.5 ± 8.7				
<i>Pseudodiaptomus</i>	0.2	0.2	1.8 ± 2.5			0.3	16.1 ± 28.6
<i>Labidocera</i>	0.2	0.2	0.9 ± 2.1			0.3	16.0 ± 28.4
<i>Temora</i>	>0.0					>0.0	1.0 ± 2.0

Source: The author, 2022.

5.2.3.3 Composition of the copepod assemblage by size class

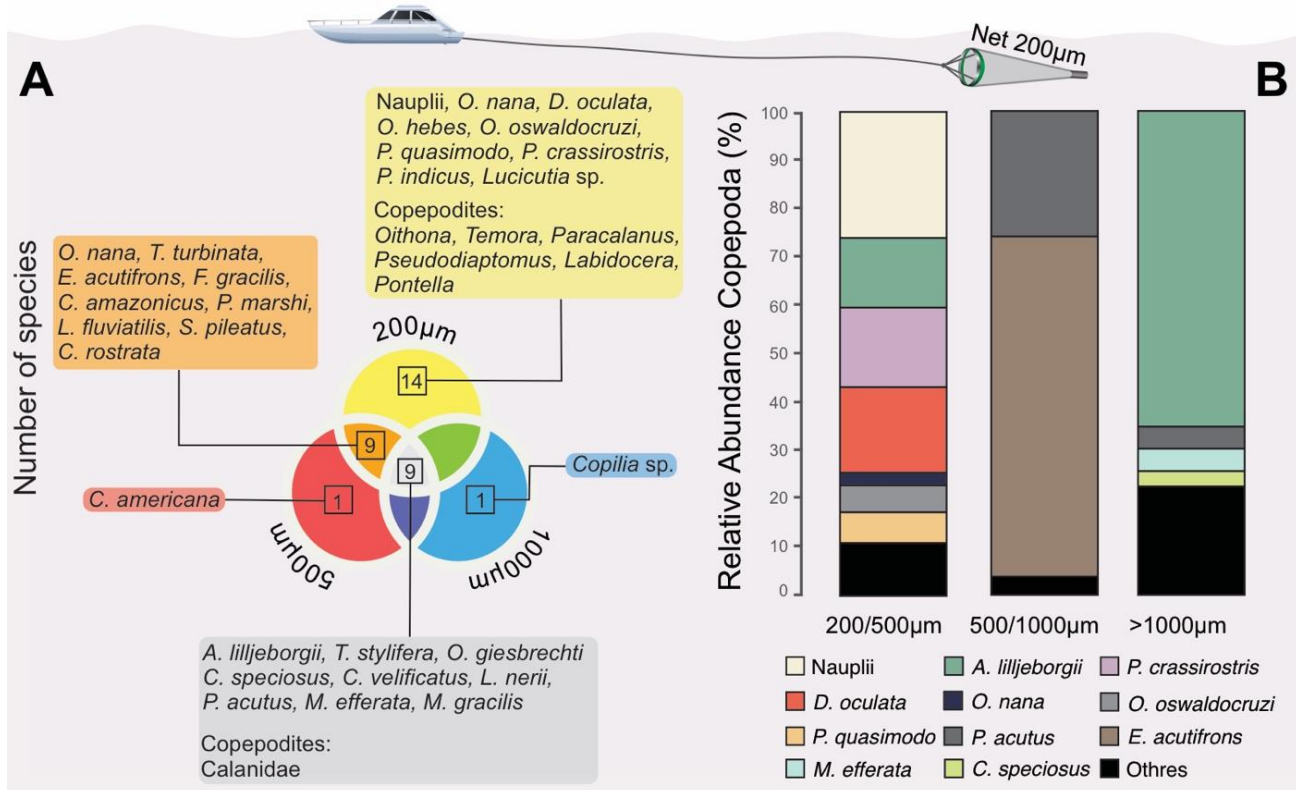
The Vann diagram showed that the number of copepod species (14) was highest in the smallest size spectrum (200 µm), all small-sized and juvenile stages of larger species (including nauplius) (Figure 4a). Nine species occurred in the 200~500µm intercession (small/medium-sized species). Nine species were in the intercession of all size classes, i.e., these species occurred in all three size classes analyzed in the paper. Only one species occurred only in the 500µm spectrum and one in the 1000µm

spectrum (Figure 4a). From the diagram it can be seen that the assembly was mainly characterized by small species.

A total of seven, two and four taxa were considered dominant in the 200-500 μm , 500-1000 μm and >1000 μm class, representing respectively 88.2%, 94.6% and 75.2% of the total abundance of the copepod assembly (Figure 4b). Noteworthy is the important contribution of the small-sized (<1.5mm) species *P. crassirostris* and *D. oculata* in the 200-500 μm class (16.1% and 17.6%), of the medium-sized species *E. acutifrons* to the 500-1000 μm fraction (69.1%) and of the medium/large species *A. lilljeborgii* to >1000 μm (64.1%).

Statistically significant differences were identified in mean abundance between size classes (Kruskall-Wallis, $p = 0.000$), where multiple comparisons analysis showed that the 200-500 μm size class had a significantly higher mean abundance of copepods ($720.2 \pm 1516.5 \text{ ind m}^{-3}$) significantly higher ($p = 0.000$) than that recorded for the 500-1000 μm size class ($94.8 \pm 321.4 \text{ ind m}^{-3}$) ($p = 0.04$) and the >1000 μm size class ($0.7 \pm 1.3 \text{ ind m}^{-3}$) ($p = 0.000$) (Figure 5c).

Figure 4 – Composition by size class: (A) Venn diagram based on the number of species among size fractions; (B) Relative abundance (%) of Copepoda assemblage by size fraction in Rio Formoso, Brazil.



Source: The author, 2022.

5.2.3.4 Biomass and secondary production

The total biomass (more abundant species) recorded in the area was 11.9 mg C m^{-3} , ranging from 0.4 mg C m^{-3} (February - RF1 and 0.9 mg C m^{-3} in March - RF3) to 5.4 mg C m^{-3} (September - RF2 and October - RF3). Spatially, a high numerical biomass value was recorded at station RF3 (7.2 mg C m^{-2}), followed by RF2 (4.2 mg C m^{-3}) and RF1 (0.6 mg C m^{-3}).

The mean biomass of the copepod assembly ranged from $0.04 \pm 0.03 \text{ mg C m}^{-3}$ (February - RF1) to $0.59 \pm 0.065 \text{ mg C m}^{-3}$ (September - RF2 and October - RF3). The months of February and March ($0.09 \pm 0.07 \text{ mg C m}^{-3}$) recorded the lowest means, although the temporal effect was not detected (Figure 5d). Among sampling stations, the average biomass was $0.07 \pm 0.06 \text{ mg C m}^{-3}$ in RF1, $0.46 \pm 0.43 \text{ mg C m}^{-3}$ RF2 and $0.79 \pm 0.85 \text{ mg C m}^{-3}$ RF3, however, statistical differences were not recorded (Figure 5e).

Among size classes, the mean biomass was $0.97 \pm 1.23 \text{ mg C m}^{-3}$ $200/500\mu\text{m}$, $0.35 \pm 0.71 \text{ mg C m}^{-3}$ $500/1000\mu\text{m}$ and $0.002 \pm 0.007 \text{ mg C m}^{-3}$ $>1000\mu\text{m}$. The effect of size was recorded on copepod biomass (Kruskal-Wallis, $p = 0.000$), where values identified for the $200/500\mu\text{m}$ class were significantly greater than those identified for the $500/1000\mu\text{m}$ and $>1000\mu\text{m}$ classes (Multiple comparisons a posteriori test: $200/500\mu\text{m}$ vs. $500/1000\mu\text{m}$, $p = 0.0004$; $200/500 \mu\text{m}$ vs. $>1000\mu\text{m}$, $p = 0.0000$) (Figure 5f).

The species that had the highest contributions to the overall biomass of the assembly were: *P. crassirostris*, *E. acutifrons*, *A. lilljeborgii*, *P. acutus* and *D. oculata* (Table 3). Among the months, in terms of total biomass, September and October recorded the highest biomass values of copepods (September: *E. acutifrons*, *P. crassirostris*, *P. quasimodo* and *D. oculata*; October: *P. crassirostris*, *D. oculata* and *A. lilljeborgii*) (Figure 6a).

Spatially, the high contribution of the species *E. acutifrons* and *P. crassirostris* in RF2 and in RF3 *P. crassirostris* was the species that contributed most in biomass (Figure 6b). Among the size classes, most species had their highest values in the $200/500 \mu\text{m}$ size class, where *P. crassirostris*, *A. lilljeborgii*, *P. quasimodo* and *D. oculata* were the species that contributed the most in this size class. In the $500/1000\mu\text{m}$ size class the medium/large size species *E. acutifrons* and *P. acutus*. In the largest size class $>1000 \mu\text{m}$ the biomass value was very low (Figure 6c).

Table 3 – Biomass (total and mean \pm SD, mg C m $^{-3}$) and Production (total and mean SD, mg C m $^{-3}$ d $^{-1}$) of the most abundant taxonomic groups from the Copepoda assemblage captured from Rio Formoso, Brazil.

Taxa	Biomass		Production	
	Total	Mean \pm SD	Total	Mean \pm SD
Copepod nauplii	0.21	0.02 \pm 0.02		
<i>Acartia lilljeborgii</i>	1.42	0.05 \pm 0.13	3.97	0.14 \pm 0.38
<i>Paracalanus quasimodo</i>	1.21	0.11 \pm 0.16	3.04	0.27 \pm 0.38
<i>Parvocalanus crassirostris</i>	4.00	0.36 \pm 0.55	10.16	0.92 \pm 1.37
<i>Pseudodiaptomus acutus</i>	1.39	0.08 \pm 0.12	3.52	0.21 \pm 0.33
<i>Dioithona oculata</i>	1.12	0.11 \pm 0.22	3.20	0.31 \pm 0.66
<i>Oithona nana</i>	0.19	0.01 \pm 0.02	0.53	0.04 \pm 0.05
<i>Oithona oswaldoocruzi</i>	0.34	0.03 \pm 0.03	0.95	0.09 \pm 0.10
<i>Euterpina acutifrons</i>	2.08	0.29 \pm 0.47	5.18	0.74 \pm 1.21

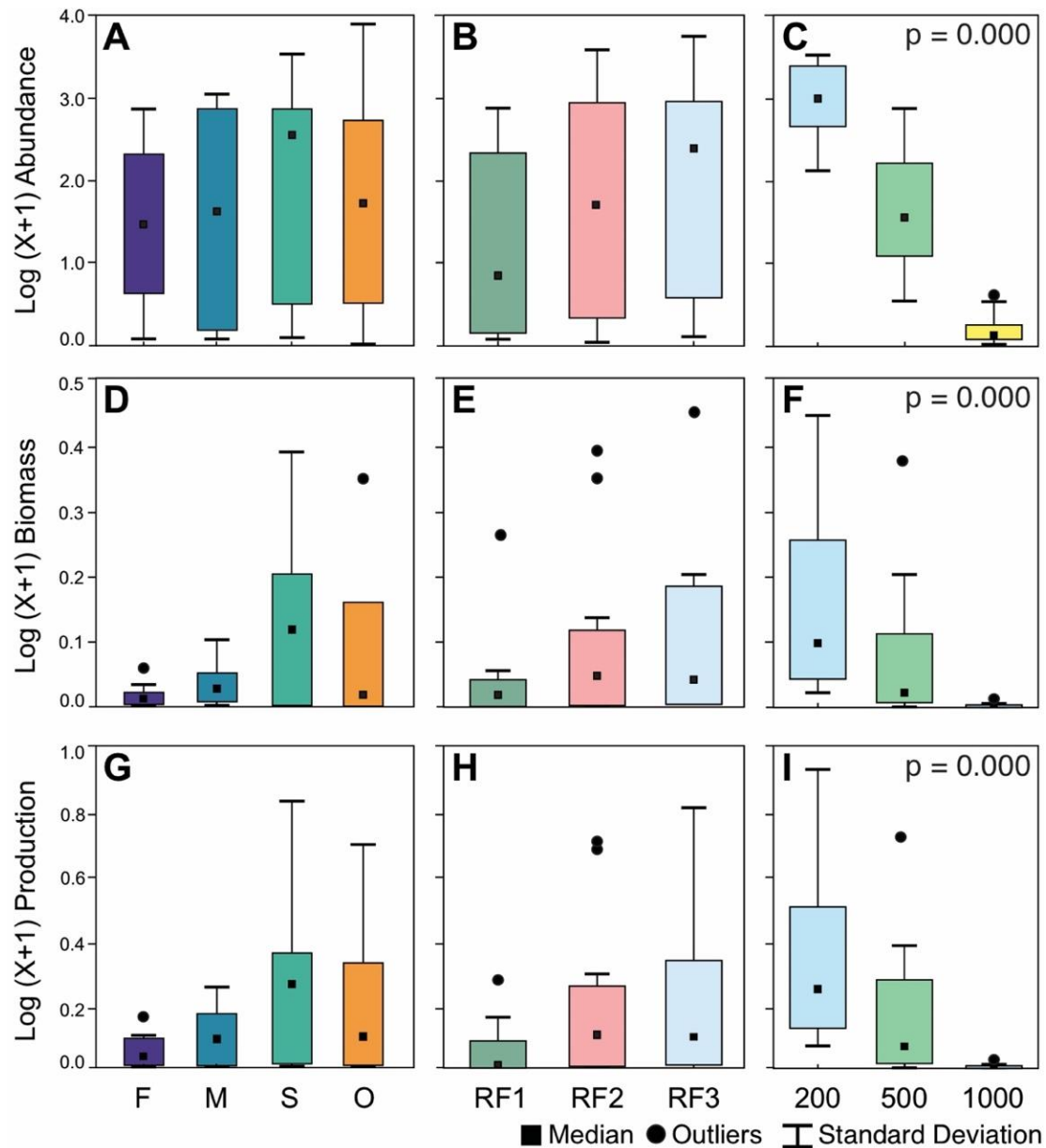
Source: The author, 2022.

The total production (more abundant species) recorded in the area was 31.2 mg C m $^{-3}$ d $^{-1}$, ranging from 1.0 mg C m $^{-3}$ d $^{-1}$ (February - RF1) to 15.0 mg C m $^{-3}$ d $^{-1}$ (October - RF3). The first two months of the study showed similar low biomass: 1.0 mg C m $^{-3}$ d $^{-1}$ February and 2.2 mg C m $^{-3}$ d $^{-1}$ March. In the last two months there has been a 10x increase compared to the first two months: 13.0 mg C m $^{-3}$ d $^{-1}$ September and 15.0 mg C m $^{-3}$ d $^{-1}$ October. Among the stations as well as the biomass, the distribution of production showed a gradient from the outermost to the innermost: 9.4 mg C m $^{-3}$ d $^{-1}$ RF1, 6.9 mg C m $^{-3}$ d $^{-1}$ RF2, and 1.4 mg C m $^{-3}$ d $^{-1}$ RF3.

The average production of the assembly ranged from 0.11 \pm 0.08 mg C m $^{-3}$ d $^{-1}$ (February - RF1) to 1.7 \pm 1.8 mg C m $^{-3}$ d $^{-1}$ (October - RF3). The other months averaged: 0.3 \pm 0.2 mg C m $^{-3}$ d $^{-1}$ February and 1.4 \pm 1.8 mg C m $^{-3}$ d $^{-1}$ September. Temporally, no statistical differences were recorded (Figure 5g). Among sampling stations, the mean production was 0.2 \pm 0.1 mg C m $^{-3}$ d $^{-1}$ RF1, 0.8 \pm 1.1 mg C m $^{-2}$ d $^{-1}$ RF2 and 1.0 \pm 1.2 mg C m $^{-3}$ d $^{-1}$ RF3, also no spatial difference was recorded (Figure 5h).

Among the size classes, the average production was 2.5 \pm 3.1 mg C m $^{-3}$ d $^{-1}$ 200/500 μ m, 0.9 \pm 1.7 mg C m $^{-3}$ d $^{-1}$ 500/1000 μ m and 0.006 \pm 0.01 mg C m $^{-3}$ d $^{-1}$ >1000 μ m. Size classes statistical differences was recorded on copepod production (Kruskal-Wallis, p = 0.000), where values recorded for the 200/500 μ m class were higher than those recorded for the 500/1000 μ m and >1000 μ m classes (Multiple comparisons a posteriori test: 200/500 μ m vs. 500/1000 μ m, p = 0.000; 200/500 μ m vs. >1000 μ m, p = 0.006) (Figure 5i).

Figure 5 – Box-Plot (median and quartiles) representing the Log(X+1) of abundance, biomass and production of the Copepoda assemblage by: **Abundance:** (A) Temporal, (B) Spatial: RF1, RF2 e RF3 and (C) Size fraction 200/500 μm , 500/1000 μm and >1000 μm . **Biomass:** (D) Temporal, (E) Spatial and (F) Size fraction. **Production:** (G) Temporal, (H) Spatial and (I) Size classes. Samples collected using the 200 μm mesh in 2020 in Rio Formoso, Brazil.



Source: The author, 2022.

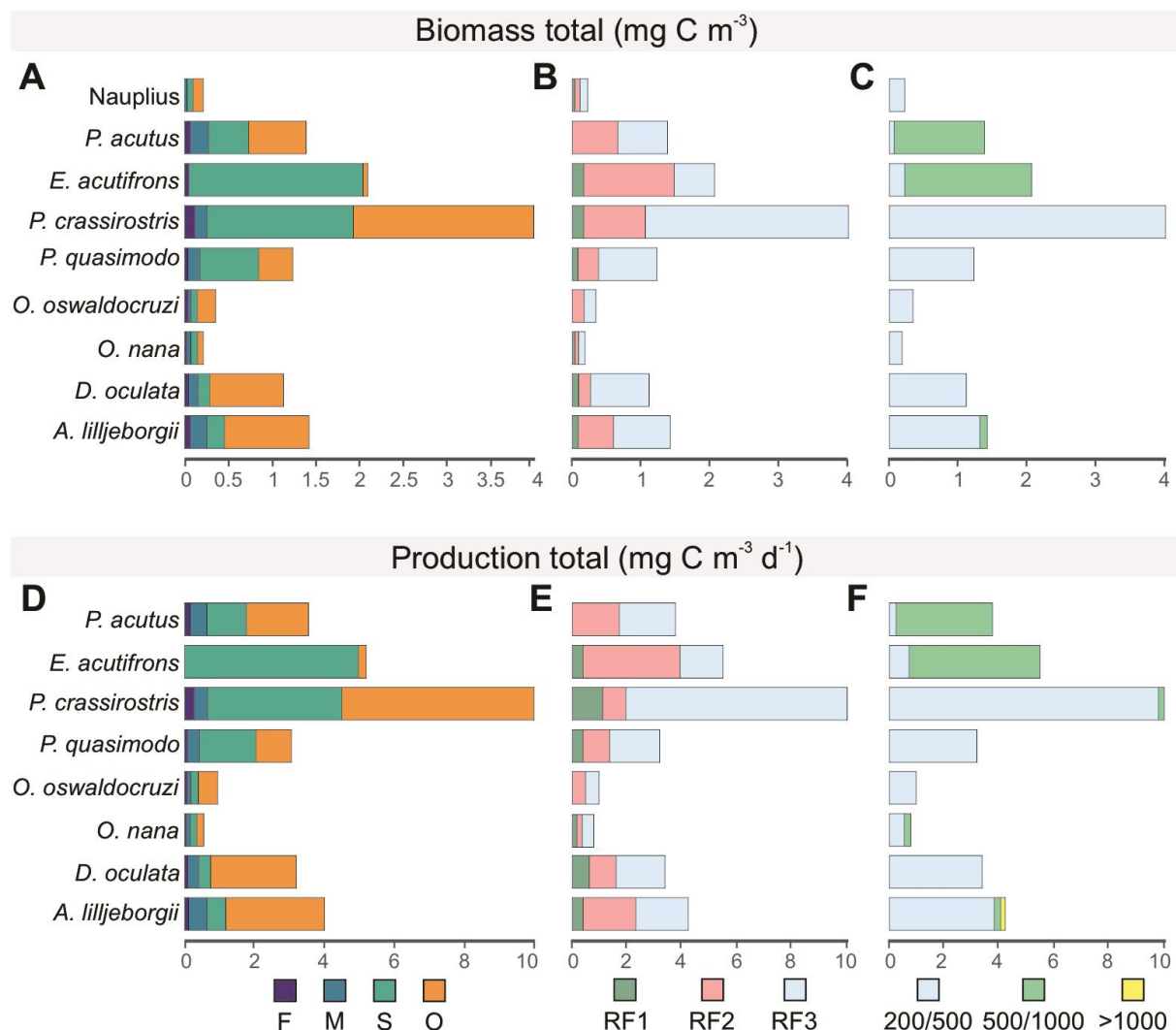
The species with the highest contribution to overall assembly production were: *P. crassirostris*, *E. acutifrons*, *A. lilljeborgii*, *P. acutus* and *D. oculata*, following the same pattern as for biomass (Table 3). As with the biomass between months, in terms of total production, September and October

had the largest contributions (September: *E. acutifrons*, *P. crassirostris*, *P. quasimodo* and *D. oculata*; October: *P. crassirostris*, *A. lilljeborgii* and *D. oculata*) (Figure 6e).

Among the stations, in terms of total production, in station RF1 the contributions were low, but the species *P. quasimodo* stands out. For station RF2 we highlighted the species *E. acutifrons*, *P. acutus* and *A. lilljeborgii* and for RF3 the species *P. crassirostris* (Figure 6f).

Between size classes, in terms of total production per specific contribution, as well as abundance and biomass, most species had their highest values in the 200/500 μm size class (Most contributed: *P. crassirostris*, *A. lilljeborgii*, *P. quasimodo* e *D. oculata*). In the 500/1000 μm class the medium/large size species *E. acutifrons* and *P. acutus* were most productive, and these same species contributed in the >1000 μm class (Figure 6g).

Figure 6 – Biomass (mg C m^{-3}) and production ($\text{mg C m}^{-3} \text{ d}^{-1}$) of Copepoda by time series species (A - E), season (B - F) and size class (C - G) in Rio Formoso, northeast of Brazil.



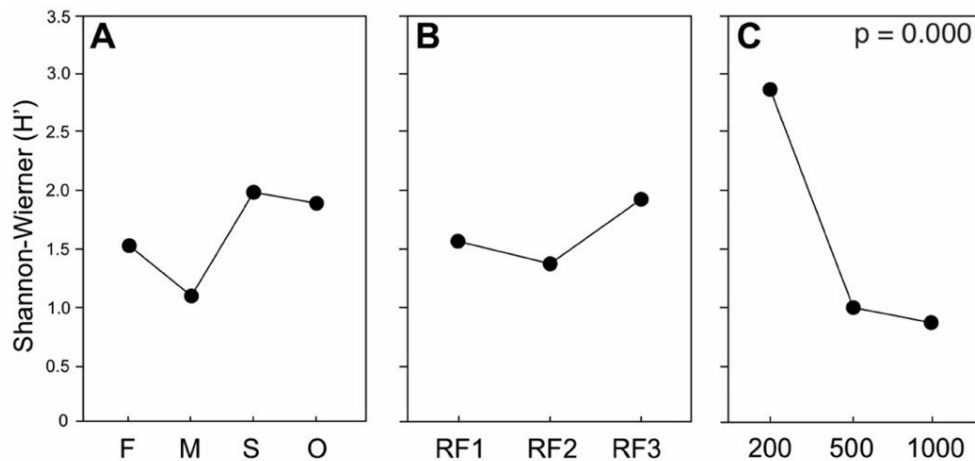
Source: The author, 2022.

5.2.3.5 Diversity

The mean values of Shannon's (H') species diversity index observed on the investigated factors (temporal, spatial and size fraction), indicate low diversity for the month of February (RF1: 1.5 ± 1.1 bits ind^{-1}) and March (RF2: 0.9 ± 1.3 bits ind^{-1}) and medium in September (RF2 2 ± 0.8 bits ind^{-1}) and October (RF3: 1.9 ± 1 bits ind^{-1}) (Figure 7a). On the spatial factor it was possible to observe higher diversity at the outermost station (RF3 - 1.9 ± 1 bits ind^{-1}) and the two inner ones had similar diversities (RF1 - 1.6 ± 1 and RF2 - 1.4 ± 1.2 bits ind^{-1}) (Figure 7b). Analysis of variance identified no significant differences between the means recorded for the temporal and spatial factor.

As for the size fraction factor, it was possible to observe medium diversity in the 200/500 μm size class - 2.7 ± 0.3 bits ind^{-1} and low in the other classes: 500/1000 μm - 1.2 ± 0.8 bits ind^{-1} and $>1000\mu\text{m}$ - 0.9 ± 0.8 bits ind^{-1} (Figure 7c). The means differed significantly (ANOVA, $p = 0.000$), where it was observed that the mean value recorded in the 200/500 μm size class differed from the other two classes 500/1000 μm (Tukey HSD, $p = 0.0001$) and $>1000\mu\text{m}$ (Tukey HSD, $p = 0.0001$).

Figure 7 – Average values of the Shannon diversity index (H') in Rio Formoso: (A) Annual variability of diversity; (B) Variety in terms of spatial diversity; (C) Variety in terms of the size fractions of the diversity.



Source: The author, 2022.

5.2.3.6 Structure of the copepod assemblage

PERMANOVA indicated that the structure of the copepod assembly in terms of abundance, biomass and production differed according to size class factor (Table 4). Paired tests for the size fraction factor in relation to abundance the three size classes (200/500 μm vs. 500/1000 μm vs. $>1000\mu\text{m}$) differ significantly in the quantitative taxonomic composition of the copepod assembly

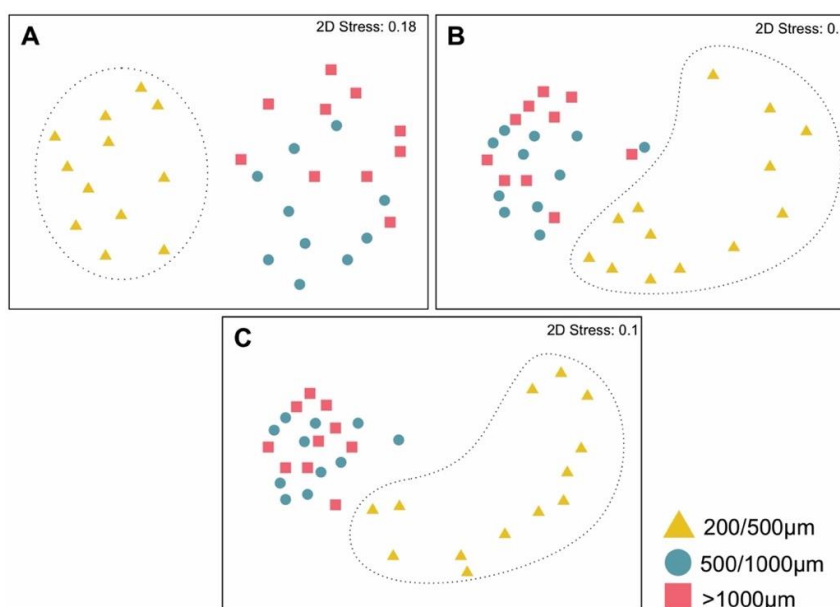
(abundance, biomass and production). Regarding biomass and production, the paired test showed that the 200-500 μm fraction is different from 500-1000 μm and >1000 μm . The MDS graphically shows these differences recorded by PERMANOVA in copepod assembly structure in response to the size fraction factor for abundance, biomass and production (Figure 8).

Table 4 – PERMANOVA analysis for the most abundant taxa (>2%) based on the abundance, biomass and production of the copepod assemblage structure in relation to the factors Size class and Spatial.

PERMANOVA	df	MS	Pseudo-F	<i>P</i> (perm)	<i>P</i> (MC)
Abundance					
Size Class	2	12725	113.72	0.001	0.001
Spatial	2	331.2	2.9599	0.227	0.2073
Size class x Spatial	4	125.2	1.119	0.477	0.4261
Biomass					
Size Class	2	873.78	12.408	0.001	0.003
Spatial	2	247.59	3.5161	0.117	0.104
Size class x Spatial	4	113.93	1.6179	0.302	0.297
Production					
Size Class	2	3942.5	40.905	0.001	0.001
Spatial	2	458.17	4.7537	0.082	0.085
Size class x Spatial	4	168.57	1.749	0.271	0.281

Source: The author, 2022.

Figure 8 – Multidimensional Scaling (MDS) for the copepod assemblage in response to the Size Fraction factor in (A) abundance, (B) biomass and (C) production: 200/500 μm (yellow triangle), 500/1000 μm (blue circle) and >1000 μm (pink square).



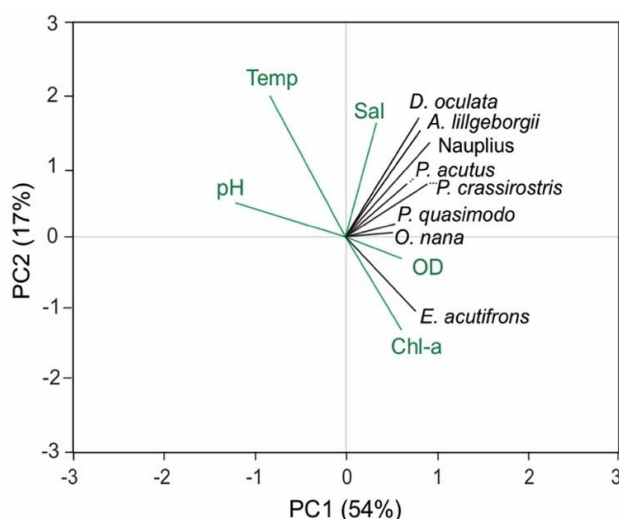
Source: The author, 2022.

The MDS formed two distinct groups. The first corresponds to the size class 200/500 µm and the second a merged group of the classes 500/1000 µm and >1000 µm (Figure 8 a, b and c).

In abundance, SIMPER shows a dissimilarity of 89.7% between size classes 200/500µm vs. 500/1000µm, where the taxa nauplii (16.8%), *P. crassirostris* (14.1%), *P. quasimodo* (12%), *D. oculata* (11.5%) contribute 54.5% of this dissimilarity. Between the 200/500µm vs. >1000µm classes there was 98.4% dissimilarity and the same taxa above mentioned (Nauplii 17.9%, *P. crassirostris* 15%, *P. quasimodo* 12%, *D. oculata* 12.7%) contributed 57.6%. Between the fractions 500/1000µm vs. >1000µm there was 92.5% dissimilarity and the species *P. acutus* (47.3%) and *A. lilljeborgii* (24.4%) contributed with 71.7%.

SIMPER, for biomass, shows 96.8% dissimilarity between the 200/500µm vs. 500/1000µm size classes, where the species *P. crassirostris* (23.3%), *P. acutus* (18.4%), *E. acutifrons* (13.4%), and *A. lilljeborgii* (12.6%) contribute with 67.8% of this dissimilarity. Between the 200/500 µm vs. >1000 µm classes there was 97.2% dissimilarity, where the species *P. crassirostris* (30.4%), *P. quasimodo* (17.4%), *A. lilljeborgii* (17.1%) and *D. oculata* (12.1) contributed with 77%. For production SIMPER showed a 96.5% dissimilarity between the 200/500 µm vs. 500/1000µm size classes where *P. crassirostris* (21.9%), *P. acutus* (17.9%), *A. lilljeborgii* (13.2%) and *P. quasimodo* (12.7%) contributed 65.8%. Between classes 200/500 µm vs. >1000µm there was 98.2% dissimilarity as *P. crassirostris* (28.2%), *A. lilljeborgii* (17.7%), *P. quasimodo* (17.3%) and *D. oculata* (12.4) contributed with 75.6%.

Figure 9 – Principal component analysis (PCA) results of environmental variable vectors (Temp = temperature, pH, DO = dissolved oxygen, Sal = salinity and Chl-a = chlorophyll-a / green vectors) and black vectors dominant species.



Source: The author, 2022.

The principal component analysis (PCA) explained 71% of the data variation (Figure 9); axis 1 explained 54% (PC1) and the axis 2 explained 17% (PC2). Salinity and pH were the main factors responsible for the distribution of *D. oculata*, *O. nana*, *P. crassirostris* and *F. gracilis*, showing that the distribution of these species correlated positively with the salinity gradient and also neutral pH. The species *E. acutifrons*, *P. quasimodo*, Copepoda nauplii, *A. lilljeborgii* and *L. nerii* were positively related to dissolved oxygen and chlorophyll-a factors. Evidencing that the abundance of these species is favored by high dissolved oxygen levels in the water and high chlorophyll-a concentrations, it is also possible to observe that temperature has a negative effect on these species.

5.2.4 Discussion

This paper is the first attempt to investigate the spatial and temporal variability of copepod abundance, biomass and production in the estuarine EPA of Rio Formoso. The results did not show considerable spatial-temporal variability in trends of copepod abundance, biomass and production. This fact may be related to our number of samples. Although trends were observed and considered, especially when considering different size categories within the copepod assemblage.

5.2.4.1 Environmental variables and phytoplanktonic biomass (chlorophyll-a)

In estuarine environments, factors such as temperature, salinity and pH are key parameters for the successful development of biological communities (FEITOSA *et al.*, 1999; SANTOS *et al.*, 2009). They can act directly on the spatial distribution and timing of aquatic organisms, providing a great importance in biological productivity, and can be considered ecological barriers for the speciation of more sensitive organisms (FEITOSA *et al.*, 1999; SANTOS *et al.*, 2009). The patterns of monthly variation for the dry season, recorded, correspond to those characteristics for the region (rainfall, salinity and temperature) (LIMA *et al.*, 2012; MOURA, 1991; NEUMANN-LEITÃO *et al.*, 1995; SILVA *et al.*, 2009). The estuary is classified as mesohaline/euhaline, well mixed without thermal stratification in the water column (HANSEN; JR, 1966; LIRA *et al.*, 1979; SILVA *et al.*, 2009).

According to Macêdo *et al.* (2000), the values attributed to dissolved oxygen and pH are influenced by the photosynthetic rate/respiration and the tidal cycles, however, the capacity of neutralization existing in the aquatic ecosystem due to the buffer effect prevents the occurrence of great variation of pH and the highest values are obtained in the most saline areas. In the results

presented here dissolved oxygen is within the standard for the region (SILVA *et al.*, 2009; SILVA *et al.*, 2019), as is pH (neutral/alkaline) (LIRA *et al.*, 1979; MARQUES *et al.*, 2015; SILVA *et al.*, 2009). These patterns were due to the input of marine waters/salt wedge amplitude (LIRA *et al.*, 1979) and response of the physiology of organisms the biogeochemical cycles of the environment (BECK; BRULAND, 2000; MACÊDO *et al.*, 2000).

The RF2 station showed an increase in phytoplankton biomass compared to the other two (RF1 and RF3). These high values would be associated with the meeting of the Formoso River flow with the Ariquindá River mouth, causing an increase in productivity in this area. Seasonally, phytoplankton biomass varied from oligotrophic (February and March) to hypereutrophic (September and October) according to Passavante (2003) classification. Honorato da Silva *et al.* (2004), when analyzing for the first time the phytoplankton in the Formoso River estuary, observed a very high phytoplankton biomass variation (2.45 to 70.22 mg.m⁻³ - higher values in the dry period), similar to the present study.

5.2.4.2 Composition and abundance of the copepod assemblage

The major differences between estuarine and marine zooplankton are related to high abundance and low diversity, being characterized basically by small species of the orders Cyclopoida and Calanoida (ARA, 1998; DAVID *et al.*, 2006; DUGGAN *et al.*, 2008). When papers published in several Brazilian estuaries are analyzed, a pattern is seen among the dominant genera (*Acartia*, *Paracalanus* and *Oithona*) (NEUMANN-LEITÃO, 1994; ARA, 2004; DIAS; BONECKER, 2008; GONÇALVES, 2016).

The results indicate that the taxonomic groups identified are similar to those verified by previous studies carried out in Rio Formoso and follow the pattern of domain specificity in Brazilian estuaries. The important contribution of the copepod species *P. crassirostris*, *A. lilljeborgii*, *D. oculata* and *E. acutifrons*, which are also evidenced by studies developed in the area (LIMA *et al.*, 2012; MOURA, 1991; NEUMANN-LEITÃO *et al.*, 1995). Additionally, the marine influence on the estuary was evident through the occurrence of coastal water indicator species (*Corycaeus speciosus* and *Farranula gracilis*).

P. crassirostris it was the species that contributed the most in abundance and was constant in all months of the study. Its success in the estuarine/coastal environment is related to its great tolerance to salinity and temperature, occurring in several parts of the world (limited by coastal waters) (MATSUMURA-TUNDISI, 1972). NEUMANN-LEITÃO *et al.* (1995) studying the zooplankton

communities in Rio Formoso found that *P. crassirostris* contributed the most to the copepod assemblage, corroborating our data.

A. lilljeborgii is a predominant species in several neritic/ estuarine environments, has been recorded in almost all Brazilian estuaries and is commonly associated with eutrophicated environments (BJÖRNBERG, 1981; DIAS, 1999; NEUMANN-LEITÃO, 1995). In the present study it was the second species that most contributed to the abundance of the assembly. Usually, copepods of the genus *Acartia* dominate the biomass in most bays, lagoons and estuaries due to their body size and high tolerance to environmental variations such as salinity (AZEITERIO *et al.*, 2005; BJÖRNBERG, 1972; LEANDRO *et al.*, 2007; TEIXEIRA *et al.*, 1965).

D. oculata and congeneric species are commonly found in estuarine environments due to food availability (large number of suspended particles), wide tolerance to salinity variation and are indicators of estuarine areas (BJÖRNBERG, 1981; CALBET, 2008). As for *E. acutifrons*, like the other dominant species, it is a typical coastal species and can be found as far inland as the estuary (BJÖRNBERG, 1963). According to Matsumura-Tundisi (1972), the species can occur throughout the year with peaks of abundance following at certain times of the year (associated with food availability).

All species have tolerance to variation in salinity, temperature, and are favored in eutrophic environments. All these characteristics are found in Rio Formoso, making the environment favorable for the success of these species. An increasing gradient from the inner estuary to the mouth was recorded in terms of copepod abundance. This same pattern has been observed in other studies in the region, at stations positioned close to the present ones (LIMA *et al.*, 2012; NEUMANN-LEITÃO *et al.*, 1995). The higher abundance of organisms in the outer stations would be associated with the contribution of the Ariquindá river exporting nutrients and contributing to local productivity (increasing primary producers and reflecting from consumers). This increase in nutrients and productivity at the outer stations was demonstrated by Honorato da Silva *et al.* (2004).

Temporally it was possible to observe an increase in abundance in the last two months of the study (September and October). In October, in particular, there was a spike in phytoplankton biomass (section 4.1) and also a spike in the species *P. crassirostris* and *E. acutifrons*. The peak of these two species may be in response to the peak producers, since *P. crassirostris* feeds on picoplankton and nanoplankton (CALBET *et al.*, 2000) and *E. acutifrons* is herbivorous (COSTA; FERNÁNDEZ, 2002). The principal component analysis indicated that the distribution of *E. acutifrons* would be positively correlated to chlorophyll-a.

Studies with mesozooplankton in Rio Formoso show a high diversity (justified by the high marine influence in the area) (LIMA *et al.*, 2012; NEUMANN-LEITÃO *et al.*, 1995), even though

classically estuaries are expected to have low diversities (TUNDISI; TUNDISI, 1968). The results reported here follow the classification of Valentin *et al.* (1991). The data in this study corroborate with the results of Tundisi e Tundisi (1968), where the authors explain that estuarine environments are characterized by high population abundance, but with a reduced number of dominant species (five or six). The low to medium diversity in Rio Formoso was due to the dominance of eight species, which accounted for up to 90% of the entire assemblage abundance.

5.2.4.3 Biomass and secondary productivity

Silva *et al.* (2019) when studying the seston biomass and suspended particles in Rio Formoso, found that the area has a high rate of suspended particles and is intensified in the summer, coinciding with the local high season. It is known that when copepods are exposed to an environment with high concentrations of detritus, the feeding rate is reduced. The detritus can decrease the phytoplankton consumption rate by the copepods, due to the obstruction of the buccal apparatus responsible for filtration, decreasing the assimilation rate and ends up decreasing the secondary production of the copepods (CHERVIN, 1978). Because of this, the most efficient methodology was used to determine the growth rates (one of the steps to obtain productivity (HIRST; BUNKER, 2003).

Estuarine ecosystems are usually characterized by high values of zooplankton biomass and secondary production (DAVID *et al.*, 2006). The present study was conducted during the dry period, and when comparing the average biomass ($1.3 \pm 1.2 \text{ mg C m}^{-3}$) and production ($3.4 \pm 3.0 \text{ mg C m}^{-3} \text{ d}^{-1}$) it is within the average of other Brazilian estuaries for the same period (with the same growth rate methodologies). Taperaçu estuary (Amazonas, Brazil) in the dry period was observed an average biomass of $2.9 \pm 1.0 \text{ mg C m}^{-3}$ and an average production of $6.9 \pm 2.4 \text{ mg C m}^{-3} \text{ d}^{-1}$ (MAGALHÃES *et al.*, 2011). Pina basin estuary (Pernambuco, Brazil) recorded a total biomass of $10 \pm 13.7 \text{ mg m}^{-3}$ and a mean production $1.2 \pm 1.2 \text{ mg C m}^{-3} \text{ d}^{-1}$ (MAGALHÃES, 2014).

In the present study, the species that contributed most in biomass and production were: *P. crassirostris*, *E. acutifrons* (only in September), *A. lilljeborgii*, *P. acutus* and *D. oculta*. Magalhães (2014) studying the copepod assemblage of the estuary in the Pina's Basin (Pernambuco, Brazil), found that small species contribute the most in biomass and production, with the highest values recorded in the dry season. Neumann-Leitão (2010) studying the abundance and biomass in the estuaries of rivers Botafogo and Carrapicho (North of Pernambuco), saw that the largest contributions also occur in the dry season and that small/medium sized species were more representative. This higher input in the dry period can be explained by the rainfall patterns in Pernambuco, because,

according to Nordi (1982) and Schwamborn *et al.* (2006), northeastern Brazil presents a pattern of sudden and heavy rains that decrease the salinity causing organisms to die and escape. In the present study, *P. crassirostris* and *D. oculata* contributed the most in biomass and recurrent production and *E. acutifrons* in the month of October (in response to high food availability).

In a study by Paiva *et al.* (2008), on the ichthyofauna of Rio Formoso, it was found that the trophic structure of fish in the estuary is composed of 8.4% planktonic fish (phytoplankton and zooplankton). It is known that fish are part of the meroplankton, that is, they have their larval stage in the plankton (OMORI; IKEDA, 1984). While they are larvae, fish are efficient predators of plankton, especially, smaller species of zooplankton (due to the difficulty of escaping predators) (RÉ, 1999). The species *P. crassirostris*, *D. oculata* and *E. acutifrons* are very important contributors in terms of biomass and production in the estuary of Rio Formoso and are species that are within the size range of larval fish and adult planktonic fishes like *Anchoa tricolor* and *Anchovia clupeoides* (species verified by Paiva et al. 2008 that occur in Rio Formoso), therefore justifying their importance in the maintenance of local stocks and energy transfer along the estuarine trophic web.

5.2.5 Conclusions

- The Rio Formoso estuary presents a great marine influence. This influence can be demonstrated by the occurrence of typically coastal/oceanic species and by the salinity explaining the distribution of most of the samples;
- As in other estuaries, the diversity in Rio Formoso was considered low with high abundance of species resilient to environmental variation;
- The peak phytoplankton biomass in the months of September and October favored grazing species, reinforced by the increase in biomass of herbivorous species in the last two months;
- The species *P. crassirostris*, *A. lilljeborgii*, *D. oculata* and *E. acutifrons* contributed the most in biomass and production in the assembly, suggesting that they are the main Copepoda species for the maintenance of the food web in Tamandaré.
- Due to its high contributions of biomass and production, *P. crassirostris* was considered the key species in the estuarine of Rio Formoso. Its dominance may be related to its feeding plasticity, low ingestion, mortality and metabolism rates, which makes it more stable, based on its high abundance, biomass and production rates, for all areas and months investigated.

5.2.6 Acknowledgments

This work was financed by the Fundação de Amparo à Ciência e Tecnologia de Pernambuco (FACEPE) under the grant number PBPG-0069-1.08/20. And to the same organ, we would like to express our thanks for granting the scholarship to the first author. We thank the Sustainable Tamandaré Long-Term Ecological Program (PELD TAMS) for providing all the necessary structure for the collections. To the Laboratory of Phytoplankton Laboratory (LabFito/UFPE) for granting the data of chlorophyll-a and phytoplankton biomass. And to the Oceanography Department of the Federal University of Pernambuco, for granting the use of the Marine Zooplankton Laboratory (LabZoo/UFPE).

6 CONSIDERAÇÕES FINAIS

- A presente dissertação teve como objetivo observar a heterogeneidade espaço-temporal da estrutura da assembleia de copépodes mesozooplanctônicos em duas áreas costeiras, bem como observar quaisquer alterações em relação a estrutura dos copépodes pelo derreamento de petróleo. Em decorrência da pandemia (COVID-19 em 2020 - *lockdown*) o programa de amostragem do trabalho foi afetado. A proposta inicial seria analisar o efeito do petróleo sobre os copépodes durante o ano (12 meses, seco e chuvoso), porém, não foi possível a realização das coletas para a obtenção dos dados de HPA e dos copépodes no período chuvoso (apenas seco). Para Tamandaré (única área de estudo com dados HPA) possuímos apenas dados para dois meses, dados estes insuficientes para correlacionar quaisquer alterações sobre a estrutura da assembleia de copépodes com o derramamento de petróleo. Devido a plasticidade adaptativa que os copépodes possuem, analisar os efeitos de poluentes na água se torna um desafio, uma vez que seu curto período de vida os efeitos são demonstrados de forma aguda e não crônica. Apesar disso, este foi o primeiro trabalho em Tamandaré a estudar as três principais áreas encontradas na região (pluma estuarina, baía e recife), pois, estudos na região com os copépodes apenas foram feitos sobre o topo recifal e comunidades demersais. E para o complexo estuarino do Rio Formoso foi o primeiro trabalho investigar o fluxo de biomassa e produtividade da assembleia de copépodes residentes.
- Entre as áreas foi possível observar um número semelhante de taxa, sendo observados 38 em Tamandaré e 34 no Rio Formoso. Por se tratarem de regiões próximas, a composição da assembleia e as espécies mais abundantes também foram semelhantes. Todas as espécies dominantes possuíam alta tolerância a variações ambientais, principalmente salinidade e temperatura.
- As espécies *Dioithona oculata* e *Paracalanus quasimodo* foram as que mais produziram em Tamandaré. A primeira devido ao enxame registrado (comumente encontrado na região) e a segunda condicionada a disponibilidade alimentar (principalmente na estação baía onde foi registrados seus maiores valores de abundância e produtividade secundária). No Rio Formoso *Parvocalanus crassirostris* foi a espécie que mais produziu e sua produção foi influenciada pelos picos nos produtores primários (sua fonte de alimento) nos dois últimos meses. Esse mesmo comportamento foi visto para outras espécies no estuário.
- Foi visto que a rede de 200 μm não é eficiente para a coleta de *Acartia lilljeborgii*, evidenciada por sua grande contribuição em classes de tamanho maiores. Comparou-se trabalhos entre as redes de 200 μm vs. 300 μm , essa espécie apresentou com maiores abundâncias na rede de 300 μm .

- A pluma estuarina em Tamandaré possui grande influencia na região como todo, servindo como exportador de produtividade primaria (evidenciado pela biomassa fitoplanctônica) aumentando a produtividade secundaria na região. Espacialmente também foi visto que a dinâmica ecossistêmica na região recifal age como sumidouro de produtividade secundária.
- Os dados (abundância, biomassa, produção e diversidade) para Tamandaré reafirmaram o período favorável para o mesozooplâncton descrito por trabalhos anteriores na região.
- O Rio Formoso possui uma grande influencia marinha, este ponto ficou evidenciado ao registrarmos espécies tipicamente costeiras na estações mais internas do estuário.
- Seguindo o padrão para áreas costeiras, nas duas regiões a salinidade e temperatura foram as principais variáveis ambientais responsáveis pela distribuição da assembleia de copépodes.
- De forma geral, os resultados obtidos aqui possibilitaram um maior conhecimento sobre a assembleia de copépodes mesozooplânctônica costa brasileira. Ressaltando dois pontos: 1 - a importância do uso de metodologias de análises do zooplâncton por classes de tamanho, uma vez que as redes de amostragem de plâncton podem selecionar os organismos e a metodologia clássica de quarteamento da amostra total pode superestimar espécies de grande porte (em especial para a rede de 200µm); 2 - a distribuição da assembleia de copépodes em regiões costeiras está condicionada a variações de parâmetros ambientais e ecossistêmicos, sobretudo a disponibilidade alimento influenciada pelo escoamento continental (proporcionando incremento dos produtores primários e refletindo na produtividade de seus consumidores).

REFERÊNCIAS

ABESSA, D.M.S.; ALBUQUERQUE, H.C.; MORAIS, L.G.; ARAÚJO, G.S. *et al.* Pollution status of marine protected areas worldwide and the consequent toxic effects are unknown. **Environmental pollution**, 243, p. 1450-1459, 2018.

AGUILAR, T.I.M. **Distribuição espacial e sazonal de grupos do microzooplâncton na Bacia de Campos em cinco massas de água, da superfície ao batipelágio**. 2013. Dissertação (Mestrado) -, Instituto Oceanográfico, Universidade de São Paulo, São Paulo - SP.

AKIN, S.; WINEMILLER, K.O.; GELWICK, F.P. Seasonal and spatial variations in fish and macrocrustacean assemblage structure in Mad Island Marsh estuary, Texas. **Estuarine, Coastal and Shelf Science**, 57, n. 1-2, p. 269-282, 2003.

ALMEDA, R.; BACA, S.; HYATT, C.; BUSKEY, E.J. Ingestion and sublethal effects of physically and chemically dispersed crude oil on marine planktonic copepods. **Ecotoxicology**, 23, n. 6, p. 988-1003, 2014.

ALMEDA, R.; WAMBAUGH, Z.; WANG, Z.; HYATT, C. *et al.* Interactions between zooplankton and crude oil: toxic effects and bioaccumulation of polycyclic aromatic hydrocarbons. **PloS one**, 8, n. 6, p. e67212, 2013.

ALVARES, C.A.; STAPE, J.L.; SENTELHAS, P.C.; GONÇALVES, J.L.d.M. *et al.* Köppen's climate classification map for Brazil. **Meteorologische Zeitschrift**, 22, n. 6, p. 711-728, 2013.

AMBLER, J.W.; FERRARI, F.D.; FORNSHELL, J.A. Population structure and swarm formation of the cyclopoid copepod *Dioithona oculata* near mangrove cays. **Journal of Plankton Research**, 13, n. 6, p. 1257-1272, 1991.

ANACLETO, E.I.; GOMES, E.T. Relações tróficas no plâncton em um ambiente estuarino tropical: Lagoa dos Patos (RS), Brasil. **Saúde Amb. Rev**, 1, n. 2, p. 26-39, 2006.

ARA, K. Variabilidade temporal dos copepodos no complexo estuarino-lagunar de Cananeia, São Paulo, Brasil. **Ph. D. Thesis, Universidade de São Paulo**, 308, 1998.

ARA, K. Length-weight relationships and chemical content of the planktonic copepods in the Cananéia Lagoon estuarine system, São Paulo, Brazil. **Plankton Biology and Ecology**, 48, n. 2, p. 121-127, 2001.

ARA, K. Temporal variability and production of the planktonic copepod community in the Cananéia Lagoon estuarine system, São Paulo, Brazil. **Zoological Studies**, 43, n. 2, p. 179-186, 2004.

ARAÚJO, M.E.d.; RAMALHO, C.W.N.; MELO, P.W.d. Pescadores artesanais, consumidores e meio ambiente: consequências imediatas do vazamento de petróleo no Estado de Pernambuco, Nordeste do Brasil. **Cadernos de Saúde Pública**, 36, 2020.

AZEITERIO, U.M.; MAQUES, S.C.; VIERA, L.M.R.; PASTORINHO, M.R.D. *et al.* Dynamics of the *Acartia* genus (Calanoida: Copepoda) in a temperate shallow estuary (the Mondego estuary) on the western coast of Portugal. **Acta Adriatica: International Journal of Marine Sciences**, 46, n. 1, p. 7-20, 2005.

AZEVEDO-SANTOS, V.M.; FREDERICO, R.G.; FAGUNDES, C.L.; POMPEU, P.S. *et al.* Protected areas: A focus on Brazilian freshwater biodiversity. **Diversity and Distributions**, 25, n. 3, p. 442-448, 2019.

BÅMSTEDT, U.; CORNER, E.D.S.; O'HARA, S.C.M. The biological chemistry of marine copepods. and O'Hara, SC M.(eds.), **The biological chemistry of marine copepods**. Clarendon Press, Oxford, p. 1-58, 1986.

BATES, A.E.; COOKE, R.S.; DUNCAN, M.I.; EDGAR, G.J. *et al.* Climate resilience in marine protected areas and the ‘Protection Paradox’. **Biological Conservation**, 236, p. 305-314, 2019.

BECK, N.G.; BRULAND, K.W. Diel biogeochemical cycling in a hyperventilating shallow estuarine environment. **Estuaries**, 23, n. 2, p. 177-187, 2000.

BEGON, M.; TOWNSEND, C.R. **Ecology: from individuals to ecosystems.** John Wiley & Sons, 2020. 1119279313.

BERGGREEN, U.; HANSEN, B.; KIØRBOE, T. Food size spectra, ingestion and growth of the copepod *Acartia tonsa* during development: Implications for determination of copepod production. **Marine biology**, 99, n. 3, p. 341-352, 1988.

BERROJALBIZ, N.; LACORTE, S.; CALBET, A.; SAIZ, E. *et al.* Accumulation and cycling of polycyclic aromatic hydrocarbons in zooplankton. **Environmental Science & Technology**, 43, n. 7, p. 2295-2301, 2009.

BEYER, J.; TRANNUM, H.C.; BAKKE, T.; HODSON, P.V. *et al.* Environmental effects of the Deepwater Horizon oil spill: a review. **Marine pollution bulletin**, 110, n. 1, p. 28-51, 2016.

BJÖNBERG, T.K.S. On the free living Copepods of Brazil. **Bolm. Inst. Oceanogr**, 13, n. 1, p. 1-142, 1963.

BJORNBERG, T. Copepoda. **Altas del Zooplancton del Atlántico sudoccidental y me'todos de Trabajo con Zooplancton marine**, p. 587-689, 1981.

BJÖRNBERG, T.K.S. Developmental stages of some tropical and subtropical planktonic marine copepods. **Studies on the fauna of Curacao and other Caribbean Islands**, 40, n. 1, p. 1-185, 1972.

BLAXTER, J.H.; DOUGLAS, B.; TYLER, P.A.; MAUCHLINE, J. **The biology of calanoid copepods.** Academic Press, 1998. 0080579566.

BOLTOVSKOY, D. **Atlas del zooplancton del Atlántico Sudoccidental y métodos de trabajo con el zooplancton marino.** Instituto Nacional de Investigación y Desarrollo Pesquero Mar del Plata. 1981.

BOLTOVSKOY, D.; CORREA, N.; BOLTOVSKOY, A. Marine zooplanktonic diversity: a view from the South Atlantic. **Oceanologica Acta**, 25, n. 5, p. 271-278, 2002.

BRADFORD-GRIEVE, J.M.; BOYD, P.W.; CHAN, F.H.; CHISWELL, S. *et al.* Pelagic ecosystem structure and functioning in the Subtropical Front region east of New Zealand in austral winter and spring 1993. **Journal of Plankton Research**, 21, n. 3, 1999.

BRAGA, E.S.; BONETTI, C.V.D.H.; BURONE, L.; FILHO, J.B. Eutrophication and bacterial pollution caused by industrial and domestic wastes at the Baixada Santista Estuarine System—Brazil. **Marine Pollution Bulletin**, 40, n. 2, p. 165-173, 2000.

BRANDINI, F.P. **Planctonologia na plataforma continental do Brasil: diagnose e revisão bibliográfica.** CEMAR/MMA/CIRM/FEMAR, 1997.

BRANDINI, F.P.; LOPES, R.M.; GUTSEIT, K.S. Planctonologia na plataforma continental do Brasil: diagnose e revisao bibliografica. In: **Planctonologia na plataforma continental do Brasil: diagnose e revisao bibliografica:** MMA, 1997.

BRITO-LOLAIA, M.; SANTOS, G.S.; NEUMANN-LEITÃO, S.; SCHWAMBORN, R. Micro-and mesozooplankton at the edges of coastal tropical reefs (Tamandaré, Brazil). **Helgoland Marine Research**, 74, n. 1, p. 1-14, 2020.

BRODIE, J.; DE'ATH, G.; DEVLIN, M.; FURNAS, M. *et al.* Spatial and temporal patterns of near-surface chlorophyll a in the Great Barrier Reef lagoon. **Marine and Freshwater Research**, 58, n. 4, p. 342-353, 2007.

BRUM, H.D.; CAMPOS-SILVA, J.V.; OLIVEIRA, E.G. Brazil oil spill response: Government inaction. **Science**, 367, n. 6474, p. 155-156, 2020.

BURKILL, P.H.; KENDALL, T.F. Production of the copepod *Eurytemora-Affinis* in the Bristol channel. **Marine Ecology Progress Series**, 7, n. 1, p. 21-31, 1982.

BUSKEY, E.J.; PETERSON, J.O.; AMBLER, J.W. he swarming behavior of the copepod *Dioithona oculata*: In situ and laboratory studies. **Limnology and Oceanography**, 41, n. 3, p. 513-521, 1996.

CALBET, A. The trophic roles of microzooplankton in marine systems. **ICES Journal of Marine Science**, 65, n. 3, p. 325-331, 2008.

CALBET, A.; LANDRY, M.R. Phytoplankton growth, microzooplankton grazing, and carbon cycling in marine systems. **Limnology and Oceanography**, 49, n. 1, p. 51-57, 2004.

CALBET, A.; LANDRY, M.R.; SCHEINBERG, R.D. Copepod grazing in a subtropical bay: species-specific responses to a midsummer increase in nanoplankton standing stock. **Marine Ecology Progress Series**, 193, p. 75-84, 2000.

CAMPELO, R.P.d.S.; LIMA, C.D.M.d.; SANTANA, C.S.d.; SILVA, A.J.d. *et al.* Oil spills: the invisible impact on the base of tropical marine food webs. **Marine Pollution Bulletin**, 167, p. 112281, 2021.

CAMPELO, R.P.S.; LIMA, C.D.M.; SANTANA, C.S.; SILVA, A.J. *et al.* Oil spills: the invisible impact on the base of tropical marine food webs. **Marine Pollution Bulletin**, 167, p. 112281, 2021.

CAVALCANTI, E.A.H.; NEUMANN-LEITÃO, S.; NASCIMENTO-VIEIRA, D.A.d. Mesozooplâncton do sistema estuarino de Barra das Jangadas, Pernambuco, Brasil. **Revista Brasileira de Zoologia**, 25, p. 436-444, 2008.

CERQUEIRA, W.R.P. Provável mortalidade de *Holothuria (Halodeima) grisea* (Selenka, 1867)(Echinodermata, Holothuroidea) após impacto agudo do derramamento de petróleo no Nordeste brasileiro em 2019. 2021.

CHERVIN, M.B. Assimilation of particulate organic carbon by estuarine and coastal copepods. **Marine Biology**, 49, n. 3, p. 265-275, 1978.

CHISHOLM, L.A.; ROFF, J.C. Abundances, growth rates, and production of tropical neritic copepods off Kingston, Jamaica. **Marine Biology**, 106, n. 1, p. 79-89, 1990.

CHUWEN, B.M.; HOEKSEMA, S.D.; POTTER, I.C. The divergent environmental characteristics of permanently-open, seasonally-open and normally-closed estuaries of south-western Australia. **Estuarine, Coastal and Shelf Science**, 85, n. 1, p. 12-21, 2009.

CIOTTI, M.; CICCOZZI, M.; TERRINONI, A.; JIANG, W.-C. *et al.* The COVID-19 pandemic. **Critical reviews in clinical laboratory sciences**, 57, n. 6, p. 365-388, 2020.

COSTA, K.; QUEIROZ, C.; MACÊDO, S. Hidrologia e plankton da Plataforma Continental de Pernambuco 1. Variação das características físico-químicas da água. **Encontro Brasileiro de Gerenciamento Costeiro III**, p. 337-371, 1985.

COSTA, R.r.M.d.; FERNÁNDEZ, F. Feeding and survival rates of the copepods *Euterpina acutifrons* Dana and *Acartia grani* Sars on the dinoflagellates *Alexandrium minutum* Balech and *Gyrodinium corsicum* Paulmier and the Cryptophyta *Rhodomonas baltica* Karsten. **Journal of Experimental Marine Biology and Ecology**, 273, n. 2, p. 131-142, 2002.

CRAVEIRO, N.; DE ALMEIDA ALVES, R.V.; DA SILVA, J.M.; VASCONCELOS, E. *et al.* Immediate effects of the 2019 oil spill on the macrobenthic fauna associated with macroalgae on the tropical coast of Brazil. **Marine Pollution Bulletin**, 165, p. 112107, 2021.

DASGUPTA, S.; PENG, X.; CHEN, S.; LI, J. *et al.* Toxic anthropogenic pollutants reach the deepest ocean on Earth. **Geochem. Perspect. Lett.**, 7, p. 22-26, 2018.

DAVID, V.; SAUTOUR, B.; GALOIS, R.; CHARDY, P. The paradox high zooplankton biomass–low vegetal particulate organic matter in high turbidity zones: what way for energy transfer? **Journal of Experimental Marine Biology and Ecology**, 333, n. 2, p. 202-218, 2006.

DAY, J.W.; YANEZ-ARANCIBIA, A.; KEMP, W.M.; CRUMP, B.C. Introduction to estuarine ecology. **Estuarine ecology**, 2, p. 1-19, 2012.

DELVIGNE, G.A.L.; SWEENEY, C.E. Natural dispersion of oil. **Oil and Chemical Pollution**, 4, n. 4, p. 281-310, 1988.

DIAS, C.d.O. Morphological abnormalities of *Acartia lilljeborgi* (Copepoda, Crustacea) in the Espírito Santo Bay (ES Brazil). **Hydrobiologia**, 394, p. 249-251, 1999.

DIAS, C.d.O.; BONECKER, S.L.C. Long-term study of zooplankton in the estuarine system of Ribeira Bay, near a power plant (Rio de Janeiro, Brazil). **Hydrobiologia**, 614, n. 1, p. 65-81, 2008.

DIAS, C.d.O.; BONECKER, S.L.C. The copepod assemblage (Copepoda: Crustacea) on the inner continental shelf adjacent to Camamu Bay, northeast Brazil. **Zoologia (Curitiba)**, 26, p. 629-640, 2009.

DOWNING, J.A. Assessment of secondary production: the first step. In: DOWNING, J. A. e RIGLER, F. H. (Ed.). **A manual on methods for the assessment of secondary productivity in fresh waters**. Oxford: Blackwell Sci. Publ., 1984. v. 2, p. 1-18.

DUGGAN, S.; MCKINNON, A.D.; CARLETON, J.H. Zooplankton in an Australian tropical estuary. **Estuaries and coasts**, 31, n. 2, p. 455-467, 2008.

DUYL, F.V.; GAST, G.; STEINHOFF, W.; KLOFF, S. *et al.* Factors influencing the short-term variation in phytoplankton composition and biomass in coral reef waters. **Coral Reefs**, 21, n. 3, p. 293-306, 2002.

ESCOBAR, H. Mysterious oil spill threatens marine biodiversity haven in Brazil. **Science**, 366, n. 6466, p. 672, 2019.

ESKINAZI-LEÇA, E.; KOENING, M.L.; SILVA-CUNHA, M.G.G. Estrutura e dinâmica da comunidade fitoplanctônica. In: ESKINAZI-LEÇA, E.; NEWMANN-LEITÃO, S., *et al* (Ed.). **Oceanografia um cenário tropical**. Recife: Edições Bagaço, 2004. p. 353-373.

ESKINAZI-SANT'ANNA, E.M.; TUNDIST, J.G. Zooplâncton do estuário do Pina (Recife-Pernambuco-Brasil): composição e distribuição temporal. **Revista Brasileira de Oceanografia**, 44, p. 23-33, 1996.

ESTRADA, R.; HARVEY, M.; GOSSELIN, M.; STARR, M. *et al.* Late-summer zooplankton community structure, abundance, and distribution in the Hudson Bay system (Canada) and their relationships with environmental conditions, 2003–2006. **Progress in Oceanography**, 101, n. 1, p. 121-145, 2012.

FARIAS, G.B. **Estrutura, migração e fluxo de biomassa da comunidade zooplânctonica demersal em duas áreas recifais do Nordeste brasileiro**. 2019. 68 f. Dissertação (Mestrado) - Departamento de Oceanografia, Universidade Federal de Pernambuco, Recife, Brasil.

FEITOSA, F.A.N.; NASCIMENTO, F.C.R.; COSTA, K.M.P. Distribuição espacial e temporal da biomassa fitoplanctônica relacionada com parâmetros hidrológicos na Bacia do Pina (Recife-PE). **Trabalhos Oceanográficos da Universidade Federal de Pernambuco**, 27, n. 2, p. 1-13, 1999.

FERREIRA, B.P.; MAIDA, M.; CAVA, F., 2001, **Características e perspectivas para o manejo da pesca na APA Marinha Costa dos Corais**. 50-58.

FIDELIS, V.T.P. **Estrutura da comunidade e produção dos Copépodes Pelágicos dos recifes da APA Costa dos Corais (Tamandaré, PE, Brasil)**. 2014. 147 f. Tese (Doutorado) - Departamento de Oceanografia CTG, Universidade Federal de Pernambuco, Recife, Brasil.

FIDEM. Proteção das áreas estuarinas. **Séries Desenvolvimento Urbano e Meio Ambiente**, 1987.

FIGUEIRÊDO, L.G.P. **Estrutura da comunidade e produção dos copepoda do microzooplâncton da Apa Costa dos Corais, Tamandaré, PE, Brasil**. 2014. 65 f. Dissertações (Mestrado) - Departamento de Oceanografia, Universidade Federal de Pernambuco, Recife, Brasil.

FORWARD, R.B. Diel vertical migration: zooplankton photobiology and behaviour. **Oceanogr. Mar. Biol. Annu. Rev**, 26, n. 36, p. 1-393, 1988.

FULTON, R.S. Predation, production and the organization of an estuarine copepod community. **Journal of Plankton Research**, 6, n. 3, p. 399-415, 1984.

GARCIA, K.C.; LA ROVERE, E.L. Petróleo: acidentes ambientais e riscos à biodiversidade. **Interciência (Rio de Janeiro)**, p. 232, 2011.

GARCIA, T.M.; SANTOS, N.M.O.; CAMPOS, C.C.; COSTA, G.A.S. *et al.* Plankton net mesh size influences the resultant diversity and abundance estimates of copepods in tropical oligotrophic ecosystems. **Estuarine, Coastal and Shelf Science**, 249, p. 107083, 2021.

GIFFORD, D.J.; CARON, D.A. Sampling, preservation, enumeration and biomass of marine protozooplankton. **ICES zooplankton methodology manual**, p. 193-221, 2000.

GLYNN, P.W. Ecology of a Caribbean coral reef. The Porites reef-flat biotope: Part II. Plankton community with evidence for depletion. **Marine Biology**, 22, n. 1, p. 1-21, 1973.

GONÇALVES, É.D.A. **Estrutura e diversidade funcional de Copepoda em dois estuários tropicais**. 2016. Dissertação (Mestrado) - Programa de Pós-Graduação em Ciência e Tecnologia Ambiental - PPGCTA, Universidade Estadual da Paraíba, Paraíba, Brasil.

GORSKY, G.; OHMAN, M.D.; PICHERAL, M.; GASPARINI, S. *et al.* Digital zooplankton image analysis using the ZooScan integrated system. **Journal of plankton research**, 32, n. 3, p. 285-303, 2010.

GRAHAME, J. Zooplankton of a tropical harbour: the numbers, composition, and response to physical factors of zooplankton in Kingston Harbour, Jamaica. **Journal of Experimental Marine Biology and Ecology**, 25, n. 3, p. 219-237, 1976.

GRAY, J.S. Biomagnification in marine systems: the perspective of an ecologist. **Marine Pollution Bulletin**, 45, n. 1-12, p. 46-52, 2002.

GREGO, C.S.; FEITOSA, F.A.d.N.; SILVA, M.H.d.; SILVA, M.d.G.G.d. *et al.* Fitoplâncton do ecossistema estuarino do Rio Ariquindá (Tamandaré, Pernambuco, Brasil): variáveis ambientais, biomassa e produtividade primária. **Atlântica (Rio Grande)**, 31, n. 2, p. 183-198, 2009.

GROSS, M.G.; GROSS, E. **Oceanography: A view of the Earth**. New Jersey, Prentice Hall: 1996.

HÄDER, D.-P.; GAO, K. Interactions of anthropogenic stress factors on marine phytoplankton. **Frontiers in Environmental Science**, 3, p. 14, 2015.

HANSEN, B.; BJORNSEN, P.K.; HANSEN, P.J. The size ratio between planktonic predators and their prey. **Limnology and oceanography**, 39, n. 2, p. 395-403, 1994.

HANSEN, D.V.; JR, M.R. New dimensions in estuary classification 1. **Limnology and oceanography**, 11, n. 3, p. 319-326, 1966.

HEAD, R.N.; PHARRIS, R.; BONNET, D.; IRIGOIEN, X. A comparative study of size-fractionated mesozooplankton biomass and grazing in the North East Atlantic. **Journal of Plankton Research**, 21, n. 12, p. 2285-2308, 1999.

HIROTA, R. Zooplankton. **The Oceanographic Society of Japan (Ed.), Coastal Environmental Research Manual**, 1986.

HIRST, A.G.; BUNKER, A.J. Growth of marine planktonic copepods: global rates and patterns in relation to chlorophyll a, temperature, and body weight. **Limnology and Oceanography**, 48, n. 5, p. 1988-2010, 2003.

HOFFMEYER, M.S. Decadal change in zooplankton seasonal succession in the Bahía Blanca estuary, Argentina, following introduction of two zooplankton species. **Journal of plankton research**, 26, n. 2, p. 181-189, 2004.

HONORATO DA SILVA, M.; PASSAVANTE, J.d.O.; SILVA-CUNHA, M.; NASCIMENTO-VIEIRA, D. *et al.* Distribuição espacial e sazonal da biomassa fitoplanctônica e dos parâmetros hidrológicos no estuário do rio Formoso (Rio Formoso, Pernambuco, Brasil). **Tropical Oceanography**, 32, n. 1, p. 89-106, 2004.

HOPCROFF, R.; ROFF, J.C.; CHAVEZ, F. Size paradigms in copepod communities: a re-examination. **Hydrobiologia**, 453, n. 1, p. 133-141, 2001.

HUANG, Y.-J.; JIANG, Z.B.; ZENG, J.N.; CHEN, Q.Z. *et al.* The chronic effects of oil pollution on marine phytoplankton in a subtropical bay, China. **Environmental monitoring and assessment**, 176, n. 1, p. 517-530, 2011.

HUGHES, C.E.; PENNINGTON, R.T.; ANTONELLI, A. Neotropical plant evolution: assembling the big picture. **Botanical Journal of the Linnean Society**, 171, n. 1, p. 1-18, 2013.

HUGHES, T.P.; KERRY, J.T.; BAIRD, A.H.; CONNOLLY, S.R. *et al.* Global warming transforms coral reef assemblages. **Nature**, 556, n. 7702, p. 492-496, 2018.

HUNTLEY, M.E.; LOPEZ, M.D. Temperature-dependent production of marine copepods: a global synthesis. **The American Naturalist**, 140, n. 2, p. 201-242, 1992.

HUYSEN, R. Copepod evolution. **The Ray Society**, 1991.

IBAMA. **Manchas de óleo: litoral brasileiro**. Brasilia, 2020. Disponível em: <http://ibama.gov.br/manchasdeoleo>. Acesso em: 20 de Julho - 2020.

JACOBS, F.; GRANT, G.C. **Guidelines for zooplankton sampling in quantitative baseline and monitoring programs**. National Information Service, 1978.

JOHANNES, R.E.; GERBER, R. Import and export of net plankton by an Eniwetok coral reef community. **Great Barrier Reef Committee (Brisbane, Australia)**, 1, p. 97-104, 1974.

KENNISH, M.J. Ecology of estuaries: biological aspects. Volume II. : London: CRC Press 1990.

KIMMERER, W.J. The theory of secondary production calculations for continuously reproducing populations. **Limnology and Oceanography**, 32, n. 1, p. 1-13, 1987.

KIØRBOE, T. Population regulation and role of mesozooplankton in shaping marine pelagic food webs. **Hydrobiologia**, 363, n. 1-3, p. 13-27, 1997.

KIØRBOE, T. What makes pelagic copepods so successful? **Journal of Plankton Research**, 33, n. 5, p. 677-685, 2010.

KIORBOE, T.; SABATINI, M. Scaling of fecundity, growth and development in marine planktonic copepods. **Marine ecology progress series**. Oldendorf, 120, n. 1, p. 285-298, 1995.

KLEPPEL, G.S.; DAVIS, C.S.; CARTER, K. Temperature and copepod growth in the sea: a comment on the temperature-dependent model of Huntley and Lopez. **The American Naturalist**, 148, n. 2, p. 397-406, 1996.

KNAP, A.H.; BURNS, K.A.; DAWSON, R.; EHRHARDT, M. *et al.* Dissolved/dispersed hydrocarbons, tarballs and the surface microlayer: Experiences from an IOC/UNEP Workshop in Bermuda, December, 1984. **Marine pollution bulletin**, 17, n. 7, p. 313-319, 1986.

LEANDRO, S.M.; MORGADO, F.; PEREIRA, F.; QUEIROGA, H. Temporal changes of abundance, biomass and production of copepod community in a shallow temperate estuary (Ria de Aveiro, Portugal). **Estuarine, Coastal and Shelf Science**, 74, n. 1-2, p. 215-222, 2007.

LEFÈVRE, M., 1985, **Spatial variability of zooplanktonic populations in the lagoons of a high island (Moorea, French Polynesia)**. Museum-EPHE. Pages 39-45.

LIMA, B.F.R.; PESSOA, V.T.; GUSMÃO, L.c.M.d.O.; SILVA, A.a.P. *et al.* Mesozooplâncton do Estuário do Rio Formoso, Pernambuco, Brasil, Com Ênfase Em Cnidaria. **Tropical Oceanography**, 2012.

LIRA, A.L.d.O.; CRAVEIRO, N.; DA SILVA, F.F.; ROSA FILHO, J.S. Effects of contact with crude oil and its ingestion by the symbiotic polychaete Branchiosyllis living in sponges (*Cinachyrella* sp.) following the 2019 oil spill on the tropical coast of Brazil. **Science of The Total Environment**, 801, p. 149655, 2021.

LIRA, L.; FONSECA, V.G. Composição e distribuição faciológica do estuário do rio Formoso-PE. **Anais da Universidade Federal Rural de Pernambuco**, 5, p. 77-104, 1980.

LIRA, L.; ZAPATA, M.C.; FONSECA, V.G.d. Aspect of the Formoso river estuary, PE (Pernambuco, Brazil). **Caderno Omega**, 1979.

LIRA, M.C.d.A. Distribuicao dos Copepoda do complexo estuarino-lagunar Mandau/Manguaba-AL (Brasil). **Bol. Estud. Ciênc. Mar**, 9, p. 47-62, 1996.

LOPES, R.M. Zooplankton distribution in the Guaraú river estuary (South-eastern Brazil). **Estuarine, Coastal and Shelf Science**, 39, n. 3, p. 287-302, 1994.

LOPES, R.M.; VALE, R.d.; BRANDINI, F.P. Composição, abundância e distribuição espacial do zooplâncton no complexo estuarino de Paranaguá durante o inverno de 1993 e o verão de 1994. **Revista Brasileira de Oceanografia**, 46, p. 195-211, 1998.

LOSADA, A.P.M.; FEITOSA, F.A.N.; LINS, I.C. Variação sazonal e espacial da biomassa fitoplanctônica nos estuários dos rios Ilhetas e Mamucaba (Tamandaré-PE) relacionada com parâmetros hidrológicos. **Tropical Oceanography**, 31, n. 1, p. 1-29, 2003.

LOURENÇO, R.A.; COMBI, T.; DA ROSA ALEXANDRE, M.; SASAKI, S.T. *et al.* Mysterious oil spill along Brazil's northeast and southeast seaboard (2019–2020): Trying to find answers and filling data gaps. **Marine Pollution Bulletin**, 156, p. 111219, 2020.

MACÊDO, S.J.; MONTES, M.J.F.; LINS, I.C. Características abióticas da área. **Gerenciamento participativo de estuários e manguezais**, p. 7-25, 2000.

MAGALHÃES, A.; NOBRE, D.S.B.; BESSA, R.S.C.; PEREIRA, L.C.C. *et al.* Seasonal and short-term variations in the copepod community of a shallow Amazon estuary (Taperaçu, Northern Brazil). **Journal of Coastal Research**, p. 1520-1524, 2011.

MAGALHÃES, G.M.D.O. **Produção de copepoda do plâncton em um estuário impactado no nordeste brasileiro** 2014. 89 f. Tese (Doutorado) - Programa de Pós- Graduação em Oceanografia da Universidade Federal de Pernambuco (PPGO – UFPE), Universidade Federal De Pernambuco Recife, Brasil.

MAIDA, M.; FERREIRA, B.P. Estudo preliminar sobre o assentamento de corais em um Recife na Baía de Tamandaré-PE. **Bol. Téc. Cient. CEPENE**, 3, p. 23-37, 1995.

MARCHAND, M.H. The Amoco Cadiz oil spill. Distribution and evolution of hydrocarbon concentrations in seawater and marine sediments. **Environment international**, 4, n. 5-6, p. 421-429, 1980.

MARQUES, V.M.; SILVA-FALCÃO, E.C.; SEVERI, W. Estrutura da assembleia ictioplanctônica em dois estuários tropicais de Pernambuco (Brasil), sujeitos a diferentes condições hidrológicas. **Revista Brasileira de Ciências Agrárias**, 10, n. 2, p. 304-314, 2015.

MATSUMURA-TUNDISI, T. Aspectos ecologicos do zooplanton da regiao lagunar de Cananeia com especial referencia aos Copepoda (Crustacea). **Ph. D. Thesis. Universidade de São Paulo, Instituto de Biociencias, São Paulo**, 1972.

MELO, P.A.M.C.; SILVA, T.A.; NEUMANN-LEITÃO, S.; SCHWAMBORN, R. *et al.* Demersal zooplankton communities from tropical habitats in the southwestern Atlantic. **Marine Biology Research**, 6, n. 6, p. 530-541, 2010.

MELO-JUNIOR, M.; MARCOLIN, C.R.; MIYASHITA, L.K.; LOPES, R.M. Temporal changes in pelagic copepod assemblages off Ubatuba, Brazil. **Marine Ecology**, 37, n. 4, p. 877-890, 2016.

MILLER, C.B. The zoology of zooplankton. **Biological Oceanography**. Blackwell Publishing, Malden, p. 111-128, 2004.

MIRANDA, L.B.d.; CASTRO, B.M.d.; KJERFVE, B. Circulation and mixing due to tidal forcing in the Bertioga Channel, São Paulo, Brazil. **Estuaries**, 21, n. 2, p. 204-214, 1998.

MISHRA, S.; PANIGRAHY, R.C. Zooplankton ecology of the Bahuda estuary (Orissa), east coast of India. 1999.

MORRONE, J.J. Cladistic biogeography of the Neotropical region: identifying the main events in the diversification of the terrestrial biota. **Cladistics**, 30, n. 2, p. 202-214, 2014.

MOURA, R.T. **Biomassa, produção primária do fitoplâncton e alguns fatores ambientais da Baía de Tamandaré, Rio Formoso, Pernambuco, Brasil.** . 1991. 290 f. Dissertação (Mestrado) - Departamento de Oceanografia, Universidade Federal de Pernambuco, Recife.

MOURA, R.T.; PASSAVANTE, J.Z.d.O. Taxa de assimilação do fitoplâncton da baía de Tamandaré-Rio Formoso-PE-Brasil. **Boletim Técnico e Científico CEPENE, Tamandaré**, 1, n. 1, p. 17-23, 1993.

MOURA, R.T.; PASSAVANTE, J.Z.d.O. Biomassa fitoplanctônica na baía de Tamandaré, Rio Formoso-Pernambuco, Brasil. **Trabalhos Oceanográficos da Universidade Federal de Pernambuco**, 23, p. 1-15, 1995.

MÜLLER, M.N.; YOGUI, G.T.; GÁLVEZ, A.O.; DE SALES JANNUZZI, L.G. *et al.* Cellular accumulation of crude oil compounds reduces the competitive fitness of the coral symbiont *Symbiodinium glynnii*. **Environmental Pollution**, 289, p. 117938, 2021.

MUSCHENHEIM, D.K.; LEE, K. Removal of oil from the sea surface through particulate interactions: review and prospectus. **Spill Science & Technology Bulletin**, 8, n. 1, p. 9-18, 2002.

NASCIMENTO-VIEIRA, D.A.d.; FERNANDO DE FIGUEIREDO; NETO, P. Mesozooplâncton de área recifal do atlântico sudoeste tropical. **Tropical Oceanography**, p. 13, 2010.

NEUMANN-LEITÃO, S. **Impactos antropicos na comunidade zooplânctonica estuarina, Porto de Suape - PE - brasil.** 1994. Tese (Doutorado) -, Universidade de São Paulo, São Carlos, São Paulo.

NEUMANN-LEITÃO, S. Resenha literária sobre zooplâncton estuarino no Brasil. **Trab. Oceanogr. Univ. Fed. PE**, 23, p. 25-53, 1995.

NEUMANN-LEITÃO, S. O zooplâncton como indicador da qualidade ambiental de dois estuários do Brasil tropical. **Professorship Thesis, Universidade Federal de Pernambuco, Recife**, 2010.

NEUMANN-LEITÃO, S.; FEITOSA, F.A.N.; MAYAL, E.; SCHWAMBORN, R. *et al.* The plankton from Maracajaú reef ecosystem (Brazil)–offshore coral reefs under multiple human stressors. **WIT Trans. Ecol. Environ.**, 122, p. 173-182, 2009.

NEUMANN-LEITÃO, S.; GUSMÃO, L.M.D.O.; VIEIRA, D.A.d.N.; PARANHOS, J.D.N. Zooplâncton da área estuarina do Rio Formoso - PE (Brasil). **Trabalhos Oceanográficos da Universidade Federal de Pernambuco**, p. 55-64, 1995.

NEUMANN-LEITÃO, S.; GUSMÃO, L.M.O.; NASCIMENTO-VIEIRA, D.; SILVA, T.A. *et al.* Biodiversidade do mesozooplâncton do nordeste do Brasil. **Trabs Oceanogr. Univ. Fed. PE**, 26, n. 1, p. 27-34, 1998.

NEUMANN-LEITÃO, S.; MATSUMURA-TUNDISI, T. Dynamics of a perturbed estuarine zooplanktonic community: Port of Suape, PE, Brazil. **Internationale Vereinigung für theoretische und angewandte Limnologie: Verhandlungen**, 26, n. 4, p. 1981-1988, 1998.

NEWELL, G.E.; NEWELL, R.C. **Marine plankton: a practical guide**. 1963.

NORDI, N. **Ecologia do zooplâncton no estuário do Rio Paraíba do Norte (Paraíba-Brasil)**. 1982. Dissertação (Mestrado) - Departamento de Ciências Biológicas, Universidade Federal de São Carlos, São Paulo, Brasil.

ODUM, E.P.; BARRETT, G.W. **Fundamentals of ecology**. Saunders Philadelphia, 1971.

OMORI, M.; IKEDA, T. **Methods in marine zooplankton ecology**. 1984.

OMORI, M.; IKEDA, T. Methods in marine zooplankton ecology. Florida. : Krieger. 332p 1992.

PAFFENHÖFER, G.-A. Vertical zooplankton distribution on the northeastern Florida shelf and its relation to temperature and food abundance. **Journal of Plankton Research**, 5, n. 1, p. 15-33, 1983.

PAGANO, M.; LUCIEN SAINT-JEAN. Biomass and production of the calanoid copepod *Acartia clausi* in a tropical coastal lagoon: Lagune Ebrie, Ivory Coast. **SCI. MAR.**, 53, n. 2, p. 617-624, 1989.

PAIVA, A.C.G.d.; CHAVES, P.d.T.d.C.; ARAÚJO, M.E.d. Estrutura e organização trófica da ictiofauna de águas rasas em um estuário tropical. **Revista brasileira de Zoologia**, 25, p. 647-661, 2008.

PASSAVANTE, J.Z.O., 2003, **Produção fitoplanctônica do estuário do rio Capibaribe (Recife, Pernambuco, Brasil)**.

PATIL, N.N.; GOLDIN, Q.; SOMANI, V.U.; KURVE, P.N. *et al.*, 2002, **Study of zooplankton distribution from Ulhas river estuary and Thane creek**. 109-115.

PEREIRA, J.B. **Composição, distribuição, biomassa e produção secundária do zooplâncton do sistema estuarino de Santos, São Paulo, Brasil**. 2011. Tese (Doutorado) - Instituto Oceanográfico (USP), Universidade de São Paulo, São Paulo, Brasil.

PETERSON, W.T.; TISELIUS, P.; KIØRBOE, T. Copepod egg production, moulting and growth rates, and secondary production, in the Skagerrak in August 1988. **Journal of Plankton Research**, 13, n. 1, p. 131-154, 1991.

RAMSEUR, J.L. Oil spills in U.S. coastal waters: background, governance, and issues for congress. **Congressional research service**, 2010.

RÉ, P.M.A.B. **Ictioplâncton estuarino da Península Ibérica: guia de identificação dos ovos e estados larvares planctônicos**. Lisboa: Camara municipal de Cascais Cascais, 1999. 9726370655.

REBOUÇAS, A.C. Sedimentos da Baía de Tamandaré-Pernambuco. **Trabalhos Oceanográficos da Universidade Federal de Pernambuco**, 7, n. 9, p. 187-206, 1966.

ROBERTIS, A.D. Size-dependent visual predation risk and the timing of vertical migration: An optimization model. **Limnology and Oceanography**, 47, n. 4, p. 925-933, 2002.

SANTANA-BARRETO, M.S.; NÓBREGA, M.N.C.; FILHO, B.d.M. Revisão e atualização do zooplâncton no estuário do Rio Ariquinda, Rio Formoso-Pernambuco. **Proceedings of the Encontro Brasileiro de Plâncton**, 4, p. 415-430, 1991.

SANTOS, T.G.d.; BEZERRA-JUNIOR, J.L.; COSTA, K.M.P.d.; FEITOSA, F.A.d.N. Dinâmica da biomassa fitoplanctônica e variáveis ambientais em um estuário tropical (Bacia do Pina, Recife, PE). **Revista Brasileira de Engenharia de Pesca**, 4, n. 1, p. 95-109, 2009.

SCHWAMBORN, R.; EKAU, W.; SILVA, A.P.; SCHWAMBORN, S.H.L. *et al.* Ingestion of large centric diatoms, mangrove detritus, and zooplankton by zoeae of *Aratus pisonii* (Crustacea: Brachyura: Grapsidae). **Hydrobiologia**, 560, n. 1, p. 1-13, 2006.

SHANNON, C.E. A mathematical theory of communication. **The Bell system technical journal**, 27, n. 3, p. 379-423, 1948.

SHERR, E.B.; SHERR, B.F. Significance of predation by protists in aquatic microbial food webs. **Antonie van Leeuwenhoek**, 81, n. 1-4, p. 293-308, 2002.

SIEBURTH, J.M.; WILLIS, P.-J.; JOHNSON, K.M.; BURNEY, C.M. *et al.* Dissolved organic matter and heterotrophic microneuston in the surface microlayers of the North Atlantic. **Science**, 194, n. 4272, p. 1415-1418, 1976.

SILVA, A.P.; NEUMANN-LEITÃO, S.; SCHWAMBORN, R.; GUSMÃO, L.M.d.O. *et al.* Mesozooplankton of an impacted bay in North Eastern Brazil. **Brazilian Archives of Biology and Technology**, 47, p. 485-493, 2004.

SILVA, L.; FIGUEIREDO FILHO, D.; FERNANDES, A. O efeito do lockdown sobre a epidemia da COVID-19 no Brasil: evidências a partir de uma análise de séries temporais interrompidas. **Cadernos de Saúde Pública**, 36, 2020.

SILVA, L.S.C.d.; LIMA PICANÇO, J.d.; CALIL, J.G.S. O grande desastre esquecido: análise preliminar do derramamento de óleo na costa brasileira (agosto/2019–março/2020) e seus impactos no litoral da Bahia. **Revista da Universidade Federal de Minas Gerais**, 27, n. 3, p. 54-79, 2020.

SILVA, M.H.d.; CUNHA, M.d.G.G.d.S.; PASSAVANTE, J.Z.d.O.; GREGO, C.K.d.S. *et al.* Estrutura sazonal e espacial do microfitoplâncton no estuário tropical do rio Formoso, PE, Brasil. **Acta botanica brasiliaca**, 23, p. 355-368, 2009.

SILVA, N.L.; MARCOLIN, C.R.; SCHWAMBORN, R. Using image analysis to assess the contributions of plankton and particles to tropical coastal ecosystems. **Estuarine, Coastal and Shelf Science**, 219, p. 252-261, 2019.

SKJOLDAL, H.R.; WIEBE, P.H.; POSTEL, L.; KNUTSEN, T. *et al.* Intercomparison of zooplankton (net) sampling systems: Results from the ICES/GLOBEC sea-going workshop. **Progress in Oceanography**, 108, p. 1-42, 2013.

SOARES, M.d.O.; TEIXEIRA, C.E.P.; BEZERRA, L.E.A.; PAIVA, S.V. *et al.* Oil spill in South Atlantic (Brazil): Environmental and governmental disaster. **Marine Policy**, 115, p. 103879, 2020.

SOROKIN, Y.I. Aspects of trophic relations, productivity and energy balance in coral-reef ecosystems. **Ecosystems of the world**, 25, p. 401-418, 1990a.

SOROKIN, Y.I. Plankton in the reef ecosystems. **Ecosystems of the World**, 25, p. 291-327, 1990b.

SZEWCZYK, A.; BOROWIEC, F.; HANCZAKOWSKA, E. Fatty acid and cholesterol content of meat of broilers fed linseed oil or different linseed varieties. **NATIONAL RESEARCH INSTITUTE OF ANIMAL PRODUCTION**, 6, n. 1, p. 109-116, 2006.

TADA, K.; SAKAI, K.; NAKANO, Y.; TAKEMURA, A. *et al.* Size-fractionated phytoplankton biomass in coral reef waters off Sesoko Island, Okinawa, Japan. **Journal of Plankton Research**, 25, n. 8, p. 991-997, 2003.

TEIXEIRA, C.; TUNDISI, J.; KUTNER, M.B. Plankton studies in a mangrove environment II: the standing stock and some ecological factors. **Boletim do Instituto Oceanográfico**, 14, p. 13-41, 1965.

TRANTER, D.; GEORGE, J. Zooplankton abundance at Kavaratti and Kalpeni atolls in the Laccadives. **Proceedings of the First Symposium on Coral and Coral Reefs, Conchin**, 1, p. 239-256, 1972.

TUNDISI, J.; ESTUARINO, P. Contribuições Avulsas do instituto Oceanográfico da Universidade de São Paulo. 1970.

TUNDISI, J.; TUNDISI, T.M. Plankton studies in a mangrove environment: V. Salinity tolerances of some planktonic crustaceans. **Boletim do Instituto Oceanográfico**, 17, p. 57-65, 1968.

TUNDISI, J.G.O. Contribuições Avulsas do instituto Oceanográfico da Universidade de São Paulo. 1970.

TURNER, J.T. Planktonic copepods of Boston Harbor, Massachusetts Bay and Cape Cod Bay, 1992. *In: Ecology and Morphology of Copepods*: Springer, 1994. p. 405-413.

UEDA, H.; KUWAHARA, A.; TANAKA, M.; AZETA, M. Underwater observations on copepod swarms in temperate and subtropical waters. 1983.

UNESCO. Determination of photosynthetic pigments. **Determination of Photosynthetic Pigments in Sea-water**, p. 9-18, 1966.

UNESCO. Zooplankton sampling. *In: Monographs in Oceanographic Methodology*. Paris: UNESCO, 1968. p. 74.

UYE, S.-i.; NAGANO, N.; SHIMAZU, T. Abundance, biomass, production and trophic roles of micro-and net-zooplankton in Ise Bay, central Japan, in winter. **Journal of Oceanography**, 56, n. 4, p. 389-398, 2000.

VALENTIN, J.L.; MACEDO-SAIDAH, F.E.; TENENBAUM, D.R.; SILVA, N.M.L.d. A diversidade específica para a análise das sucessões fitoplanctônicas. Aplicação ao ecossistema da ressurgência de Cabo Frio (RJ). **Revista Nerítica**, 6, n. 1-2, p. 7-26, 1991.

WALSH, G.E. Toxic effects of pollutants on Plankton. **Principles of Ecotoxicology**. John Wiley & Sons, Inc., New York, p. 257-274, 1978.

WEBBER, M.K.; ROFF, J.C. Annual biomass and production of the oceanic copepod community off Discovery Bay, Jamaica. **Marine Biology**, 123, p. 481-495, 1995.

WILLIAMS, G.J.; GRAHAM, N.A.; JOUFFRAY, J.B.; NORSTRÖM, A.V. *et al.* Coral reef ecology in the Anthropocene. **Functional Ecology**, 33, n. 6, p. 1014-1022, 2019.

WILLIAMSON, P.; GRIBBIN, J. How plankton change the climate. **New Scientist**, 129, n. 1760, p. 48-52, 1991.

WILSON, D.S. Food size selection among copepods. **Ecology**, 54, n. 4, p. 909-914, 1973.

WILSON, K.L.; TITTENSOR, D.P.; WORM, B.; LOTZE, H.K. Incorporating climate change adaptation into marine protected area planning. **Global Change Biology**, 26, n. 6, p. 3251-3267, 2020.

YAMAZI, I. Plankton investigation in inlet waters along the coast of japan-xvii. seasonal succession of zooplankton in the inner area of tanabe bay from june to october, 1954. **PUBLICATIONS OF THE SETO MARINE BIOLOGICAL LABORATORY**, 4, n. 2-3, p. 311-320, 1955.

ZARAUZ, L.; IRIGOIEN, X.; FERNANDES, J.A. Modelling the influence of abiotic and biotic factors on plankton distribution in the Bay of Biscay, during three consecutive years (2004–06). **Journal of plankton research**, 30, n. 8, p. 857-872, 2008.

ZIOLLI, R.L. Aspectos ambientais envolvidos na poluição marinha por petróleo. **Revista Saúde e Ambiente**, vol.3, p. 32-41, 2002.